Title
A Hybrid Dynamical Systems Theory for Legged Locomotion

Author
Burden, Samuel A.

Publication Date
2014

Peer reviewed|Thesis/dissertation

A Hybrid Dynamical Systems Theory for Legged Locomotion

by

Samuel A. Burden

A dissertation submitted in partial satisfaction of the
requirements for the degree of
Doctor of Philosophy

in

Engineering—Electrical Engineering and Computer Sciences

in the

Graduate Division

of the

University of California, Berkeley

Committee in charge:

Professor S. Shankar Sastry, Chair
Professor Robert J. Full
Professor Ruzena Bajcsy
Professor Maciej Zworski

Fall 2014

A Hybrid Dynamical Systems Theory for Legged Locomotion

Abstract

A Hybrid Dynamical Systems Theory for Legged Locomotion

by

Samuel A. Burden

Doctor of Philosophy in Engineering—Electrical Engineering and Computer Sciences

University of California, Berkeley

Professor S. Shankar Sastry, Chair

Legged locomotion arises from intermittent contact between limbs and terrain. Since it emerges from a closed–loop interaction, reductionist study of body mechanics and terrestrial dynamics in isolation have failed to yield comprehensive strategies for forward– or reverse–engineering locomotion. Progress in locomotion science stands to benefit a diverse array of engineers, scientists, and clinicians working in robotics, neuromechanics, and rehabilitation. Eschewing reductionism in favor of a holistic study, we seek a systems–level theory tailored to the dynamics of legged locomotion.

Parsimonious mathematical models for legged locomotion are *hybrid*, as the system state undergoes continuous *flow* through limb stance and swing phases punctuated by instantaneous *reset* at discrete touchdown and liftoff events. In their full generality, hybrid systems can exhibit properties such as nondeterminism and orbital instability that are inconsistent with observations of organismal biomechanics. By specializing to a class of intrinsically self–consistent dynamical models, we exclude such pathologies while retaining emergent phenomena that arise in closed–loop studies of locomotion.

Beginning with a general class of hybrid control systems, we construct an intrinsic state–space metric and derive a provably–convergent numerical simulation algorithm. This resolves two longstanding problems in hybrid systems theory: non–trivial comparison of states from distinct discrete modes, and accurate simulation up to and including *Zeno* events. Focusing on models for periodic gaits, we prove that isolated discrete transitions generically lead the hybrid dynamical system to reduce to an equivalent classical (smooth) dynamical system. This novel route to reduction in models of rhythmic phenomena demonstrates that the closed–loop interaction between limbs and terrain is generally simpler than either taken in isolation. Finally, we show that the non–smooth flow resulting from arbitrary footfall timing possesses a non–classical (*Bouligand*) derivative. This provides a foundation for design and control of multi–legged maneuvers. Taken together, these contributions yield a unified analytical and computational framework—a hybrid dynamical systems theory—applicable to legged locomotion.

to Mary Louise

Contents

List of Figures

List of Tables

Acknowledgments

First and foremost I thank Shankar Sastry and Bob Full, who advised and guided my thesis work. Shankar's generous spirit, limitless enthusiasm for research, and unflagging dedication to the welfare of his mentees serves as a model for us all. Bob's heroic investment of time and effort cultivating me as an academic and interdisciplinary researcher yields a debt I may never repay. As I transition to the next stage of my academic career, I can only hope to instill in my students the same passion and loyalty I learned.

I give my heartfelt gratitude to the faculty who mentored and supported me throughout my education: to Eric Klavins, for introducing me, as a high school student, to academia; to Ruzena Bajcsy, for her singular role as a pioneer in research and devoted "grandmother"; to Dan Koditschek, for his exceptional academic standards and conscientious mentorship; to Claire Tomlin, for her sterling achievements as a researcher and teacher; to Maciej Zworski, for his generous service and personal accommodation; and to Ron Fearing, for his provocative questions and openness to collaboration. I aspire to justify the considerable investment you have each made on my behalf.

At UW, UPenn, and Berkeley, I've had the honor and pleasure of befriending and collaborating with an extraordinary cohort: Nils Napp and the SOSLab; Jonathan Clark, Joel Weingarten, Goran Lynch, Aaron Johnson, Gavin Kenneally, and the Kod*Lab; Shai Revzen, Talia Moore, Jean–Michel Mongeau, and the Poly–PEDAL Lab; Aaron Hoover and the Biomimetic Millisystems Lab; Saurabh Amin, Humberto Gonzalez, Ram(anaryan[an]) Vasudevan, Nikhil Naikal, Henrik Ohlsson, Lily Ratliff, Insoon Yang, Dheeraj Singaraju, Ehsan Elhamifar, and the rest of our (Semi–)Autonomous Group.

For their selfless dedication to instilling the next generation with a passion for engineering, I admire Matt Spencer, Sam (#2) Coogan, Dan Calderone, Dorsa Sadigh, and the rest of the EEGSA Outreach folks.

I am grateful to the sponsors and staff that enabled my research: Jessica Gamble, Gary Given, Mary Stewart, Annie Ren, and ERSO from Berkeley Engineering; Diedra Krieger from UPenn Engineering; a Graduate Research Fellowship from the National Science Foundation; and the Micro–Autonomous Systems and Technology grant from the Army Research Lab. This enterprise would not be possible without your support!

For their tireless efforts in rehabilitation, I thank Mary Popylisen and Jamie Hampton.

I owe a special debt to a cadre of intellectuals who significantly influenced my thinking: Michael Duncan, Branko Kerkez, Pavan Vaswani, Brian Wolfe, Henry Jacobs, Baruch Sterin, Avital Steinitz, Brian Pepin, and Joe Jardine.

I am extremely fortunate to be part of a loving and ever–expanding family. I particularly wish to acknowledge: Denise and Rick, who unfailingly encouraged me to seek personal satisfaction over material rewards; Jess, who buoyed me throughout my adolescence and education; Nancy and Ken, who welcomed me into their home; and Aaron, whose camaraderie kept me grounded.

Finally, I dedicate this thesis to Mary Louise. I am humbled to be your partner.

Chapter 1

Introduction

Dynamic interaction with the environment provides the foundation for autonomy. An agent's perception of the world, and its action in it, is directly mediated by the physical phenomena governing the coupling of its *self* with the *non–self*. It is the agent's primary aim to respond appropriately to the consequences of its motor actions in the world. Biological organisms have developed exquisite strategies to achieve this aim across a staggering array of physical scales, material compositions, and body morphologies. In contrast, *artifacts*[1] are numb, dumb, and clumsy, struggling with each step in the perception → action loop depicted in Figure 1.1. As scientists and engineers, we will not be permitted the luxury of uncovering the principles underlying autonomy through random experimentation over evolutionary timescales. Instead, we must derive systematic methodologies for reverse– and forward–engineering of sensorimotor control.

Given the astounding range of ecological contexts populated by autonomous agents, our insights will necessarily be specialized to the dominant physical phenomena at a particular scale of interest. At interplanetary scales we concern ourselves with propulsion through gravitational landscapes, while at microscopic scales stochastic diffusion dominates. Between these two extremes, agents interact with viscous media governed by aero–, hydro–, and terra–dynamics. Though a significant fraction of Earth's biomass is buoyed throughout its life by fluids, the human condition is relentlessly held at the terrestrial interface between air and water. Thus in this thesis we attend to sensorimotor control of intermittent interaction with *terra firma*.

[1] artifact, *n.* An object made or modified by human workmanship, as opposed to one formed by natural processes [OED].

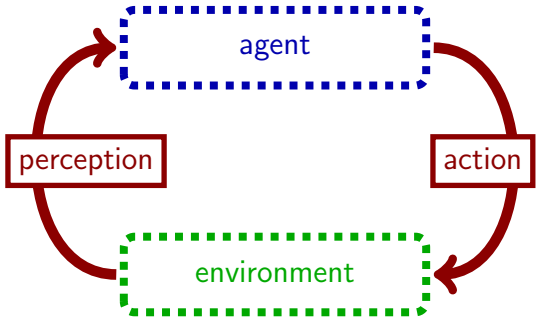

Figure 1.1: *Sensorimotor control loop.* Autonomous agents interact continually with their environments through a closed loop that transforms perception to action. The coupled system can exhibit emergent behavior not predicted by a reductionist analysis of the agent or its environment in isolation.

1.1 Robotics, Neuromechanics, and Rehabilitation

Recent decades have witnessed a confluence of approaches to study sensorimotor control stemming from disparate areas in engineering, science, and medicine. Three such incident fields have direct bearing on the macro scale: *robotics*, *neuromechanics*, and *rehabilitation*. The aims of these three fields are complementary in that an advance in one area can lead to progress in either of the others. This provides a unique opportunity to conduct fruitful research at the disciplinary boundary. However, systematically translating results between domains requires development of a common conceptual framework. We contend that the potential for transformative payoffs and co–benefits justifies the effort required, and briefly summarize some trends and targets of opportunity.

Robotics: *engineering discipline concerned with programming matter to perform work.* Artifacts must move out of structured and sterile environments into the "real world" characterized by dynamically–changing environments and autonomous external agents. Driven by a societal need for safe collaboration between robots and humans both in the factory and in homes [NRI], requirements for rigid manipulation and noiseless observations [Mur+94; Ma+04] must be relaxed in favor of task–driven perception and action [Baj88; Kod92; Soa13].

Neuromechanics: *scientific discipline focused on the coupling between a nervous system and environment through musculoskeletal structures.* A reductionist focus on either neurophysiology or biomechanics alone will fail to yield understanding of the mechanisms leading to animal behavior [Nis+07]; Figure 1.2a. Similarly, we must reject the false dichotomy of "sensory" and "motor" neuroscience that splits the sensorimotor loop within the processing system, recognizing instead that "neural computation is inescapably closed–loop" [Rot+14]; Figure 1.2b. Aspects of this closed–loop approach have been championed under various

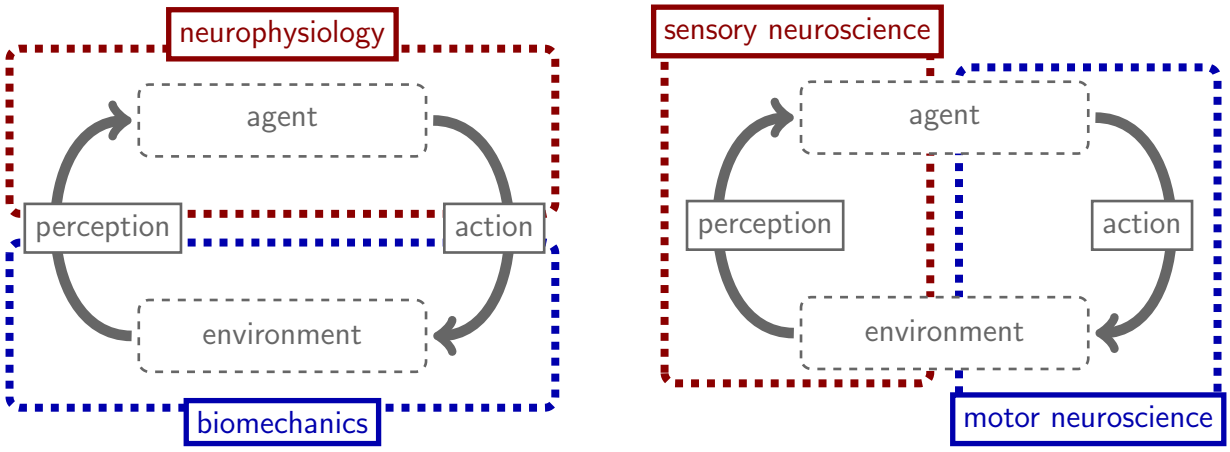

(a) neurophysiology vs. biomechanics (b) sensory vs. motor neuroscience

Figure 1.2: *False dichotomies in the sensorimotor control loop.* (a) Biomechanics focuses on the dynamic interaction between an agent's body and the environment, whereas neurophysiology studies the internal transformation of sensory data to motor commands. (b) Cognitive neuroscience focuses on representations in the nervous system formed from impinging sensory data, whereas motor control seeks principles underlying behavior synthesis.

labels: Wiener's "cybernetics" [Wie48]; Bernstein's "emergent problems in the regulation of motor acts" [Ber67]; Full and Koditschek's "templates–and–anchors" hypothesis [FK99]. This effort is supported by early–career awards at the disciplinary interface [BWF; SF].

Rehabilitation: *medical discipline concerned with enhancing natural human ability and mitigating disability.* Of particular interest are novel therapies, prostheses, and assistive devices that augment the intrinsic ability of individuals. Originally conceived in the realm of individualized genomic diagnosis and pharmacological treatment [Hoo+04; HC10], the paradigm of *personalized healthcare* should extend to neurophysiological, behavioral, and rehabilitative therapy. The need to automatically tailor healthcare to an individual's trauma, pathology, and deficiency is driven by the increase in elderly, underserved, and military veteran populations, both domestically and abroad. This area is bolstered by initiatives in translational medicine [Col11] and neurotechnology [Ins+13].

1.1.1 Common Cause

Engineers have in organisms proof–of–concept designs that dramatically outperform their robotic counterparts: insects survive in the wild despite loss of multiple limbs [Guf99]; the cost of transport in animals is orders of magnitude smaller than comparable robots [Col+05]. The disparity in performance between extant animals and robots is especially galling since animal body designs meet many conflicting constraints (ontogeny, reproduction, metabolism)

that do not burden artifacts [Ram+04]. Scientists can use robotic surrogates in comparative studies to overcome limitations in diversity of scale, morphology, and material composition found in the animal kingdom [QR98; Rit+00; Kla+00; Kod+04; Del04; LB11]. Clinicians stand to benefit both from the forward engineering and design capabilities devised by engineers as well as the reverse engineering techniques and results derived by scientists, for instance in the design of active assistive devices [Fer+05; Don+08; Mar+11].

1.1.2 Common Challenge

In each discipline, one essential challenge lies in the dynamical complexity arising from the interaction of an agent with its environment. From a reductionist viewpoint, this interaction seems hopelessly complex, combining distributed hierarchies of feedback loops in the sensorimotor system with the hydro–, aero–, or terra–dynamics and Newtonian mechanics that dominate the macro scale. As a consequence, recent years have seen an emergence of systems–level approaches that study the closed–loop dynamics of an agent interacting with its environment. In robotics, concepts of *embodied* [Pfe+07] or *mechanical* [Bli+07] *intelligence* as well as *morphological computation* [Hau+11], *communication* [Rie+10], or *control* [Füc+12] assert that behaviors of interest arise from the dynamical coupling of feedback and information processing elements distributed throughout the body and environment. Neuromechanics itself arose from the recognition that neither neuroscience nor biomechanics alone could provide a full account of animal behavior [Nis+07], and capitalizes on broader trends toward integrative and comparative approaches to organismal biology [Vog07; Sch+09].

1.2 Systems Theory for Sensorimotor Control

Given the aforementioned complexity of the physical phenomena under investigation, it may seem misguided to seek a systems–level theory for sensorimotor control. While we struggle to understand the principles of perception and action in isolation, it seems hopeless to directly study their interaction. In actual fact, there exists a wealth of evidence—*experimental*, *phenomenological*[2], and *sociological*—that justifies the systems–level approach as a viable alternative to reductionism. We review this evidence before proceeding to specify the essential elements that constitute a systems theory. Drawing analogies from successful examples of the systems approach, we focus attention on the underpinnings of a systems theory for sensorimotor control.

[2] phenomenology, *n.* The division of any science which is concerned with the description and classification of its phenomena, rather than causal or theoretical explanation. [OED]

1.2.1 Justification for a Systems–Level Approach

Experimental

Animal musculoskeletal structure is highly overdetermined; there are many more mechanical degrees–of–freedom and enervated muscles than would be strictly necessary to achieve any given task. Initially viewed as as the "problem of motor redundancy" [Ber67], this excess may actually provide significant benefits without incurring substantive costs. In the modern view, organisms "exploit the bliss of motor abundance" [Lat12] via predictable strategies including muscle synergies [TM05; dB05; TM07], internal degrees–of–freedom (or *uncontrolled manifolds*) [SS99], and optimality [FH85; TJ02; Tod04; Sco04]. These emergent phenomena resolve redundancy, maintain stability, and aid perturbation recovery [Loe+99]. Thus whole–body behaviors such as locomotion can be achieved largely through mechanical means [Kod+04]. Even complex environments comprised of flowing, fluidizing granular media do not necessarily increase the dynamical complexity of the closed–loop interaction that gives rise to locomotion [Li+13].

Phenomenological

Terrestrial locomotion of animals shares striking similarities across a range of scales, morphologies, and material compositions. Animals as diverse as hexapedal cockroaches, quadrupedal canines, and bipedal birds bounce like a monopode in the saggital plane [Bli89; BF93; Ghi+03; Hol+06], and a prosthesis tuned for competitive athletics restored biomechanically similar functionality to a human [Wey+09]. Turning the monopode on its side yields qualitative agreement with sprawled–posture gaits of hexapods and quadrupeds in the lateral plane [SH00b; SH00a; SH01; Sch+02]. These "template" models embody and exploit "self–stabilization" [KF99] mechanisms underlying turning and perturbation recovery [JF99; JF02; Ful+02; KH07; Kuk+09] and properly embed in "anchored" neuromechanical variants [Hol+06; Pro+10]. Biologically–inspired robots can rely on purely feedforward inputs to execute dynamically–stable rhythmic locomotion [Sar+01; Kim+06; Bir+09; Hoo+10; McG90; Col+05] and manipulation [SA93; RD12] tasks. This synergistic interaction between the nervous system and body can be studied with system–level neuromechanical simulation models [Edw10]. Thus, "integrative approaches reveal not only how each component within a locomotor system operates but how they function as a collective whole" [Dic+00].

Sociological

Engineering, science, and medicine stand to benefit tremendously from interdisciplinary collaborative investigation of sensorimotor control. However, disparities in the detailed physics of perception, processing, and action in the different domains threaten to obstruct efficient transmission of advances across disciplinary boundaries. Despite progress in the areas of biologically–inspired materials, sensors, actuators, and processors, robots and animals will remain comprised of vastly different components for the foreseeable future. Given this in-

herent disparity, the systems–level approach possesses a major advantage over reductionism in that its advances are not tied to the underlying physics. Representations for mechanisms discovered in one domain are necessarily abstracted in the systems approach, facilitating translation to other fields. This has been demonstrated most strikingly in the qualitative translation of mechanisms for rapid running [Sar+01; Kim+06; Bir+09], turning [Hoo+10], and inversion [Mon+12] from neuromechanics to robotics. Thus, "systems theory, especially dynamical systems theory, may provide [a] shared language and fruitful avenues of interdisciplinary integration" [Sch+09].

1.2.2 Elements of a Systems Theory

The notion that one can fruitfully study aspects of a class of physical phenomena holistically without necessarily expending the substantial effort required to distill a collection of fundamental mechanisms is appealing. This has led some to develop a theory of systems [Ber84] that provides concepts of equivalence and generic properties of graphical representations. However, the generality inherent in this approach is unlikely to provide design or mechanistic principles useful for practitioners of engineering, science, or medicine. Therefore we seek an approach tailored to sensorimotor control.

For our purposes, a *systems theory* is a unified *analytical*, *computational*, and *experimental* framework that enables systematic study of a class of physical phenomena.

Analytical elements: *intrinsically self–consistent techniques for dynamical modeling.* Concepts include: genericity, minimality, and equivalence of model structures; interconnection and feedback between subsystems; stability, sensitivity, and robustness to uncertainty; reduction, embedding, (bi–)simulation, and approximation between models; controllability and observability.

Computational elements: *tractable algorithms for studying models on a computer.* Techniques include: numerical simulation algorithms to approximate trajectories and reachable sets; statistical inference methods for parameter estimation and state filtering; optimization tools including dynamic programming and the calculus of variations; schemes for verification and model checking.

Experimental elements: *practical procedures for transforming between models and data.* For instance: system identification and adaptation transform data collected from a physical system to model structure or parameters; control synthesis and machine learning transform models to behaviors on a physical system.

This classification is intended as a conceptual aid rather than a rigid partition. Although analogous to the division into (1) system structures, (2) system dynamics, (3) control methods, (4) design methods in [Kit02b], our definition emphasizes the contributions from disciplines spanning applied mathematics, control theory, optimization, and statistics.

1.2.3 Linear Systems Theory

Linear systems theory is the exemplar of what we seek in sensorimotor control. It arose from the unification of complementary efforts to model, control, and design stationary regulatory processes in the telecommunications, electronics, mechatronics, and aerospace industries [ÅK14]. The culmination of nearly a century of dedicated effort, it is comprised of a unified framework [Kal59] for analysis [Bro70; CD91], computation [Lue69; And+99], and experimentation [SB89; Lju99].

It is important to note that linear systems theory succeeds only within prescribed experimental contexts. Linear lumped–parameter models of electrical circuits or flexible beams must be augmented or replaced with continuum models in the presence of high–frequency or high–amplitude driving signals. Linear state feedback stabilizes physical phenomena only in a neighborhood of the operating point, and topological obstacles can preclude the possibility of global stabilization via linear feedback [May10]. Many fundamental biological and biochemical processes exhibit stable oscillatory behavior precluded by the class of linear dynamical systems [HB71; Td90; Gol96; Win01; Buz06].

The applicability of this theory to such a broad range of stationary regulatory phenomena in mechanics, chemistry, electromagnetics, and biochemistry may be singular. We do not expect other systems–level theories to apply to a similarly diverse collection of physical phenomena. In fact, this broad applicability may be viewed as a consequence of the genericity of linear dynamics (in the dynamical systems sense [Har60; GH83; Abb04]) amongst the ubiquitous class of smooth stationary phenomena. In this view, the breadth of other systems theories may be limited largely by the generality of their underlying class of models. Nevertheless, linear systems theory provides a conceptual template for the framework we seek. In generalizing to sensorimotor control, this example instructs us to focus on dynamic phenomena that proliferate in the wider non–smooth and non–stationary world.

1.2.4 Other Systems Sciences

Although the systems–level approach has been fruitfully applied to formulate biological hypotheses for many years [Ros58; Mes68; Mil73; Rie77], it is presently enjoying a resurgence in interest across biology, bioengineering, and biomedicine. Systems biology focuses on analysis [Alo06] and computational modeling [Kit02a] of intact biochemical reaction networks, cells, tissues, and organisms [Kit02b]. Synthetic biology [And+06; BS05] seeks to repurpose biomolecules and reaction networks to construct systems that achieve new engineering aims. Advancements from both systems and synthetic biology translate to medicine, with hopes of achieving a "systems approach to disease" [Hoo+04; PW09]. Despite tremendous progress and intensive interest, "many breakthroughs in experimental devices, advanced software, and analytical methods are required before the achievements of systems biology can live up to their much–touted potential" [Kit02b]. Nevertheless, this rapidly–growing area provides another instructive example for the development of a systems–level theory that merges complementary efforts in science, engineering, and medicine.

1.3 Dynamical Systems Theory for Locomotion

Realizing a systems–level theory for sensorimotor control is a broad agenda that will require contributions from a multi–disciplinary team of investigators over many years. As an example, the systematic development of linear systems theory began in earnest with frequency–domain methods developed by telephony researchers [Nyq32; Bod40] matured decades later after combining contributions from numerous disciplines. In the space of a single dissertation, we can only aspire to contribute rudiments of the unified framework we seek, and even then must restrict the class of physical phenomena under consideration. Thus in this thesis we attend to derivation of a *hybrid dynamical systems theory* for *legged locomotion*. We devote the remainder of this chapter to motivating and outlining our contributions.

1.3.1 Focus on Legged Locomotion

Mobility is critical for autonomy. Though artificial environments are increasingly navigable via wheels and tracks, the existence of stairs, curbs, and other obstacles imply locomotion will inevitably involve intermittent contact with the substrate. Consequently, legged locomotion ought to be a primary focus of the systems–level approach to sensorimotor control.

Dynamic legged locomotion is characterized by intermittent interaction between limbs and terrain. We coarsely divide limb motion into four epochs (*swing*, *touchdown*, *stance*, *liftoff*) as follows: limbs reciprocate freely (*swing*) above the ground, initiate contact with the terrain (*touchdown*) and rapidly develop reaction force, leverage sustained contact with the substrate (*stance*) to propel the body forward, and detach (*liftoff*) to terminate the interaction with the ground. Although the fundamental physical laws governing each epoch are continuous, the *touchdown* and *liftoff* transitions typically comprise a small fraction of the gait cycle. Thus a parsimonious approach to modeling locomotion compresses these transitions into an instantaneous period of time. This results in a *hybrid* dynamical system whose state evolution is governed by continuous–time *flow* punctuated by discrete–time *reset*.

1.3.2 Hybrid Dynamical Systems Theory Foundations

Each element of the unified framework we seek rests upon a shared modeling foundation. As linear systems theory demonstrates, the success of a systems–level approach need not depend on faithfulness to the underlying physics. Therefore we seek a modeling paradigm that is phenomenological, i.e. one whose predictions agree well with empirical observations of robot and animal locomotion, but whose consistency with contemporary reductionist theory is not enforced. The parsimonious class of models proposed in the previous section—*hybrid* dynamical systems—could fill this role. However, general hybrid systems exhibit behaviors such as nondeterminism and orbital instability that are inconsistent with our observations of the physical world. Therefore we derive foundations of a hybrid dynamical systems theory for legged locomotion by focusing on the simplest pattern of locomotion: the periodic gait.

1.3.3 Our Contributions

Overview Beginning with a general class of *hybrid control systems*, in Chapter 2 we derive a state space metric and a provably–convergent numerical simulation algorithm. Specializing to *hybrid dynamical systems* in Chapter 3, we demonstrate that models for periodic gaits undergoing isolated transitions generically reduce to classical continuous–time dynamical systems. Focusing further on discontinuous vector field dynamics in an individual hybrid domain, we provide conditions in Chapter 4 that ensure the flow is continuous and piecewise–differentiable near general periodic gaits.

Chapter 2 The study of hybrid control systems requires practical tools for approximation and comparison of system executions. Existing approaches to these problems impose restrictions on the system's continuous and discrete dynamics that are not satisfied for models of legged locomotion. To compare system states in distinct hybrid modes, we derive an intrinsic state–space metric. This enables construction of the first trajectory–space metric with respect to which the closed orbits that model periodic gaits are orbitally stable. This metric is applied to develop a numerical simulation algorithm that converges uniformly to any orbitally stable execution. Incidentally, the algorithm's convergence is guaranteed up to and including *Zeno* events, i.e. points where an execution's transition times accumulate.

Chapter 3 Near an exponentially stable periodic orbit undergoing isolated transitions in a hybrid dynamical system, we prove that executions generically contract superexponentially to a constant–dimensional subsystem. Under a non–degeneracy condition on the rank deficiency of the associated Poincaré map, the contraction occurs in finite time regardless of the stability properties of the orbit. Hybrid transitions may be removed from the resulting subsystem via a topological quotient that admits a smooth structure to yield an equivalent smooth dynamical system. We demonstrate reduction of a high–dimensional underactuated mechanical model for terrestrial locomotion, assess structural stability of deadbeat controllers for rhythmic locomotion and manipulation, and derive a normal form for the stability basin of a hybrid oscillator.

Chapter 4 Legged animals with four, six, and more legs exhibit gaits with near–simultaneous touchdown of two or more limbs. The overlapping transition surfaces inherent in hybrid models of such gaits introduce non–determinism or orbital instability in general hybrid systems. Under a non–degeneracy condition ensuring trajectories pass transversally through transitions, we show that such models possess a well–defined flow that is Lipschitz continuous and piecewise–differentiable. The definition of piecewise–differentiability we use implies that although the flow is not classically differentiable, nevertheless it admits a first–order approximation. We exploit this first–order approximation to infer existence of piecewise–differentiable Poincaré maps, study structural stability of the flow, and derive techniques for assessing stability, optimality, and controllability of periodic gaits.

Chapter 2

Metrization and Simulation of Hybrid Control Systems

For continuous–state dynamical systems and finite–state automata there separately exist rich sets of tools for metrization and simulation. The interaction of discrete transitions with continuous dynamics that is characteristic of hybrid control systems requires a new approach. To address this limitation, in this chapter we construct a distance metric over the state space of a hybrid control system and apply this metric to develop a provably–convergent numerical simulation algorithm. Our framework imposes mild restrictions, enabling formal investigation of a wide range of systems: the dynamics may be nonlinear, the continuous dynamics may be controlled, and multiple discrete transitions may occur simultaneously, so long as executions are orbitally stable.

Efforts to topologize and subsequently metrize hybrid control systems have been significant but fragmented. Nerode and Kohn [NK93] consider state–space topologies induced by the finite–state automaton associated with the hybrid system. We propose a metric topology over the state space of hybrid control systems, effectively metrizing the *hybrifold* proposed by Simic *et al.* [Sim+05], as well as the *colimit* topology constructed by Ames and Sastry [AS05] over the *regularization* proposed by Johansson *et al.* [Joh+99]. In contrast, Tavernini [Tav87] directly metrized the space of executions of hybrid systems, and Gokhman [Gok08] later demonstrated the equivalence of the resulting topology with that generated by the Skorohod trajectory metric (see Chapter 6 in [Pol84]). We highlight the technical and practical limitations imposed by metrizing the trajectory space rather than state space in Section 2.4.4.

The notion of *regularization* or *relaxation* of a hybrid system should not be confused with the "relaxation" of hybrid inclusions described by Cai *et al.* [Cai+08]. Since interpreting our hybrid control systems as hybrid inclusions yields singleton–valued "flow" and "jump" maps, relaxation in this sense does not yield a distinct hybrid system. Sanfelice and Teel [ST10] subsequently prove existence of approximating executions for a given "simulation" of a hybrid inclusion. In this chapter we consider the opposite problem of proving convergence of approximating simulations for a given execution of a hybrid control system.

The literature on numerical simulation of deterministic hybrid systems may be broadly partitioned into two groups: practical algorithm development focused on obtaining high–precision estimates of discrete event times, and theoretical proofs of convergence for simulations of certain classes of hybrid systems. Practical algorithms aim to place time–steps close to discrete event times using root–finding [Car78; Sha+91; GN92]. Theoretical proofs of convergence have generally required restrictive assumptions. Esposito *et al.* [Esp+01], for instance, apply feedback linearization to asymptotically guarantee event detection for semi–algebraic guards, while Paoli and Schatzman [PS03] develop a provably–convergent simulation algorithm for second–order mechanical states undergoing impact specified by a unilateral constraint. The most general convergence results relax the requirement that discrete transition times be determined accurately [Tav87; Tav09; Bur+11b], and consequently can accommodate arbitrary nonlinear transition surfaces, Lipschitz continuous vector fields, and continuous discrete transition maps. We extend this approach using our proposed metric topology to prove convergence of simulations to executions of hybrid control systems that satisfy an *orbital stability* property described in Section 2.3. Our simulation algorithm may be applied to hybrid systems possessing control inputs and overlapping guards, representing a substantial contribution beyond our previous efforts [Bur+11b] and those of others [Tav87; Tav09].

The remainder of this chapter is organized as follows. Section 2.1 contains definitions of the topological, metric, and dynamical system concepts used throughout. We present our technique for metrization and relaxation of hybrid control systems in Section 2.2 and apply these constructions to define a metric for comparing trajectories in hybrid control systems. We then develop our algorithm for numerical simulation of hybrid control system executions in Section 2.3, where we apply our trajectory metric to prove uniform convergence of simulations to orbitally stable executions. The technique is illustrated in Section 2.4 using examples for accuracy, verification, and novel hybrid control system behavior.

2.1 Preliminaries

2.1.1 Topology [Kel75]

The 2–norm is our finite–dimensional norm of choice unless otherwise specified. Given P, the set of all finite partitions of $\mathbb{R}$, and $n \in \mathbb{N}$, we define the *total variation* of $f \in L^\infty(\mathbb{R}, \mathbb{R}^n)$ by:

$$\mathrm{V}(f) = \sup\left\{ \sum_{j=0}^{m-1} \|f(t_{j+1}) - f(t_j)\|_1 \mid \{t_k\}_{k=0}^{m} \in P,\ m \in \mathbb{N} \right\}, \tag{2.1.1}$$

where $L^\infty(\mathbb{R}, \mathbb{R}^n)$ is the set of all almost everywhere bounded functions from $\mathbb{R}$ to $\mathbb{R}^n$. The total variation of f is a semi–norm, i.e. it satisfies the Triangle Inequality, but does not separate points. f is of *bounded variation* if $\mathrm{V}(f) < \infty$, and we define $BV(\mathbb{R}, \mathbb{R}^n)$ to be the set of all functions of bounded variation from $\mathbb{R}$ to $\mathbb{R}^n$.

Given $n \in \mathbb{N}$ and $D \subset \mathbb{R}^n$, ∂D is the boundary of D, and $\text{int}(D)$ is the interior of D. Recall that given a collection of sets $\{S_\alpha\}_{\alpha\in\mathcal{A}}$, where $\mathcal{A}$ might be uncountable, the *disjoint union* of this collection is $\coprod_{\alpha\in\mathcal{A}} S_\alpha = \bigcup_{\alpha\in\mathcal{A}} S_\alpha \times \{\alpha\}$, a set that is endowed with the piecewise–defined topology. Throughout this chapter we will abuse notation and say that given $\bar{\alpha} \in \mathcal{A}$ and $x \in S_{\bar{\alpha}}$, then $x \in \coprod_{\alpha\in\mathcal{A}} S_\alpha$, even though we should write $\iota_{\bar{\alpha}}(x) \in \coprod_{\alpha\in\mathcal{A}} S_\alpha$, where $\iota_{\bar{\alpha}} \colon S_{\bar{\alpha}} \to \coprod_{\alpha\in\mathcal{A}} S_\alpha$ is the *canonical identification* $\iota_{\bar{\alpha}}(x) = (x, \bar{\alpha})$.

In this chapter we make extensive use of the concept of a *quotient topology* induced by an equivalence relation defined on a topological space. We regard a detailed exposition of this important concept as outside the scope of this document, and refer the reader to Chapter 3 in [Kel75] or Section 22 in [Mun00] for more details. The next definition formalizes equivalence relations in topological spaces induced by functions. If $f \colon A \to B$, $V \subset A$, and $V' \subset B$, then we let $f(V) = \{f(a) \in B \mid a \in V\}$ denote the image of V under f, and $f^{-1}(V') = \{a \in A \mid f(a) \in V'\}$ denote the pre–image of V under f.

Definition 2.1.1. *Let $\mathcal{S}$ be a topological space, $A, B \subset \mathcal{S}$ two subsets, and $f \colon A \to B$ a function. We define an* f–induced equivalence relation $\Lambda_f \subset \mathcal{S} \times \mathcal{S}$ *as the transitive closure of the following relation:*

$$\big\{(a,b) \in \mathcal{S} \times \mathcal{S} \mid a \in f^{-1}(b), \text{ or } b \in f^{-1}(a), \text{ or } a = b\big\}. \tag{2.1.2}$$

$a, b \in \mathcal{S}$ are f–related, *denoted by $a \overset{f}{\sim} b$, if $(a,b) \in \Lambda_f$. Moreover, the* equivalence class of *$x \in \mathcal{S}$ is defined as $[x]_f = \Big\{a \in \mathcal{S} \mid a \overset{f}{\sim} x\Big\}$, and the set of equivalence classes is defined as $\frac{\mathcal{S}}{\Lambda_f} = \Big\{[x]_f \mid x \in \mathcal{S}\Big\}$. We endow the* quotient $\frac{\mathcal{S}}{\Lambda_f}$ *with the quotient topology.*

Note that Λ_f is an equivalence relation. An important application of the function–induced quotient is the construction of a single topological space out of several disconnected sets. Indeed, given a collection of sets $\{S_\alpha\}_{\alpha\in\mathcal{A}}$, where $\mathcal{A}$ is some index set, and a function $f \colon U \to \coprod_{\alpha\in\mathcal{A}} S_\alpha$, where $U \subset \coprod_{\alpha\in\mathcal{A}} S_\alpha$, then $\widehat{S} = \frac{\coprod_{\alpha\in\mathcal{A}} S_\alpha}{\Lambda_f}$ is a topological space.

Next, we present a useful concept from graph theory that simplifies our ensuing analysis.

Definition 2.1.2. *Let $(\mathcal{J}, \Gamma)$ be a directed graph, where $\mathcal{J}$ is the set of vertices and $\Gamma \subset \mathcal{J} \times \mathcal{J}$ is the set of edges. Then, given $j \in \mathcal{J}$, define the* neighborhood of j, *denoted $\mathcal{N}_j$, by:*

$$\mathcal{N}_j = \{e \in \Gamma \mid \exists j' \in \mathcal{J} \text{ s.t. } e = (j, j')\}. \tag{2.1.3}$$

2.1.2 Length Metrics [Bur+01]

Every metric space has an induced length metric, defined by measuring the length of the shortest curve between two points. Throughout this chapter, we use induced length metrics to metrize the function–induced quotients of disjoint unions of sets. To formalize this approach, we begin by defining the length of a curve in a metric space; the following definition is equivalent to Definition 2.3.1 in [Bur+01].

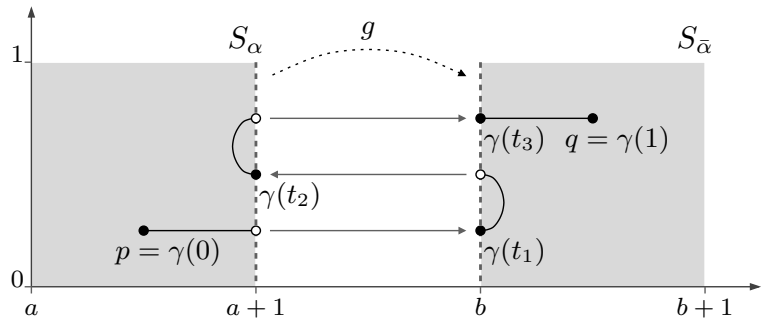

Figure 2.1: A g–connected curve γ with partition $\{t_i\}_{i=0}^4$, where $S_\alpha = [a, a+1] \times [0,1]$, $S_{\bar{\alpha}} = [b, b+1] \times [0,1]$, and $g\colon \{a+1\} \times [0,1] \to \{b\} \times [0,1]$ is defined by $g(a+1, x) = g(b, x)$.

Definition 2.1.3. *Let (S, d) be a metric space, $I \subset [0,1]$ be an interval, and $\gamma\colon I \to \mathcal{S}$ be a continuous function. Define the* length of γ under the metric d *by:*

$$L_d(\gamma) = \sup\left\{ \sum_{i=0}^{k-1} d\big(\gamma(\bar{t}_i), \gamma(\bar{t}_{i+1})\big) \mid k \in \mathbb{N},\ \{\bar{t}_i\}_{i=0}^k \subset I,\ \bar{t}_0 < \bar{t}_1 < \ldots < \bar{t}_k \right\}. \tag{2.1.4}$$

We now define a generalization of continuous curves for quotiented disjoint unions.

Definition 2.1.4. *Let $\{S_\alpha\}_{\alpha \in \mathcal{A}}$ be a collection of sets and $f\colon U \to \coprod_{\alpha \in \mathcal{A}} S_\alpha$, where $U \subset \coprod_{\alpha \in \mathcal{A}} S_\alpha$. $\gamma\colon [0,1] \to \coprod_{\alpha \in \mathcal{A}} S_\alpha$ is* f–connected *if there exists $k \in \mathbb{N}$ and $\{t_i\}_{i=0}^k \subset [0,1]$ with $0 = t_0 \leq t_1 \leq \ldots \leq t_k = 1$ such that $\gamma|_{[t_i, t_{i+1})}$ is continuous for each $i \in \{0, 1, \ldots, k-2\}$, $\gamma|_{[t_{k-1}, t_k]}$ is continuous, and $\lim_{t \uparrow t_i} \gamma(t) \overset{f}{\sim} \gamma(t_i)$ for each $i \in \{0, 1, \ldots, k-1\}$. Moreover, in that case $\{t_i\}_{i=0}^k$ is called a* partition of γ.

Note that, since each section $\gamma|_{[t_i, t_{i+1})}$ is continuous, it must necessarily belong to a single set S_α for some $\alpha \in \mathcal{A}$ because the disjoint union is endowed with the piecewise–defined topology. In the case when $\mathcal{A} = \{\alpha\}$ is a singleton, then every id_{S_α}–connected curve is simply a continuous curve over S_α, where id_{S_α} denotes the identity function in S_α. Figure 2.1 shows an example of a connected curve over a collection of two sets.

Using the concept of connected curves, we now define the induced length distance of a collection of metric spaces. The induced length distance is a generalization of the induced metric defined in Chapter 2 in [Bur+01].

Definition 2.1.5. *Let $\{(S_\alpha, d_\alpha)\}_{\alpha \in \mathcal{A}}$ be a collection of metric spaces, and let $\{X_\alpha\}_{\alpha \in \mathcal{A}}$ be a collection of sets such that $X_\alpha \subset S_\alpha$ for each $\alpha \in \mathcal{A}$. Furthermore, let $f\colon U \to \coprod_{\alpha \in \mathcal{A}} X_\alpha$, where $U \subset \coprod_{\alpha \in \mathcal{A}} X_\alpha$, and let $\widehat{X} = \frac{\coprod_{\alpha \in \mathcal{A}} X_\alpha}{\Lambda_f}$. $d_{i,\widehat{X}}\colon \widehat{X} \times \widehat{X} \to [0, \infty]$ is the* f–induced length

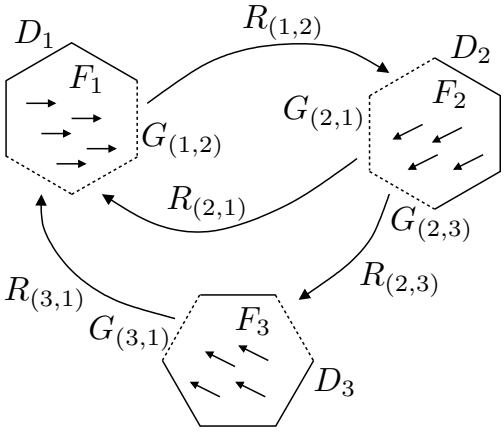

Figure 2.2: Illustration of a hybrid control system with three modes.

distance of $\widehat{X}$, *defined by:*

$$d_{i,\widehat{X}}(p,q) = \inf\Bigg\{ \sum_{i=0}^{k-1} L_{d_{\alpha_i}}\big(\gamma|_{[t_i,t_{i+1})}\big) \mid \gamma\colon [0,1] \to \coprod_{\alpha\in\mathcal{A}} X_\alpha,\ \gamma(0)=p,\ \gamma(1)=q, \\ \gamma \text{ is } f\text{–connected},\ \{t_i\}_{i=0}^{k} \text{is a partition of } \gamma, \\ \{\alpha_i\}_{i=0}^{k-1} \text{ s.t. } \gamma\big([t_i,t_{i+1})\big) \subset X_{\alpha_i}\ \forall i \Bigg\}. \tag{2.1.5}$$

We invoke this definition to metrize both subsets and disjoint unions of metric spaces. It is important to note that although $d_{i,\widehat{X}}$ is non–negative, symmetric, and subadditive, it does not necessarily separate points of $\widehat{X}$ (see Section 2.3 in [Bur+01]), and hence generally only defines a *pseudo*–metric. In the special case where no function f is supplied, then by convention we let $f = \mathrm{id}_X$, the identity function on X. This implies $\widehat{X} = X$ and the induced metric coincides with the given metric. The following Lemma is a straightforward consequence of Proposition 2.3.12 in [Bur+01].

Lemma 2.1.1. *Let (S,d) be a metric space and $X \subset S$. Then $d_{i,X}$ is a metric. Moreover, the topology on X induced by $d_{i,X}$ is equivalent to the topology on X induced by d.*

2.1.3 Hybrid Control Systems

Motivated by the definition of hybrid systems presented in [Sim+05], we define the class of hybrid systems of interest in this chapter.

Definition 2.1.6. *A* hybrid control system *is a tuple $\mathcal{H} = (\mathcal{J}, \Gamma, \mathcal{D}, U, \mathcal{F}, \mathcal{G}, \mathcal{R})$, where:*

- *$\mathcal{J}$ is a finite set indexing the discrete states of $\mathcal{H}$;*

- $\Gamma \subset \mathcal{J} \times \mathcal{J}$ *is the set of edges, forming a directed graph structure over* $\mathcal{J}$*;*
- $\mathcal{D} = \{D_j\}_{j\in\mathcal{J}}$ *is the set of domains, where each* D_j *is a subset of* $\mathbb{R}^{n_j}$*,* $n_j \in \mathbb{N}$*;*
- $U \subset \mathbb{R}^m$ *is the range space of control inputs,* $m \in \mathbb{N}$*;*
- $\mathcal{F} = \{F_j\}_{j\in\mathcal{J}}$ *is the set of vector fields, where each* $F_j \colon \mathbb{R} \times D_j \times U \to \mathbb{R}^{n_j}$ *is a vector field defined on* D_j*;*
- $\mathcal{G} = \{G_e\}_{e\in\Gamma}$ *is the set of guards, where each* $G_{(j,j')} \subset \partial D_j$ *is a guard in mode* $j \in \mathcal{J}$ *that defines a transition to mode* $j' \in \mathcal{J}$*; and,*
- $\mathcal{R} = \{R_e\}_{e\in\Gamma}$ *is the set of reset maps, where each* $R_{(j,j')} \colon G_{(j,j')} \to D_{j'}$ *defines the transition from guard* $G_{(j,j')}$*.*

For convenience, we sometimes refer to hybrid control systems as just hybrid systems, and we refer to the distinct vertices within the graph structure associated with a hybrid control system as modes. Each domain in the definition of a hybrid control system is a metric space with the Euclidean distance metric. A three–mode autonomous hybrid system, which is a particular case of Definition 2.1.6 where none the vector fields $\{F_j\}_{j\in\mathcal{J}}$ depend on the control input, is illustrated in Figure 2.2. Note that we restrict control inputs to the continuous flow, hence inputs do not have an effect during discrete transitions.

Next, we impose several technical assumptions that support existence and uniqueness of trajectories on hybrid domains.

Assumption 2.1.1. *Let* $\mathcal{H}$ *be a hybrid control system. Then the following statements are true:*

(1) *For each* $j \in \mathcal{J}$*,* D_j *is a compact* n_j*–dimensional manifold with boundary.*

(2) U *is compact.*

(3) *For each* $e \in \Gamma$*,* G_e *is a closed, embedded, codimension* 1*, submanifold with boundary.*

(4) *For each* $e \in \Gamma$*,* R_e *is continuous.*

Assumption 2.1.2. *For each* $j \in \mathcal{J}$*,* F_j *is Lipschitz continuous. That is, there exists* $L > 0$ *such that for each* $j \in \mathcal{J}$*,* $t_1, t_2 \in \mathbb{R}$*,* $x_1, x_2 \in D_j$*, and* $u_1, u_2 \in U$*:*

$$\big\|F_j(t_1, x_1, u_1) - F_j(t_2, x_2, u_2)\big\| \leq L\big(|t_1 - t_2| + \|x_1 - x_2\| + \|u_1 - u_2\|\big). \tag{2.1.6}$$

Assumption 2.1.2 guarantees the existence and uniqueness for ordinary differential equations in individual domains. In the sequel we will consider control inputs of *bounded variation* $u \in BV(\mathbb{R}, U)$. Note that without loss of generality we take 0 as the initial time in the following Lemma; a general initial time can be accommodated by a straightforward change of variables.

Lemma 2.1.2. *Let $\mathcal{H}$ be a hybrid control system. Then for each $j \in \mathcal{J}$, each initial condition $p \in D_j$, and each control $u \in BV(\mathbb{R}, U)$, there exists an interval $I \subset \mathbb{R}$ with $0 \in I$ such that the following differential equation has a unique solution:*

$$\dot{x}(t) = F_j\big(t, x(t), u(t)\big), \quad t \in I, \quad x(0) = p. \tag{2.1.7}$$

x is called the integral curve *of F_j with initial condition p and control u. Moreover, $x|_I$ is absolutely continuous.*

Proof. Let $\widetilde{F}_j \colon \mathbb{R} \times \mathbb{R}^{n_j} \times U \to \mathbb{R}^{n_j}$ be any globally Lipschitz continuous extension to F_j (guaranteed to exist by Theorem 1 in [McS34]). Given any $p \in D_j \subset \mathbb{R}^{n_j}$ and $u \in BV(\mathbb{R}, U)$, Proposition 5.6.5 in [Pol97] guarantees the existence of an integral curve $\widetilde{x} \colon \widetilde{I} \to \mathbb{R}^{n_j}$ for $\widetilde{F}_j$ with initial condition $x(0) = p$. Note that $\widetilde{x}$ is absolutely continuous by Theorem 3.35 in [Fol99]. Let $I \subset \widetilde{I}$ be the connected component of $\widetilde{x}^{-1}(D_j)$ containing 0. Then $x = \widetilde{x}|_I$ is an absolutely continuous integral curve of F_j and $x(I) \subset D_j$. Note that x is unaffected by the choice of extension $\widetilde{F}_j$. □

The following definition is used to construct executions of a hybrid control system.

Definition 2.1.7. *Let $\mathcal{H}$ be a hybrid control system, $j \in \mathcal{J}$, $p \in D_j$, and $u \in BV(\mathbb{R}, U)$. $x \colon I \to D_j$ is the* maximal integral curve *of F_j with initial condition p and control u if, given any other integral curve with initial condition p and control u, such as $\tilde{x} \colon \widetilde{I} \to D_j$, then $\widetilde{I} \subset I$.*

Given a maximal integral curve $x \colon I \to D_j$, a direct consequence[1] of Definition 2.1.7 and Assumption 2.1.1 is that either $\sup I = +\infty$, or $\sup I = t' < \infty$ and $x(t') \in \partial D_j$. This fact is critical during the definition of executions of a hybrid control systems in Section 2.3.

2.2 Metrization and Relaxation

In this section, we metrize a unified family of spaces containing all the domains of a hybrid control system $\mathcal{H}$. The constructed metric space has three appealing properties:

(1) the distance between a point in a guard and its image via its respective reset map is zero;

(2) the distance between points in different domains are properly defined and finite; and,

(3) the distance between points is based on the Euclidean distance metric from each domain.

[1] This follows from continuity of integral curves and compactness of hybrid domains.

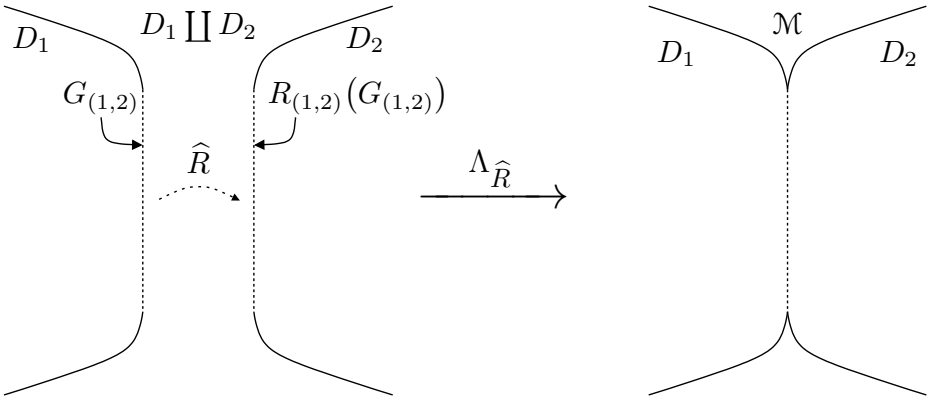

Figure 2.3: (left) Disjoint union of D_1 and D_2. (right) Hybrid quotient space $\mathcal{M}$ obtained from the relation $\Lambda_{\widehat{R}}$.

2.2.1 Hybrid Quotient Space

Using Definitions 2.1.5 and 2.1.6, we construct a metric space where the executions of a hybrid control system reside. The result is a metrization of the *hybrifold* [Sim+05].

Definition 2.2.1. *Let $\mathcal{H}$ be a hybrid control system, and let*

$$\widehat{R}\colon \coprod_{e\in\Gamma} G_e \to \coprod_{j\in\mathcal{J}} D_j \tag{2.2.1}$$

be defined by $\widehat{R}(p) = R_e(p)$ for each $p \in G_e$. Then the hybrid quotient space *of $\mathcal{H}$ is:*

$$\mathcal{M} = \frac{\coprod_{j\in\mathcal{J}} D_j}{\Lambda_{\widehat{R}}}. \tag{2.2.2}$$

Figure 2.3 illustrates the details about the construction described in Definition 2.2.1.

The induced length distance on $\mathcal{M}$ is in fact a distance metric:

Theorem 2.2.1. *Let $\mathcal{H}$ be a hybrid control system, and let $d_{i,\mathcal{M}}$ be the $\widehat{R}$–induced length distance of $\mathcal{M}$, where $\widehat{R}$ is defined in (2.2.1). Then $d_{i,\mathcal{M}}$ is a metric on $\mathcal{M}$, and the topology it induces is equivalent to the $\widehat{R}$–induced quotient topology.*

Proof. We provide the main arguments of the proof, omitting the details in the interest of brevity. First, note that each domain is a normal space, i.e. every pair of disjoint closed sets have disjoint neighborhoods. Second, note that each reset map is a closed map, i.e. the image of closed sets under the reset map are closed. This fact follows by Condition 3 in Assumption 2.1.1, since each guard is compact, thus reset maps are closed by the Closed Map Lemma (Lemma A.52 in [Lee12]).

Let $\widehat{D} = \coprod_{j\in\mathcal{J}} D_j$ and $p, q \in \widehat{D}$. We aim to show that if p and q yield distinct equivalence classes (i.e. $(p, q) \notin \Lambda_{\widehat{R}}$) then the induced distance between them is strictly positive. Note

that the equivalence classes $[p]_{\widehat{R}}$ and $[q]_{\widehat{R}}$ are each a finite collection of closed sets. Moreover, since we can construct disjoint neighborhoods around each of these closed sets, then we can conclude that there exists $\delta > 0$ such that $d_{i,\mathcal{M}}\big([p]_{\widehat{R}}, [q]_{\widehat{R}}\big) > \delta$. The proof concludes by following the argument in Exercise 3.1.14 in [Bur+01], i.e. since each connected component in $\widehat{D}$ is bounded, then $\mathcal{M}$ is also bounded (in the quotient topology). Then, using a simple extension of Theorem 5.8 in [Kel75][2], we get that the identity map from $\mathcal{M}$ to the space constructed by taking the quotient of all the points in $\widehat{D}$ such that $d_{i,\mathcal{M}}$ has zero distance is a homeomorphism, thus they have the same topology. □

It is crucial to note that all $\widehat{R}$–connected curves are continuous in the topology induced by the metric $d_{i,\mathcal{M}}$ on the hybrid quotient space $\mathcal{M}$. This implies in particular that executions of hybrid control systems (to be defined in Section 2.3) are continuous in $\mathcal{M}$ since the endpoint of the segment of an execution that lies in a guard G_e will be $\widehat{R}$–related to the start point of the subsequent segment of the execution; alternately, this follows from Theorem 3.12(b) in [Sim+05] since $\mathcal{M}$ is equivalent to the "hybrifold" construction in that paper. This important property is foundational to the convergence results for sequences of (relaxed) executions and their simulations derived in Section 2.3. For further details, we refer the interested reader to Examples 3.2 and 3.3 in [Sim+05] where continuity is clearly discussed for simple examples.

2.2.2 Relaxation of a Hybrid Control System

To construct a numerical simulation scheme which does not require the exact computation of the time instant when an execution intersects a guard, we require a method capable of introducing some slackness within the computation. This is accomplished by relaxing each domain along its guard and then relaxing each vector field and reset map accordingly in order to define a relaxation of a hybrid control system.

To formalize this approach, we begin by defining the relaxation of each domain of a hybrid control system, which is accomplished by first attaching an ε–sized strip to each guard.

Definition 2.2.2. *Let $\mathcal{H}$ be a hybrid control system. For each $e \in \Gamma$, let $S_e^\varepsilon = G_e \times [0, \varepsilon]$ be the* strip associated to guard G_e. *For each $j \in \mathcal{J}$, let*

$$\chi_j \colon \coprod_{e \in \mathcal{N}_j} G_e \to \coprod_{e \in \mathcal{N}_j} S_e^\varepsilon, \tag{2.2.3}$$

be the canonical identification *of each point in a guard with its corresponding strip defined for each $p \in G_e$ as $\chi_j(p) = (p, 0) \in S_e^\varepsilon$. Then, the* relaxation of D_j *is defined by:*

$$D_j^\varepsilon = \frac{D_j \coprod \Big(\coprod_{e \in \mathcal{N}_j} S_e^\varepsilon\Big)}{\Lambda_{\chi_j}}. \tag{2.2.4}$$

[2]The extension aims to allow the domain of the map to be bounded instead of compact. The new proof follows step–by–step the argument in [Kel75].

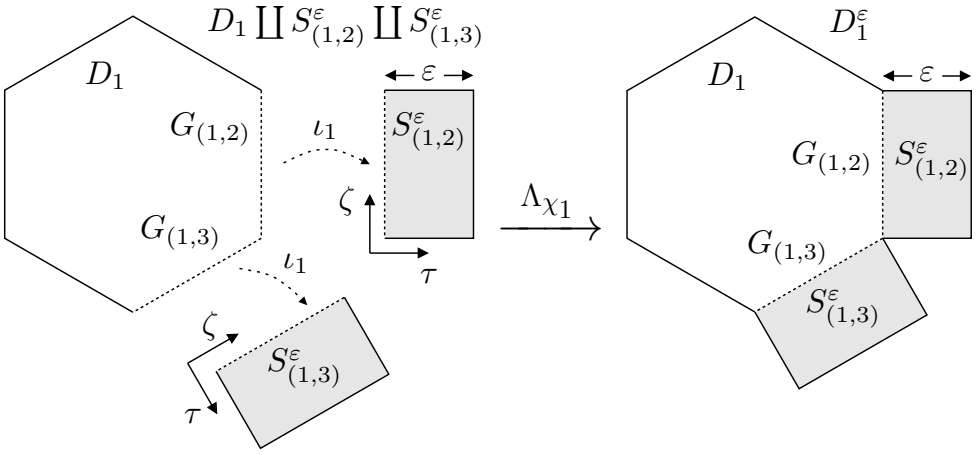

Figure 2.4: Disjoint union of D_1 and the strips in its neighborhood, $\{S^\varepsilon_e\}_{e\in\mathcal{N}_1}$ (left), and the relaxed domain D_1^ε obtained from the relation Λ_{χ_1} (right).

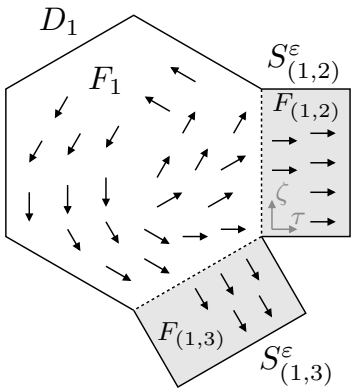

Figure 2.5: Relaxed vector field F_1^ε on relaxed domain D_1^ε.

By Condition 3 in Assumption 2.1.1, each point on a strip S^ε_e of D_j is defined using n_j coordinates $(\zeta_1, \ldots, \zeta_{n_j-1}, \tau)$, shortened (ζ, τ), where τ is called the *transverse coordinate* and is the distance along the interval $[0, \varepsilon]$. An illustration of Definition 2.2.2 together with the coordinates on each strip is shown in Figure 2.4.

We endow each S^ε_e with a distance metric in order to define an induced length metric on a relaxed domain D^ε_j.

Definition 2.2.3. *Let $j \in \mathcal{J}$ and $e \in \mathcal{N}_j$. Endow D_j with d_{i,D_j} as its metric, and $d_{S^\varepsilon_e} \colon S^\varepsilon_e \times S^\varepsilon_e \to [0,\infty)$ as the metric on S^ε_e, defined for each $\zeta, \zeta' \in G_e$ and $\tau, \tau' \in [0, \varepsilon]$ by:*

$$d_{S^\varepsilon_e}\big((\zeta,\tau),(\zeta',\tau')\big) = d_{i,G_e}(\zeta,\zeta') + |\tau - \tau'|. \tag{2.2.5}$$

We now define a length metric on relaxed domains using Definitions 2.1.4 and 2.1.5.

Theorem 2.2.2. *Let $j \in \mathcal{J}$, and let d_{i,D_j^ε} be the χ_j–induced length distance on D_j^ε, where χ_j is as defined in (2.2.3). Then d_{i,D_j^ε} is a metric on D_j^ε, and the topology it induces is equivalent to the χ_j–induced quotient topology.*

Proof. Since d_{i,D_j^ε} is non–negative, symmetric, and subadditive, it remains to show that it separates points. Let $p, q \in D_j^\varepsilon$. First, we want to show that $[p]_{\chi_j} = [q]_{\chi_j}$ whenever $d_{i,D_j^\varepsilon}(p,q) = 0$. Note that for each $e \in \mathcal{N}_j$ and each pair $p, q \in G_e$, and by the Definition 2.1.5 and 2.2.3, $d_{S_e^\varepsilon}((p,0),(q,0)) \geq d_{i,D_j}(p,q)$, hence no connected curve that "jumps" to a strip can be shorter than a curve that stays in D_j. This fact immediately shows that for $p, q \in D_j$, $d_{i,D_j^\varepsilon}(p,q) = 0$ implies that $[p]_{\chi_j} = [q]_{\chi_j}$. The case when one of the points is in $G_e \times (0,\varepsilon] \subset S_e^\varepsilon$ follows easily by noting that those points can be separated by a suitably–sized $d_{S_e^\varepsilon}$–ball. The proof concludes by following the argument in Exercise 3.1.14 in [Bur+01], as we did in the proof of Theorem 2.2.1. □

Refer to d_{i,D_j^ε} as the *relaxed domain metric*. Note that Theorem 2.2.2 can be proved using the same argument as in the proof of Theorem 2.2.1, but we prove Theorem 2.2.2 to emphasize the utility of the inequality relating the induced metric on a domain and the metric on each strip.

Next, we define a vector field over each relaxed domain.

Definition 2.2.4. *Let $j \in \mathcal{J}$. For each $e \in \mathcal{N}_j$, let the vector field on the strip S_e^ε, denoted F_e, be the unit vector pointing outward along the transverse coordinate. In coordinates, $F_e\big(t,(\zeta,\tau),u\big) = \big(\underbrace{0,\ \ldots,\ 0}_{\zeta \text{ coords.}},\ 1\big)^T$. Then, the* relaxation of F_j *is:*

$$F_j^\varepsilon(t,x,u) = \begin{cases} F_j(t,x,u) & \text{if } x \in D_j, \\ F_e(t,x,u) & \text{if } x \in G_e \times (0,\varepsilon] \subset S_e^\varepsilon, \text{ for some } e \in \mathcal{N}_j. \end{cases} \tag{2.2.6}$$

Note that the relaxation of the vector field is generally not continuous along each G_e, for $e \in \mathcal{N}_j$. As we show in Algorithm 2, this discontinuous vector field does not lead to sliding modes on the guards [Utk77; Fil88], since the vector field on the strips always points away from the guard. An illustration of the relaxed vector field F_j^ε on D_j^ε is shown in Figure 2.5.

The definitions of relaxed domains and relaxed vector fields allow us to construct a relaxation of the hybrid control systems as follows:

Definition 2.2.5. *Let $\mathcal{H}$ be a hybrid control system. The* relaxation *of $\mathcal{H}$ is a tuple $\mathcal{H}^\varepsilon = (\mathcal{J}, \Gamma, \mathcal{D}^\varepsilon, U, \mathcal{F}^\varepsilon, \mathcal{G}^\varepsilon, \mathcal{R}^\varepsilon)$, where:*

- *$\mathcal{D}^\varepsilon = \{D_j^\varepsilon\}_{j\in\mathcal{J}}$ is the set of relaxations of the domains in $\mathcal{D}$, and each D_j^ε is endowed with its induced length distance metric d_{i,D_j^ε};*
- *$\mathcal{F}^\varepsilon = \{F_j^\varepsilon\}_{j\in\mathcal{J}}$ is the set of relaxations of the vector fields in $\mathcal{F}$;*

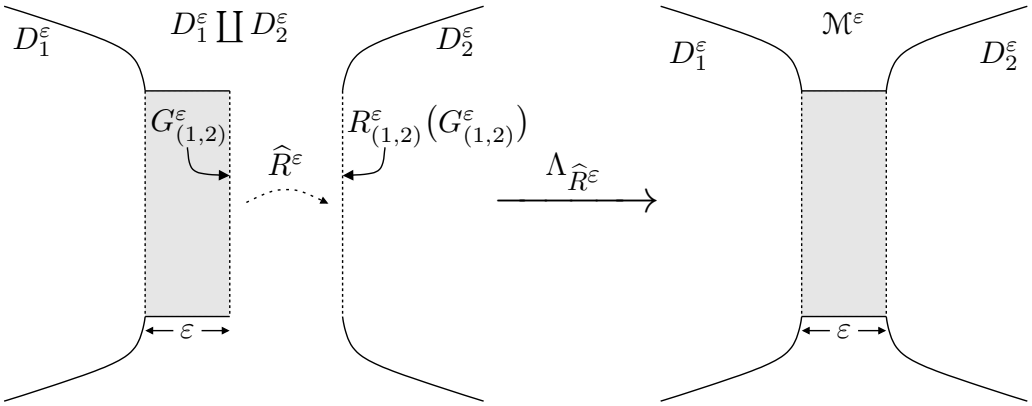

Figure 2.6: (left) Disjoint union of D_1^ε and D_2^ε. (right) Relaxed hybrid quotient space $\mathcal{M}^\varepsilon$ obtained from the relation $\Lambda_{\widehat{R}^\varepsilon}$.

- $\mathcal{G}^\varepsilon = \{G_e^\varepsilon\}_{e\in\Gamma}$ *is the set of relaxations of the guards in* $\mathcal{G}$*, where* $G_e^\varepsilon = G_e \times \{\varepsilon\} \subset S_e^\varepsilon$ *for each* $e \in \Gamma$*; and,*
- $\mathcal{R}^\varepsilon = \{R_e^\varepsilon\}_{e\in\Gamma}$ *is the set of relaxations of the reset maps in* $\mathcal{R}$*, where* $R_e^\varepsilon \colon G_e^\varepsilon \to D_{j'}$ *for each* $e = (j, j') \in \Gamma$ *and* $R_e^\varepsilon(\zeta, \varepsilon) = R_e(\zeta)$ *for each* $\zeta \in G_e^\varepsilon$*.*

2.2.3 Relaxed Hybrid Quotient Space

Analogous to the construction of the metric quotient space $\mathcal{M}$, using Definitions 2.1.5 and 2.2.5 we construct a unified metric space where executions of relaxations of hybrid control systems reside. The result is a metrization of the *hybrid colimit* [AS05] rather than a metrization of the hybrifold as in the previous section.

Definition 2.2.6. *Let* $\mathcal{H}^\varepsilon$ *be the relaxation of the hybrid control system* $\mathcal{H}$*. Also, let*

$$\widehat{R}^\varepsilon \colon \coprod_{e\in\Gamma} G_e^\varepsilon \to \coprod_{j\in\mathcal{J}} D_j^\varepsilon \tag{2.2.7}$$

be defined by $\widehat{R}^\varepsilon(p) = R_e^\varepsilon(p)$ *for each* $p \in G_e^\varepsilon$*. Then the* relaxed hybrid quotient space *of* $\mathcal{H}^\varepsilon$ *is:*

$$\mathcal{M}^\varepsilon = \frac{\coprod_{j\in\mathcal{J}} D_j^\varepsilon}{\Lambda_{\widehat{R}^\varepsilon}}. \tag{2.2.8}$$

The construction in Definition 2.2.6 is illustrated in Figure 2.6.

We now show that the induced length distance on $\mathcal{M}^\varepsilon$ is indeed a metric. We omit this proof since it is identical to the proof of Theorem 2.2.1.

Theorem 2.2.3. *Let* $\mathcal{H}$ *be a hybrid control system, let* $\mathcal{H}^\varepsilon$ *be its relaxation, and let* $d_{i,\mathcal{M}^\varepsilon}$ *be the* $\widehat{R}^\varepsilon$*–induced length distance of* $\mathcal{M}^\varepsilon$*, where* $\widehat{R}^\varepsilon$ *is defined in* (2.2.7)*. Then* $d_{i,\mathcal{M}^\varepsilon}$ *is a metric on* $\mathcal{M}^\varepsilon$*, and the topology it induces is equivalent to the* $\widehat{R}^\varepsilon$*–induced quotient topology.*

All $\widehat{R}^\varepsilon$–connected curves are continuous under the metric topology induced by $d_{i,\mathcal{M}^\varepsilon}$ which is important when we study executions of hybrid systems in Section 2.3.

As expected, the metric on $\mathcal{M}^\varepsilon$ converges pointwise to the metric on $\mathcal{M}$.

Theorem 2.2.4. *Let $\mathcal{H}$ be a hybrid control system, and let $\mathcal{H}^\varepsilon$ be its relaxation. Then for all $p, q \in \mathcal{M}$, $d_{i,\mathcal{M}^\varepsilon}(p,q) \to d_{i,\mathcal{M}}(p,q)$ as $\varepsilon \to 0$.*

Proof. Abusing notation, let $L(\gamma)$ denote the length of any connected curve γ, defined as the sum of the lengths of each of its continuous sections under the appropriate metric. First, note that $d_{i,\mathcal{M}}(p,q) \leq d_{i,\mathcal{M}^\varepsilon}(p,q)$. This inequality follows since, as we argued in the proof of Theorem 2.2.2, given an edge $(j,j') \in \Gamma$, $d_{S^\varepsilon_{(j,j')}}((p',0),(q',0)) \geq d_{i,D_j}(p',q')$ for any pair of points $p', q' \in G_{(j,j')}$. Thus, adding the strips $\{S_e\}_{e\in\gamma}$ in $\mathcal{M}^\varepsilon$ only make the length of a connected curve longer.

Now let $\widehat{D} = \coprod_{j\in\mathcal{J}} D_j$ and $\widehat{D}^\varepsilon = \coprod_{j\in\mathcal{J}} D^\varepsilon_j$. Given $\delta > 0$, there exists $\gamma\colon [0,1] \to \widehat{D}$, an $\widehat{R}$–connected curve with partition $\{t_i\}_{i=0}^k$, such that $\gamma(0) = p$, $\gamma(1) = q$, and $d_{i,\mathcal{M}}(p,q) \leq L(\gamma) \leq d_{i,\mathcal{M}}(p,q) + \delta$. Moreover, without loss of generality let $\gamma^\varepsilon\colon [0,1] \to \widehat{D}^\varepsilon$ be an $\widehat{R}^\varepsilon$–connected curve that agrees with γ on $\widehat{D}$, i.e. each section of γ^ε on $\widehat{D}$ is identical, up to time scaling, to a section of γ Thus γ^ε has at most k ε–length extra sections, and $L(\gamma) \leq L(\gamma^\varepsilon) \leq L(\gamma) + k\varepsilon$. Thus, $d_{i,\mathcal{M}^\varepsilon}(p,q) \leq L(\gamma^\varepsilon) \leq d_{i,\mathcal{M}}(p,q) + k\varepsilon + \delta$. The result follows after noting this inequality is valid for all $\delta > 0$, thus $d_{i,\mathcal{M}^\varepsilon}(p,q) \leq d_{i,\mathcal{M}}(p,q)$. □

Note that Theorem 2.2.4 does not imply that the topology of $\mathcal{M}^\varepsilon$ converges to the topology of $\mathcal{M}$. On the contrary, $\mathcal{M}^\varepsilon$ is homotopically equivalent to the graph $(\mathcal{J},\Gamma)$ for each $\varepsilon > 0$ [AS05], whereas the topology of $\mathcal{M}$ may be different [Sim+05].

We conclude this section by introducing metrics between curves on $\mathcal{M}^\varepsilon$.

Definition 2.2.7. *Let $I \subset [0,\infty)$ a bounded interval. Given any two curves $\gamma, \gamma'\colon I \to \mathcal{M}^\varepsilon$, we define:*

$$\rho^\varepsilon_I(\gamma,\gamma') = \sup\{d_{i,\mathcal{M}^\varepsilon}(\gamma(t),\gamma'(t)) \mid t \in I\}. \tag{2.2.9}$$

Our choice of the supremum among point–wise distances in Definition 2.2.7 is inspired by the sup–norm for continuous real–valued functions.

2.3 Numerical Simulation

This section contains our main result: discrete approximations of trajectories of hybrid control systems, constructed using any variable step size numerical integration algorithm, converge uniformly to the actual trajectories. This section is divided into three parts. First, we define a pair of algorithms that construct executions of hybrid control systems and their relaxations, respectively. Next, we develop a discrete approximation scheme for executions of relaxations of hybrid control systems. Finally, we prove that these discrete approximations converge to the executions of the original, non–relaxed, hybrid control system using the metric topologies developed in Section 2.2.

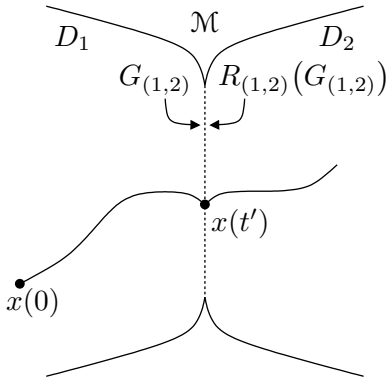

Figure 2.7: Discrete transition of an execution x.

Algorithm 1: execution of hybrid control system $\mathcal{H}$.

Input: $t = 0$, $j \in \mathcal{J}$, $p \in D_j$, and $u \in BV(\mathbb{R}, U)$.

Set $x(0) = p$.
while *True* **do**
  Let $\gamma\colon I \to D_j$ be the maximal integral curve of F_j with control u such that $\gamma(t) = x(t)$.
  Let $t' = \sup I$ and $x(s) = \gamma(s)$ for each $s \in [t, t')$. ▷ *if* $t' < \infty$, *then* $\gamma(t') \in \partial D_j$.
  if $t' = \infty$, ***or*** $\nexists e \in \mathcal{N}_j$ *such that* $\gamma(t') \in G_e$ **then**
    Stop.
  end
  Let $(j, j') \in \mathcal{N}_j$ be such that $\gamma(t') \in G_{(j,j')}$.
  Set $x(t') = R_{(j,j')}\big(\gamma(t')\big)$, $t = t'$, and $j = j'$. ▷ $\gamma(t') \overset{\widehat{R}}{\sim} x(t')$.
end

2.3.1 Execution of a Hybrid System

We begin by defining an *execution* of a hybrid control system. This definition agrees with the traditional intuition about executions of hybrid control systems which describes an execution as evolving as a standard control system until a guard is reached, at which point a discrete transition occurs to a new domain using a reset map. We provide an explicit definition to clarify technical details required in the proofs below. Given a hybrid control system, $\mathcal{H}$, as in Definition 2.1.6, Algorithm 1 defines an execution of $\mathcal{H}$ via construction. A resulting execution, denoted x, is an $\widehat{R}$–connected curve from some interval $I \subset [0, \infty)$ to $\coprod_{j \in \mathcal{J}} D_j$. Thus, abusing notation, we regard x as a continuous curve on $\mathcal{M}$. Abusing notation again, we regard x as a piece–wise continuous curve on $\mathcal{M}^\varepsilon$ for each $\varepsilon > 0$. Figure 2.7 shows an execution undergoing a discrete transition.

Note that executions constructed using Algorithm 1 are not necessarily unique. Indeed, Definition 2.1.7 implies that once a discrete transition has been performed, the execution is

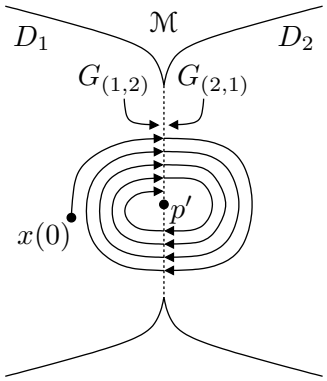

Figure 2.8: Zeno execution x accumulating at p' in a two–mode hybrid system.

unique until a new transition is made; however, the choice in Step 8 is not necessarily unique if the maximal integral curve passes through the intersection of multiple guards. It is not hard to prove that a sufficient condition for uniqueness of executions is that all the guards are disjoint, even though, as we show in Section 2.4.4, uniqueness of the executions can be obtained for some cases where guards do intersect.

With the definition of execution of a hybrid control system, we can define a class of executions unique to hybrid control systems.

Definition 2.3.1. *An execution is* Zeno *when it undergoes an infinite number of discrete transitions in a finite amount of time. Hence, there exists $T > 0$, called the* Zeno Time*, such that the execution is only defined on $I = [0, T)$.*

Zeno executions are hard to simulate since they apparently require an infinite number of reset map evaluations, an impossible task to implement on a digital computer. A consequence of Algorithm 1 is that if $x\colon I \to \mathcal{M}$ is an execution such that $T = \sup I < \infty$, then either

(1) x has a finite number of discrete transitions on $I = [0, T]$, and $x(T) \in \partial D_j$ for some $j \in \mathcal{J}$, or

(2) x is a Zeno execution and $I = [0, T)$.

We now introduce a property of Zeno executions of particular interest:

Definition 2.3.2. *Let $\mathcal{H}$ be a hybrid control system, $p \in \mathcal{M}$, $u \in BV(\mathbb{R}, U)$, and $x\colon [0, T) \to \mathcal{M}$ be a Zeno execution with initial condition p, control u, and Zeno Time T. x* accumulates at $p' \in \mathcal{M}$ *if* $\lim_{t\to T} d_{i,\mathcal{M}}\big(x(t), p'\big) = 0$.

Examples of Zeno executions that do not accumulate can be found in [Zha+01]. Figure 2.8 shows a Zeno execution that accumulates at p'. Note that for p' to be a Zeno accumulation point, it must belong to a guard of a hybrid control system.

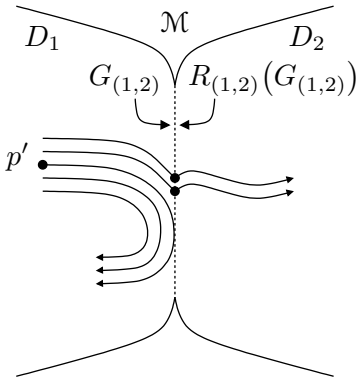

Figure 2.9: Non–orbitally stable execution with respect to the initial condition p'.

Since $\mathcal{M}$ is a metric space, we can introduce the concept of continuity of a hybrid execution with respect to its initial condition and control input in a straightforward way. Employing this definition, we can define the class of executions that are numerically approximable:

Definition 2.3.3. *Let $\mathcal{H}$ be a hybrid control system, and assume that all the executions of $\mathcal{H}$ are unique. Denote by $x_{(p,u)}\colon I_{(p,u)} \to \mathcal{M}$ the hybrid execution of $\mathcal{H}$ with initial condition $p \in \mathcal{M}$ and control $u \in BV(\mathbb{R}, U)$. Given $T > 0$, we say that the map $(p,u) \mapsto x_{(p,u)}$ is* orbitally stable in $[0,T]$ *at $(p',u') \in \mathcal{M} \times BV(\mathbb{R},U)$ if there exists a neighborhood of (p',u'), say $N_{(p',u')} \subset \mathcal{M} \times BV(\mathbb{R},U)$, such that the following conditions are satisfied:*

(1) *$[0,T] \subset I_{(p,u)}$ for each $(p,u) \in N_{(p',u')}$.*

(2) *The map $(p,u) \mapsto x_{(p,u)}(t)$ is continuous at (p',u') for each $t \in [0,T]$.*

As observed in Section III.B in [Lyg+03], executions that are not orbitally stable are difficult to approximate with a general algorithm. Figure 2.9 shows a non–orbitally stable execution that intersects the guard tangentially, and note that executions initialized arbitrarily close to $p' \in D_1$ undergo different sequences of transitions. Unfortunately, there is presently no general test (analytical or numerical) that ensures a given execution is orbitally stable. Theorem III.2 in [Lyg+03] provides one set of sufficient conditions ensuring orbital stability.

2.3.2 Relaxed Execution of a Hybrid System

Next, we define the concept of *relaxed execution* for a relaxation of a hybrid control system. The main idea is that, once a relaxed execution reaches a guard, we continue integrating over the strip with the relaxed vector field, F_e, as in Definition 2.2.4. Given the hybrid control system, $\mathcal{H}$, its relaxation, $\mathcal{H}^\varepsilon$, for some $\varepsilon > 0$, Algorithm 2 defines a relaxed execution of $\mathcal{H}^\varepsilon$ via construction. The resulting relaxed execution, denoted x^ε, is a continuous function defined from an interval $I \subset [0,\infty)$ to $\mathcal{M}^\varepsilon$. Note that this algorithm is only defined for initial conditions belonging to D_j for some $j \in \mathcal{J}$ since the strips are artificial objects that do not

appear in $\mathcal{H}$. The generalization to all initial conditions is straightforward; we omit it to simplify the presentation.

Algorithm 2: relaxed execution of hybrid control system $\mathcal{H}$.

Input: $t = 0$, $j \in \mathcal{J}$, $p \in D_j$, and $u \in BV(\mathbb{R}, U)$.

1 Set $x^\varepsilon(0) = p$.
2 **while** *True* **do**
3 Let $\gamma\colon I \to D_j$, the maximal integral curve of F_j with control u such that $\gamma(t) = x^\varepsilon(t)$.
4 Let $t' = \sup I$ and $x^\varepsilon(s) = \gamma(s)$ for each $s \in [t, t')$. ▷ *if* $t' < \infty$, *then* $\gamma(t') \in \partial D_j$.
5 **if** $t' = \infty$, ***or*** $\nexists e \in \mathcal{N}_j$ *such that* $\gamma(t') \in G_e$ **then**
6 Stop.
7 **end**
8 Let $(j, j') \in \mathcal{N}_j$ such that $\gamma(t') \in G_{(j,j')}$, thus $\big(\gamma(t'), 0\big) \in S^\varepsilon_{(j,j')}$.
9 Set $x^\varepsilon(t'+\tau) = \big(\gamma(t'), \tau\big)$ for each $\tau \in [0, \varepsilon)$.
10 Set $x^\varepsilon(t'+\varepsilon) = R^\varepsilon_{(j,j')}\big(\gamma(t'), \varepsilon\big)$, $t = t'+\varepsilon$, and $j = j'$. ▷ $\big(\gamma(t'), \varepsilon\big) \overset{\widehat{R}^\varepsilon}{\sim} x^\varepsilon(t'+\varepsilon)$.
11 **end**

Step 9 of Algorithm 2 relaxes each instantaneous discrete transition by integrating over the vector field on a strip, hence forming a continuous curve on $\mathcal{M}^\varepsilon$. Also note that our definition for the relaxed execution over each strip S^ε_e, also in Step 9, is exactly equal to the maximal integral curve of F_e. Figure 2.10a shows an example of a relaxed mode transition produced by Algorithm 2. Given a hybrid system $\mathcal{H}$ and its relaxation $\mathcal{H}^\varepsilon$, the relaxed execution of $\mathcal{H}^\varepsilon$ produced by Algorithm 2 is a delayed version of the execution of $\mathcal{H}$ produced by Algorithm 1, since the relaxed version has to expend ε time units during each discrete transition. In that sense, our definition of relaxed execution is equivalent to an execution of a *regularized hybrid systems* [Joh+99].

Note that if a relaxed execution is unique for a given initial condition and input, then the corresponding hybrid execution is also unique, but not vice versa. Indeed, consider the case of a hybrid execution performing a single discrete transition at a point, say p, where two guards intersect, i.e. $p \in G_e$ and $p \in G_{e'}$, such that $R_e(p) = R_{e'}(p)$. In this case the hybrid execution is unique, but its relaxed counterpart either evolves via S_e or $S_{e'}$, hence obtaining 2 different executions. Nevertheless, both relaxed executions reach the same point after evolving over the strip.

Next, we state our first convergence theorem.

Theorem 2.3.1. *Let $\mathcal{H}$ be a hybrid control system and $\mathcal{H}^\varepsilon$ be its relaxation. Let $p \in \mathcal{M}$, $u \in BV(\mathbb{R}, U)$, $x\colon I \to \mathcal{M}^\varepsilon$ be an execution of $\mathcal{H}$ with initial condition p and control u, and let $x^\varepsilon\colon I^\varepsilon \to \mathcal{M}^\varepsilon$ be a corresponding relaxed execution of x. Assume that the following conditions are satisfied:*

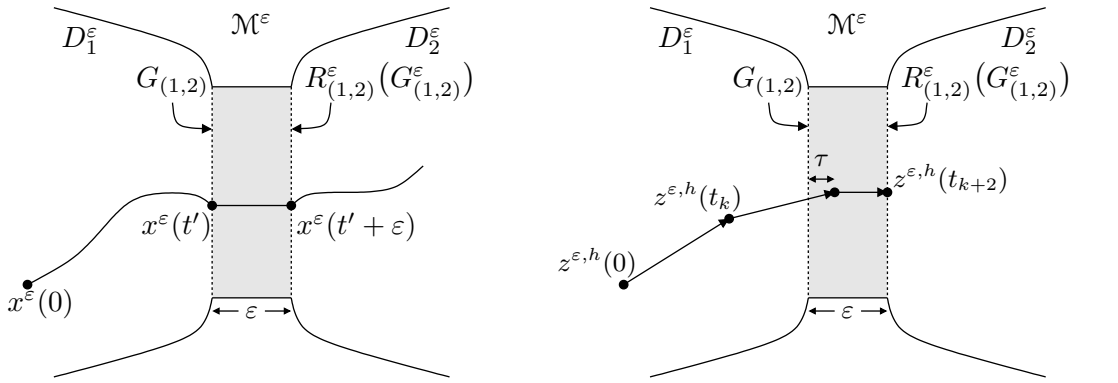

(a) Mode transition of a relaxed execution x^ε in a two–mode relaxed hybrid control system.

(b) Discrete approximation $z^{\varepsilon,h}$ of a relaxed execution in a two-mode hybrid control system.

Figure 2.10: (left) Relaxed execution and (right) its discrete approximation.

(1) *x is orbitally stable with initial condition p and control u;*

(2) *x has a finite number of discrete transitions or is a Zeno execution that accumulates; and*

(3) *there exists $T > 0$ such that for each ε small enough, $[0,T] \subset I \cap I^\varepsilon$ if x has a finite number of discrete transitions, and $[0,T) \subset I \cap I^\varepsilon$ if x is Zeno.*

Then, $\lim_{\varepsilon\to 0} \rho^\varepsilon_{[0,T]}\big(x, x^\varepsilon\big) = 0$.

Proof. We provide the main arguments of the proof, omitting some details in the interest of brevity. First, given $j \in \mathcal{J}$ and $[\tau,\tau') \subset [0,T]$ such that $x(t) \in D_j$ for each $t \in [\tau,\tau')$, then, since $x|_{[\tau,\tau')}$ is absolutely continuous, for each $t, t' \in [\tau,\tau')$,

$$d_{i,\mathcal{M}^\varepsilon}\big(x(t),x(t')\big) \le L_{d_{i,D_j}}\big(x|_{[t,t')}\big) = \int_t^{t'} \big\|F_j\big(s,x(s),u(s)\big)\big\|\,\mathrm{d}s \le K(t'-t), \tag{2.3.1}$$

where $K = \sup\big\{\big\|F_j^\varepsilon\big(t,x,u\big)\big\| \mid j \in \mathcal{J},\ t \in [0,T],\ x \in \mathcal{M}^\varepsilon, u \in U\big\} < \infty$.

Second, let $k \in \mathbb{N}$ and $\{\lambda_i\}_{i=0}^k \subset [0,1]$ be a sequence such that $0 = \lambda_0 \le \lambda_1 \le \ldots \le \lambda_k = 1$. Given $\varepsilon > 0$, let $\gamma_t\colon [0,1] \to \mathcal{M}^\varepsilon$ be defined by $\gamma_t(\lambda) = x^{\lambda\varepsilon}(t)$. Thus, by Theorem 2.2.4 and Algorithm 2, $\gamma_t(0) = x^0(t) = x(t)$ and $\gamma_t(1) = x^\varepsilon(t)$. Assume that $x^\varepsilon(t) \in D_j$ for each $t \in [\tau+\varepsilon, \tau'+\varepsilon)$, where $[\tau,\tau')$ is as defined above. Using Picard's Lemma (Lemma 5.6.3

in [Pol97]), for each $t \in [\tau+\varepsilon, \tau')$,

$$\begin{aligned}\|x^\varepsilon(t+\varepsilon) - x(t)\| &\leq e^{L(t-\tau)}\Bigg(\|x^\varepsilon(\tau+\varepsilon) - x(\tau)\| + \\ &\qquad + \int_\tau^t \big\|F_j\big(s, x(s), u(s)\big) - F_j\big(s+\varepsilon, x(s), u(s+\varepsilon)\big)\big\|\,\mathrm{d}s\Bigg) \\ &\leq e^{L(t-\tau)}\left(\|x^\varepsilon(\tau+\varepsilon) - x(\tau)\| + L\int_\tau^t \varepsilon + \|u(s) - u(s+\varepsilon)\|\,\mathrm{d}s\right) \\ &\leq e^{L(t-\tau)}\big(\|x^\varepsilon(\tau+\varepsilon) - x(\tau)\| + \big(L + \mathrm{V}(u)\big)(t-\tau)\varepsilon\big),\end{aligned} \tag{2.3.2}$$

where we have used a standard property of the functions of bounded variation (Exercise 5.1 in [Zie89]). Thus, if we assume that $\|x^\varepsilon(\tau+\varepsilon) - x(\tau)\| = O(\varepsilon)$, i.e. that there exists $C > 0$ such that $\|x^\varepsilon(\tau+\varepsilon) - x(\tau)\| \leq C\varepsilon$, then $\|x^\varepsilon(t+\varepsilon) - x(t)\| = O(\varepsilon)$ for each $t \in [\tau+\varepsilon, \tau')$. Using the same argument as above $\big\|x^{\lambda_{i+1}\varepsilon}(t+\varepsilon) - x^{\lambda_i\varepsilon}(t)\big\| = O((\lambda_{i+1}-\lambda_i)\varepsilon)$, which implies that γ_t is continuous for each $t \in [\tau+\varepsilon, \tau')$, and that $L(\gamma_t) = O(\varepsilon)$, hence $d_{i,D_j}\big(x^\varepsilon(t+\varepsilon), x(t)\big) = O(\varepsilon)$.

Assuming now that x performs 2 discrete transitions at times $\tau, \tau' \in [0,T]$, such that $\tau+\varepsilon < \tau'$, transitioning from mode j to j', and the from mode j' to j''. Note that, by definition, $x|_{[0,\tau)} = x^\varepsilon|_{[0,\tau)}$. Moreover, since x is orbitally stable, we know that x^ε performs the same 2 discrete transitions for ε small enough. Let $\tau^\varepsilon+\varepsilon \in [0,T]$ be such that $x^\varepsilon(\tau^\varepsilon+\varepsilon) \in G_{(j',j'')}$. Note that $|\tau^\varepsilon - \tau'| = O(\varepsilon)$ since $x^\varepsilon \to x$ uniformly and x is Lipschitz continuous (both propositions shown above). Assume that $\tau' \leq \tau^\varepsilon + \varepsilon$ and consider the following upper bounds:

(1) If $t \in [\tau, \tau+\varepsilon)$, then $x(t) \in D_{j'}$ and $x^\varepsilon(t) \in S^\varepsilon_{(j,j')}$, thus:

$$d_{i,\mathcal{M}^\varepsilon}\big(x(t), x^\varepsilon(t)\big) \leq d_{i,D_{j'}}\big(x(t), x(\tau)\big) + d_{S^\varepsilon_{(j,j')}}\big(x(\tau), x^\varepsilon(t)\big) = O(\varepsilon). \tag{2.3.3}$$

(2) If $t \in [\tau+\varepsilon, \tau')$, then $x(t), x^\varepsilon(t) \in D_{j'}$, thus, using the bound obtained above:

$$d_{i,\mathcal{M}^\varepsilon}\big(x(t), x^\varepsilon(t)\big) \leq d_{i,D_{j'}}\big(x(t), x(t-\varepsilon)\big) + d_{i,D_{j'}}\big(x(t-\varepsilon), x^\varepsilon(t)\big) = O(\varepsilon). \tag{2.3.4}$$

(3) If $t \in [\tau', \tau^\varepsilon+\varepsilon)$, then $x(t) \in D_{j''}$ and $x^\varepsilon \in D_{j'}$, thus, denoting $\lim_{t\uparrow\tau'} x(t) = x(\tau'^-)$:

$$\begin{aligned}d_{i,\mathcal{M}^\varepsilon}\big(x(t), x^\varepsilon(t)\big) &\leq d_{i,D_{j''}}\big(x(t), x(\tau')\big) + d_{S^\varepsilon_{(j',j'')}}\big(x(\tau'), x(\tau'^-)\big) + \\ &\quad + d_{i,D_{j'}}\big(x(\tau'^-), x^\varepsilon(\tau^\varepsilon+\varepsilon)\big) + d_{i,D_{j'}}\big(x^\varepsilon(\tau^\varepsilon+\varepsilon), x^\varepsilon(t)\big) \\ &\leq O(\varepsilon).\end{aligned} \tag{2.3.5}$$

(4) If $t \in [\tau^\varepsilon+\varepsilon, \tau^\varepsilon+2\varepsilon)$, then $x(t) \in D_{j''}$ and $x^\varepsilon \in S^\varepsilon_{(j'.j'')}$, thus:

$$d_{i,\mathcal{M}^\varepsilon}\big(x(t), x^\varepsilon(t)\big) \leq d_{i,D_{j''}}\big(x(t), x(\tau')\big) + d_{S^\varepsilon_{(j',j'')}}\big(x(\tau'), x^\varepsilon(t)\big) \leq O(\varepsilon). \tag{2.3.6}$$

(5) If $t \in [\tau^\varepsilon + 2\varepsilon, T]$, then $x(t), x^\varepsilon(t) \in D_{j''}$, thus we get the same bound as in case 2.

Therefore, $\rho^\varepsilon_{[0,T]}(x, x^\varepsilon) = O(\varepsilon)$ as desired. Note that the general case, with an arbitrary number of discrete transitions and where the discrete transitions of x^ε occur before the discrete transitions of x, follows by using the a similar argument as above by properly considering the time intervals and then applying the upper bounds inductively.

Next, let us consider the case when x is a Zeno execution that accumulates on p'. Let $\delta > 0$, then $x|_{[0,T-\delta]}$ has a finite number of discrete transitions, and as shown above, $d_{i,\mathcal{M}^\varepsilon}\big(x(T-\delta), x^\varepsilon(T-\delta)\big) = O(\varepsilon)$. Moreover, $d_{i,\mathcal{M}^\varepsilon}\big(x(T-\delta), x(t)\big) = O(\delta)$ and $d_{i,\mathcal{M}^\varepsilon}\big(x^\varepsilon(T-\delta), x^\varepsilon(t)\big) = O(\delta)$ for each $t \in [T-\delta, T)$. The conclusion follows by noting that these bounds are valid for each $\delta > 0$. □

2.3.3 Discrete Approximations

Finally, we are able to define the *discrete approximation of a relaxed execution*, which is constructed as an extension of any existing ODE numerical integration algorithm. Given a hybrid control system $\mathcal{H}$, $\mathcal{A}^h_j \colon \mathbb{R} \times \mathbb{R}^{n_j} \times U \to \mathbb{R}^{n_j}$, where $h > 0$ and $j \in \mathcal{J}$, is a *numerical integrator of order* ω, if given $p \in D_j$, $u \in BV(\mathbb{R}, U)$, x the maximal integral curve of F_j with initial condition p and control u, $N = \lfloor \frac{T}{h} \rfloor$, and a sequence $\{z_k\}_{k=0}^N$ with $z_0 = p$ and $z_{k+1} = \mathcal{A}^h_j\big(kh, z_k, u(kh)\big)$, then $\sup\big\{\|x(kh) - z_k\| \mid k \in \{0, \dots, N\}\big\} = O(h^\omega)$. This definition of numerical integrator is compatible with commonly used algorithms, including Forward and Backward Euler algorithms and the family of Runge–Kutta algorithms (Chapter 7 in [LeV07]). Algorithm 3 defines a discrete approximation of a relaxed execution of $\mathcal{H}^\varepsilon$. The resulting discrete approximation, for a step size $h > 0$, denoted by $z^{\varepsilon,h}$, is a function from a closed interval $I \subset [0, \infty)$ to $\mathcal{M}^\varepsilon$.

We now make several remarks about Algorithm 3. First, the condition in Step 6 can only be satisfied, i.e. the Algorithm only stops, if $z^{\varepsilon,h}(t_k) \in \partial D_j$ and $F_j\big(t_k, z^{\varepsilon,h}(t_k), u(t_k)\big)$ is outward–pointing, since otherwise a smaller step–size would produce a valid point. Second, the function $z^{\varepsilon,h}$ is continuous on $\mathcal{M}^\varepsilon$. Third, and most importantly, similar to Algorithm 2, the curve assigned to $z^{\varepsilon,h}$ in Step 11 is exactly the maximal integral curve of F_e while on the strip. By relaxing the guards using strips, and then endowing the strips with a trivial vector field, we avoid having to find the exact point where the trajectory intersects a guard. Our relaxation does introduce an error in the approximation, but as we show in Theorem 2.3.2, the error is of order ε. Figure 3 shows a discrete approximation produced by Algorithm 3 as it performs a mode transition.

Theorem 2.3.2. *Let $\mathcal{H}$ be a hybrid control system and $\mathcal{H}^\varepsilon$ its relaxation. Let $p \in \mathcal{M}$, $u \in BV(\mathbb{R}, U)$, and let $x \colon I \to \mathcal{M}^\varepsilon$ be a orbitally stable execution of $\mathcal{H}$ with initial condition p and control u. Furthermore, let $x^\varepsilon \colon I^\varepsilon \to \mathcal{M}^\varepsilon$ be a relaxed execution with initial condition p and control u, and let $z^{\varepsilon,h} \colon I^{\varepsilon,h} \to \mathcal{M}^\varepsilon$ be its discrete approximation. If $[0, T] \subset I^\varepsilon \cap I^{\varepsilon,h}$ for each ε and h small enough, then there exists $C > 0$ such that $\lim_{h\to 0} \rho^\varepsilon_{[0,T]}\big(x^\varepsilon, z^{\varepsilon,h}\big) \leq C\varepsilon$.*

Algorithm 3: discrete approximation of execution of relaxed hybrid control system $\mathcal{H}^\varepsilon$.

Input: $h > 0$, $k = 0$, $j \in \mathcal{J}$, and $p \in D_j$.
Set $t_0 = 0$ and $z^{\varepsilon,h}(0) = p$.
while *True* **do**
  Find $n' = \inf\{n \in \mathbb{N} \mid \mathcal{A}_j^{h2^{-n}}\big(t_k, z^{\varepsilon,h}(t_k), u(t_k)\big) \in D_j^\varepsilon\}$
  if $n' = \infty$ **then**
    return $z^{\varepsilon,h}|_{[0,t_k]}$.
  end
  Set $t_{k+1} = t_k + h2^{-n'}$, and $z^{\varepsilon,h}(t_{k+1}) = \mathcal{A}_j^{h2^{-n'}}\big(t_k, z^{\varepsilon,h}(t_k), u(t_k)\big)$.
  Set $z^{\varepsilon,h}(t) = \frac{t_{k+1}-t}{t_{k+1}-t_k} z^{\varepsilon,h}(t_k) + \frac{t-t_k}{t_{k+1}-t_k} z^{\varepsilon,h}(t_{k+1})$ for each $t \in [t_k, t_{k+1}]$.
  if $\exists (j, j') \in \mathcal{N}_j$ *such that* $z^{\varepsilon,h}(t_{k+1}) \in S^\varepsilon_{(j,j')}$ **then**
    Set $(q, \tau) = z^{\varepsilon,h}(t_{k+1}) \in S^\varepsilon_{(j,j')}$, and $t_{k+2} = t_{k+1} + \varepsilon - \tau$.
    Set $z^{\varepsilon,h}(t) = (q, t - t_{k+1} + \tau)$ for each $t \in [t_{k+1}, t_{k+2})$.
    Set $z^{\varepsilon,h}(t_{k+2}) = R^\varepsilon_{(j,j')}(q, \varepsilon)$, $k = k + 2$, and $j = j'$. ▷ *Note* $(q, \varepsilon) \overset{\widehat{R}^\varepsilon}{\sim} z^{\varepsilon,h}(t_{k+2})$.
  else
    Set $k = k + 1$.
  end
end

Proof. As we have done with the previous proofs, we only provide a sketch of the argument in the interest of brevity. Assume that x^ε performs a single discrete transition in the interval $[0, T]$ for each ε small enough, crossing the guard $G_{(j,j')}$ at time τ^ε. Then, since x is orbitally stable and $\mathcal{A}^h$ is convergent with order ω, for ε and h small enough $z^{\varepsilon,h}$ also crosses guard $G_{(j,j')}$ at time $\tau^{\varepsilon,h}_{k'} \in [t_{k'}, t_{k'+1})$ for some $k' \in \mathbb{N}$, where $\{t_k\}_{k=0}^N$ is the set of time samples associated to $z^{\varepsilon,h}$. Moreover, since $x^\varepsilon(0) = z^{\varepsilon,h}(0)$, then for each $\delta > 0$, $\left|\tau^\varepsilon - t_{k'+1}\right| \leq \delta + O(h^\omega)$ and $\left|t_{k'+2} - \tau^\varepsilon + \varepsilon\right| = O(h^\omega)$.

Define the following times:

$$\begin{aligned} \sigma_m &= \min\{t_{k'+1}, \tau^\varepsilon\}, & \sigma_M &= \max\{t_{k'+1}, \tau^\varepsilon\}, \\ \nu_m &= \min\{t_{k'+2}, \tau^\varepsilon + \varepsilon\}, & \nu_M &= \max\{t_{k'+2}, \tau^\varepsilon + \varepsilon\}, \end{aligned} \tag{2.3.7}$$

and, in order to simplify our argument, assume that $\sigma_M \leq \nu_m$. Then on the interval $[0, \sigma_m)$ we get convergence due to $\mathcal{A}^h$. On the interval $[\sigma_m, \sigma_M)$ one execution has transitioned into a strip, while the other is still governed by the vector field on D_j. On the interval $[\sigma_M, \omega_m)$ both executions are inside the strip, and on the interval $[\omega_m, \omega_M)$ one execution has transitioned to a new domain, while the second is still on the strip. After time ω_M both executions are in a new domain, and we can repeat the process.

Consider the following cases:

(1) By the convergence of algorithm $\mathcal{A}^h$, $d_{i,\mathbb{M}^\varepsilon}\big(x^\varepsilon(\sigma_m), z^{\varepsilon,h}(\sigma_m)\big) = O(h^\omega)$.

(2) Using (2.3.1) from the proof of Theorem 2.3.1,

$$d_{i,\mathcal{M}^\varepsilon}\big(x^\varepsilon(\sigma_M), z^{\varepsilon,h}(\sigma_M)\big) \le d_{i,\mathcal{M}^\varepsilon}\big(x^\varepsilon(\sigma_M), x^\varepsilon(\sigma_m)\big) + d_{i,\mathcal{M}^\varepsilon}\big(x^\varepsilon(\sigma_m), z^{\varepsilon,h}(\sigma_m)\big) + \\ + d_{i,\mathcal{M}^\varepsilon}\big(z^{\varepsilon,h}(\sigma_m), z^{\varepsilon,h}(\sigma_M)\big) = O(h^\omega). \quad (2.3.8)$$

(3) Using the same argument as in the inequality above,

$$d_{i,\mathcal{M}^\varepsilon}\big(x^\varepsilon(\nu_m), z^{\varepsilon,h}(\nu_m)\big) \le d_{i,\mathcal{M}^\varepsilon}\big(x^\varepsilon(\sigma_M), z^{\varepsilon,h}(\sigma_M)\big) + 2\varepsilon. \quad (2.3.9)$$

(4) Finally, again using the same argument as in case 2,

$$d_{i,\mathcal{M}^\varepsilon}\big(x^\varepsilon(\nu_M), z^{\varepsilon,h}(\nu_M)\big) \le d_{i,\mathcal{M}^\varepsilon}\big(x^\varepsilon(\nu_m), z^{\varepsilon,h}(\nu_m)\big) + O(h^\omega). \quad (2.3.10)$$

The generalization to any relaxed execution defined on $\mathcal{M}^\varepsilon$ and its discrete approximation follows by noting that they perform a finite number of discrete jumps on any bounded interval and that δ' can be chosen arbitrarily small. □

Next, we state the main result of this Section, which is a result of Theorems 2.3.1 and 2.3.2.

Corollary 2.3.1. *Let $\mathcal{H}$ be a hybrid dynamical system and $\mathcal{H}^\varepsilon$ be its relaxation. Let $p \in \mathcal{M}$, $u \in BV(\mathbb{R}, U)$, $x\colon I \to \mathcal{M}^\varepsilon$ be an execution of $\mathcal{H}$ with initial condition p and control u, $x^\varepsilon\colon I^\varepsilon \to \mathcal{M}^\varepsilon$ be its corresponding relaxed execution, and $z^{\varepsilon,h}\colon I^{\varepsilon,h} \to \mathcal{M}^\varepsilon$ be its corresponding discrete approximation. If the following conditions are satisfied:*

(1) *x has a finite number of mode transitions or is a Zeno execution that accumulates,*

(2) *x is orbitally stable,*

(3) *$[0,T] \subset I \cap I^\varepsilon \cap I^{\varepsilon,h}$ for each ε and h small enough,*

then $\lim_{\substack{\varepsilon\to 0\\ h\to 0}} \rho^\varepsilon_{[0,T]}\big(x, z^{\varepsilon,h}\big) = 0$.

Proof. Note that, by Theorem 2.3.1 together with the Triangle Inequality, this corollary is equivalent to proving that $\rho^\varepsilon_I\big(x^\varepsilon, z^{\varepsilon,h}\big) \to 0$ as both $\varepsilon, h \to 0$. Hence we show that $\rho^\varepsilon_I\big(x^\varepsilon, z^{\varepsilon,h}\big)$ converges uniformly on h as $\varepsilon \to 0$. Using an argument similar to the one in the proof of Theorem 7.9 in [Rud76], proving the uniform convergence on h is equivalent to showing that $\lim_{h\to 0} \limsup_{\varepsilon\to 0} \rho^\varepsilon_I\big(x^\varepsilon, z^{\varepsilon,h}\big) = 0$, but this is clearly true by Theorem 2.3.2, therefore obtaining our desired result. □

2.4 Applications

We apply our provably–convergent numerical simulation algorithm in four examples: first detailing its technical advantages over other approaches in Section 2.4.1; then comparing its performance to existing state–of–the–art algorithms in Section 2.4.2; subsequently implementing a benchmark hybrid system verification example in Section 2.4.3; and finally demonstrating its use while computing the trajectories of a legged locomotion model in Section 2.4.4. It is important to note that, to the best of our knowledge, there are no results in the literature that can allow us to prove the orbital stability of the examples in Sections 2.4.2 and 2.4.3. However, using the techniques developed in Chapter 4, we can show that the example in Section 2.4.4 is orbitally stable. In spite of our inability to formally check orbital stability in each of the examples, we experimentally checked that the trajectories in each case were continuous with respect small variations of the initial conditions and control inputs.

2.4.1 Particle in a Box

We describe a simple conceptual example that illustrates several technical advantages of our intrinsic state space metric and convergent numerical simulation algorithm. Consider the mechanical dynamics of a point mass confined to the first orthant in $\mathbb{R}^d$, some $d \in \mathbb{N}$. When the particle impacts a coordinate plane, we stipulate that it undergoes perfect plastic impact. This system is comprised of a rigid body subject to perfect unilateral constraints, hence under mild constitutive assumptions it possesses unique solutions from every initial condition defined for all forward time [Bal00, Theorem 10]. To formalize this example, let

$$D = T[0,\infty)^d \subset T\mathbb{R}^d, \tag{2.4.1}$$

for each $j \in \{1,\ldots,d\}$ let

$$G_j = \big\{(x,\dot{x}) \in \partial D : x_j = 0,\ e_j^T \dot{x}_j < 0\big\},$$

and define $R_j : G_j \to D$ by

$$\forall (x,\dot{x}) \in G : R_j(x,\dot{x}) = (x, \dot{x} - (e_j^T \dot{x}) e_j),$$

where $e_j \in \mathbb{R}^d$ is the j–th standard basis vector.

In the modeling framework of [ST10], these elements determine a hybrid system $H = (D, F, G, R)$ where: D is the *flow set* defined in (2.4.1); $F : D \to TD$ is the *flow map* (i.e. vector field) defined by

$$\forall (x,\dot{x}) \in D : F(x,\dot{x}) = (\dot{x}, 0);$$

$G = \bigcup_{j=1}^d G_j$ is the *jump set*; and $R : G \to D$ is the *jump map* defined by

$$\forall (x,\dot{x}) \in G : R(x,\dot{x}) = \prod \{R_j : j \in \{1,\ldots,d\},\ (x,\dot{x}) \in G_j\}, \tag{2.4.2}$$

where the product in (2.4.2) denotes composition; since the R_j's commute, R is well–defined.

Now fix $i, j \in \{1, \ldots, d\}$, $i \neq j$, and consider a Cauchy sequence of initial conditions $\{(x_k, \dot{x}_k)\}_{k\in\mathbb{N}} \subset G_j \setminus G_i$ such that

$$\lim_{k\to\infty} (x_k, \dot{x}_k) = (x, \dot{x}) \in G_i \cap G_j$$

for some $i \in \{1, \ldots, d\} \setminus \{j\}$; in other words, for each $k \in \mathbb{N}$ the point $(x_k, \dot{x}_k)$ is in G_j and not in G_i, but in the limit as k tends to infinity the sequence converges to a point $(x, \dot{x})$ that is in both G_i and G_j. Note that $(x_k, \dot{x}_k) \to (x, \dot{x})$ and hence $R(x_k, \dot{x}_k) = R_j(x_k, \dot{x}_k) \to R_j(x, \dot{x}) \neq R_i \circ R_j(x, \dot{x}) = R(x, \dot{x})$. This implies that R (regarded as a singleton–valued multifunction) is not outer semicontinuous, so H fails to satisfy the "hybrid basic conditions" [ST10, Assumption 2.5]. More broadly, this example illustrates that the simulation results of [ST10] cannot be applied to approximate trajectories of rigid body mechanical systems in which more than one unilateral constraint can be active. The locomotion example in Section 2.4.4 provides another practical instance where trajectories of interest pass through overlapping constraint surfaces.

2.4.2 Forced Linear Oscillator with Stop

We consider a single degree–of–freedom oscillator consisting of a mass that is externally forced and can impact a plane fixed rigid stop, as in Figure 2.11a. The state of the oscillator is the position, $x(t) \in \mathbb{R}$, and velocity, $\dot{x}(t) \in \mathbb{R}$, of the mass. The oscillator is forced with a control $u \in BV(\mathbb{R}, \mathbb{R})$. The oscillator is modeled as a hybrid control system with a single mode, denoted D, and single guard corresponding to the mass impacting the stop with non–negative velocity, denoted G:

$$\begin{aligned} D &= \big\{\big(x(t), \dot{x}(t)\big) \in \mathbb{R}^2 \mid x(t) \leq x_{\max}\big\} \\ G &= \big\{\big(x(t), \dot{x}(t)\big) \in \mathbb{R}^2 \mid x(t) = x_{\max}, \dot{x}(t) \geq 0\big\} \end{aligned} \tag{2.4.3}$$

Upon impact, the state is updated using the reset map $R(x, \dot{x}) = \big(x, -c\,\dot{x}\big)$, where $c \in [0, 1]$ is the coefficient of restitution. Within the single domain, the dynamics of the system are governed by $\ddot{x}(t) + 2a\dot{x}(t) + \omega^2 x(t) = m^{-1}\,u(t)$, where $\omega = \sqrt{m^{-1}k}$, $a = 0.5\,m^{-1}\,\mu$, k is the spring constant, and μ is the damping coefficient.

Given an initial condition $\big(x(t_0), \dot{x}(t_0)\big) = \big(x_0, \dot{x}_0\big) \in D$, the oscillator's motion is analytically determined by

$$x(t) = e^{-at}\big(A_n \cos(\tilde{\omega}t) + B_n \sin(\tilde{\omega}t)\big) + \tilde{\omega}^{-1} \int_0^t u(s) e^{-a(t-s)} \sin\big(\tilde{\omega}(t-s)\big)\, \mathrm{d}s$$

for each $t \in [t_{n-1}, t_n)$, where $\tilde{\omega} = \sqrt{\omega^2 - a^2}$ (assuming that the damping is sub–critical), with t_n such that $x(t_n^-) = x_{\max}$ for each $n \in \mathbb{N}$, and A_n and B_n are determined by the given initial conditions when $n = 0$, or those determined by applying the reset map to $x(t_n^-)$ when $n \geq 1$. Note that determining the impact times can be done analytically. The analytical solution

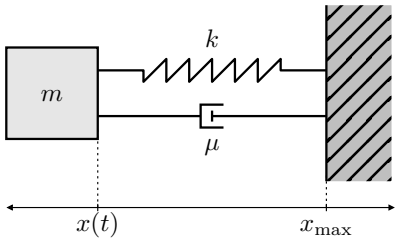

(a) Forced linear oscillator with stop.

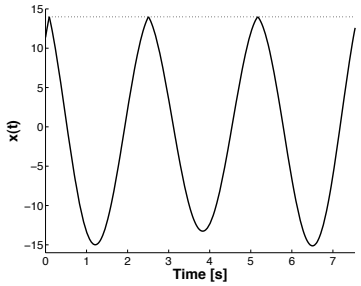

(b) Position of the analytical solution of Example 1 in Table 2.1 (solid line), and position of the stop (dotted line).

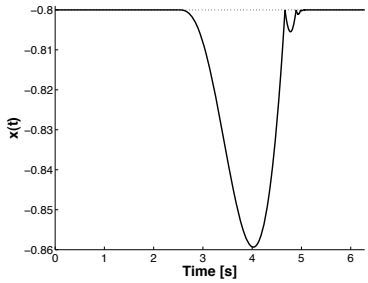

(c) Position of the analytical solution of Example 2 in Table 2.1 (solid line), and position of the stop (dotted line).

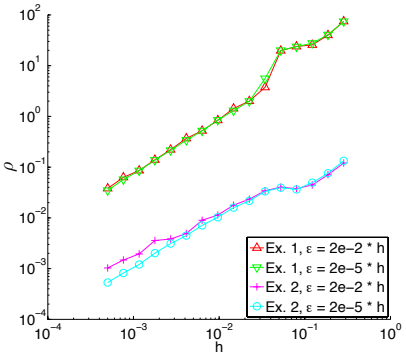

(d) Comparison of Algorithm 3 vs. the PS Method for the examples in Table 2.1 using $\rho^{\varepsilon}_{[0,t_{\max}]}$.

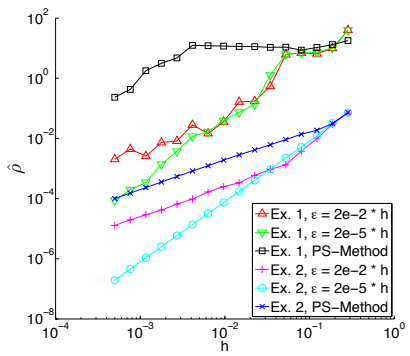

(e) Comparison of Algorithm 3 vs. the PS Method for the examples in Table 2.1 using $\hat{\rho}$.

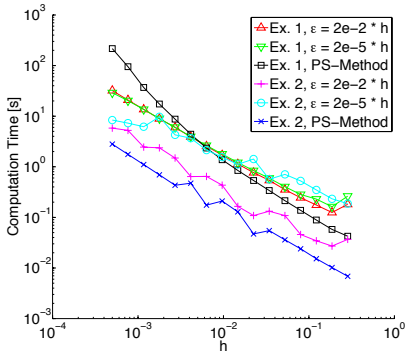

(f) Computation times of Algorithm 3 vs. the PS Method for the examples in Table 2.1.

Figure 2.11: A mechanical system (Figure 2.11a) and a pair of examples (Figs. 2.11b and 2.11c) chosen to illustrate the accuracy of Algorithm 3 vs. the PS Method (Figs. 2.11d and 2.11e) and their computation times (Figure 2.11f).

holds provided that the mass does not stick to the stop, since in that case the dynamics are given by $\ddot{x}(t) + 2a\dot{x}(t) + \omega^2 x(t) = m^{-1}\big(u(t) + \lambda(t)\big)$, where $\lambda(t) \in \mathbb{R}$ denotes the force generated by the stop to prevent movement. This equation holds as long as $x(t) = x_{\max}$, $\dot{x}(t) = \ddot{x}(t) = 0$, and the reaction of the stop is negative, i.e. $\lambda(t) \geq m\,\omega^2\,x_{\max}$. For the contact to cease, $\lambda(t) - m\,\omega^2\,x_{\max}$ must become zero and change sign. Once this happens, the analytical solution can be used again to construct the motion of the mass with the initial condition $(x_{\max}, 0)$.

Assuming that the forcing u is continuous (an assumption that is violated by many control schemes such as ones generated via optimal control) a convergent numerical simulation scheme, which we call the PS Method, to determine the position of a mechanical system with unilateral constraints was proposed in [PS03]. Fixing a step–size $h > 0$, their approach is a two–step method that for a set of time instances, $\{t_k\}_{k\in\mathbb{N}}$, computes a set of positions,

Table 2.1: Parameters for simulations of the forced linear oscillator with mechanical stop.

	a	c	$t_{\max}$	$u(t)$	x_0	$\dot{x}_0$	$x_{\max}$	ω
Example 1	0.05	0.9	40π	$20\cos(2.5\,t)$	11.36263	31.40358	14	2.5
Example 2	0.95	0.5	4π	$\cos(t)$	-0.8	0	-0.8	1

$z_{\mathrm{PS}}\colon \{t_k\}_{k\in\mathbb{N}} \to \mathbb{R}$, by:

$$\begin{aligned} z_{\mathrm{PS}}(t_0) &= x_0, \qquad z_{\mathrm{PS}}(t_1) = x_0 + \dot{x}_0 h + \frac{h^2}{2}\big(u(0) - 2a\dot{x}_0 - \omega^2 x_0\big), \\ z_{\mathrm{PS}}(t_{k+1}) &= -c\, z_{\mathrm{PS}}(t_{k-1}) + \min\big\{y_{\mathrm{PS}}(t_k), (1+c)x_{\max}\big\}, \\ y_{\mathrm{PS}}(t_k) &= \frac{1}{1+ah}\Big(h^2 u(t_k) + (2-h^2\omega^2) z_{\mathrm{PS}}(t_k) - \big((1-c) - (1+c)a\,h\big) z_{\mathrm{PS}}(t_{k-1})\Big), \end{aligned} \tag{2.4.4}$$

where $t_{k+1} = t_k + h$ for each $k \in \mathbb{N}$.

We illustrate the performance of our approach by considering the two examples described in Table 2.1 whose solutions, which are defined for all $t \in [0, t_{\max}]$, can be computed analytically. The position component of the analytical trajectory of each example is plotted in Figs. 2.11b and 2.11c. The evaluation of the performance of Algorithm 3 using ρ^{ε}, as in Definition 2.2.7, is shown in Figure 2.11d. To make our approach comparable to the PS Method, for $\mathcal{A}^h$ we use a Runge–Kutta of order two which is called the midpoint method. We cannot use ρ^{ε} to compare our discrete approximation algorithm to the PS method since the PS method does not compute the velocities of the hybrid system. Hence, we use the evaluation metric proposed in [JL01] which compares a numerically simulated position trajectory, $z_{\mathrm{pos}}\colon \{t_k\}_{k\in\mathbb{N}} \to \mathbb{R}$, to the analytically computed position trajectory, $x_{\mathrm{analytic}}\colon [0, t_{\max}] \to \mathbb{R}$, at the sample points $\{t_k\}_{k\in\mathbb{N}} \cap [0, t_{\max}]$ as follows:

$$\hat{\rho}(z_{\mathrm{pos}}, x_{\mathrm{analytic}}) = \max\big\{|z_{\mathrm{pos}}(t_k) - x_{\mathrm{analytic}}(t_k)| \mid \{t_k\}_{k\in\mathbb{N}} \cap [0, t_{\max}]\big\}. \tag{2.4.5}$$

The result of this comparison is illustrated in Figure 2.11e. Finally, the computation time on a 32 GB, 3.1 GHz *Xeon* processor computer for each of the examples as a function of the step–size and relaxation parameter is shown in Figure 2.11f. Notice in particular that we are able to achieve higher accuracy with respect to the $\hat{\rho}$ evaluation metric at much faster speeds. In Example 1, for step–sizes $h \leq 10^{-1}$, our numerical simulation method is consistently more accurate by several orders of magnitude and generally several orders of magnitude faster than the PS method. In Example 2, using a step–size of approximately $h = 10^{-2}$ and relaxation parameter $\varepsilon = 2{\cdot}10^{-7}$, our numerical simulation achieves a $\hat{\rho}$ value of approximately 10^{-4} while taking approximately 0.1 seconds, whereas the PS method requires a step–size of $h = 5 \cdot 10^{-4}$ which takes approximately 5 seconds in order to achieve the same level of accuracy.

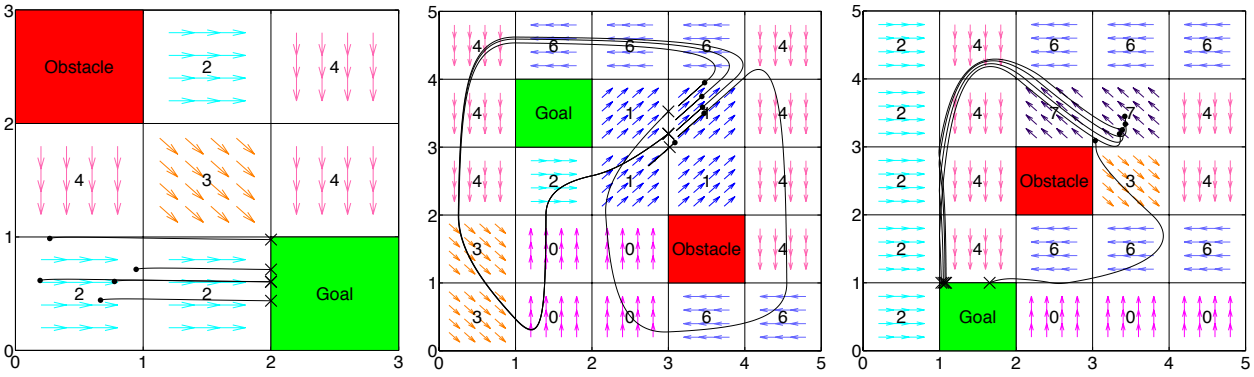

(a) Simple Instance (b) Accuracy Instance (c) Infinite Instance

Figure 2.12: *Navigation benchmark instances.* Each instance map (symbols within each square) is shown with its desired velocity (drawn in each square with an arrow). Sample trajectories (drawn as lines beginning at filled in circles and ending at crosses) begin at some of the initial conditions we attempt to verify.

2.4.3 Navigation Benchmark for Hybrid System Verification

Next, we illustrate the utility of Algorithm 3 by considering three instances of a navigation benchmark proposed in [FI04] for hybrid system verification tools. The benchmark considers an object moving in the plane while following a set of desired velocities, $v_{d_j} = \left(\sin\left(\frac{j\pi}{4}\right), \cos\left(\frac{j\pi}{4}\right)\right)$, for $j \in \{0, \ldots, 7\}$ where j is attributed to unit–sized squares according to a labeling map. Special symbols denoted "Goal" and "Obstacle" are reserved for a set of target and forbidden states, respectively. The labeling map for the three instances considered within this subsection are illustrated in Figure 2.12, where the label j in each cell refers to the desired velocity, target, or forbidden states. If the trajectory leaves the grid, the desired velocity is the velocity of the closest cell.

The dynamics of the four dimensional state, $(x, v) \in \mathbb{R}^4$, are given by $\dot{x}(t) = v(t)$, and $\dot{v}(t) = A\big(v(t) - v_{d_j}\big)$, where $A = \left(\begin{smallmatrix} -1.2 & 0.1 \\ 0.1 & -1.2 \end{smallmatrix}\right)$ for the instances illustrated in Figs. 2.12a and 2.12b and $A = \left(\begin{smallmatrix} -0.8 & -0.2 \\ -0.1 & -0.8 \end{smallmatrix}\right)$ for the instance illustrated in Figure 2.12c. For each instance, we attempt to verify that for all trajectories beginning from a set of initial conditions there exists some finite time at which the "Goal" set is reached while avoiding the "Obstacle" set. We perform this verification by discretizing over the given set of initial conditions.

For the instance illustrated in Figure 2.12a, we select a set of initial conditions $x \in [0, 1] \times [0, 1]$ and $v \in [0.1, 0.5] \times [0.05, 0.25]$. By choosing $10,000$ uniformly spaced points over the set of initial conditions, a step–size of 10^{-1}, and relaxation size of 10^{-3}, we are able to verify this system in approximately 100 seconds. For the instance illustrated in Figure 2.12b, we select a set of initial conditions $x \in [3, 4] \times [3, 4]$ and $v \in [-1, 1] \times [-1, 1]$. This instance fails the verification task as trajectories are unable to reach the "Goal" set, but do not ever intersect with the "Obstacle" set. By choosing $10,000$ uniformly spaced

points over the set of initial conditions, a step–size of 10^{-1}, and relaxation size of 10^{-3}, we discover that for this system the task is not verifiable in approximately 85 seconds. For the instance illustrated in Figure 2.12a, we select a set of initial conditions $x \in [3, 3.5] \times [3, 3.5]$ and $v \in \{0.5\} \times [-0.5, 0.5]$. In this instance, verification is possible, but trajectories get close to the "Obstacle" set. By choosing $10,000$ uniformly spaced points over the set of initial conditions, a step–size of 10^{-1}, and relaxation size of 10^{-3}, we are able to verify this system in approximately 210 seconds.

2.4.4 Simultaneous Transitions in Models of Legged Locomotion

As a terrestrial agent traverses an environment, its appendages intermittently contact the terrain. Since the equations governing the agent's motion change with each limb contact, the dynamics are naturally modeled by a hybrid control system with discrete modes corresponding to distinct contact configurations. Because the dynamics of dexterous manipulation are equivalent to that of legged locomotion [Joh+12], such hybrid control systems model a broad and important class of dynamic interactions between an agent and environment.

Legged animals commonly utilize gaits that, on average, involve the simultaneous transition of multiple limbs from aerial motion to ground contact [Ale84; Gol+99]. Similarly, many multi–legged robots enforce simultaneous leg touchdown via virtual constraints implemented algorithmically [Rai+86; Sar+01] or physical constraints implemented kinematically [Kim+06; Hoo+10]. Trajectories modeling such gaits pass through the intersection of multiple transition surfaces in the corresponding hybrid control system models. Therefore simulation of this frequently–observed behavior requires a numerical integration scheme that can accommodate overlapping guards. Algorithm 3 has this capability, and to the best of our knowledge is the only existing algorithm possessing this property. We demonstrate this advanced capability using a *pronking* gait in a saggital–plane locomotion model illustrated in Figure 2.13a.

Figure 2.13a contains an extension of the "Passive RHex–runner" in [SH06] that allows pitching motion. A rigid body with mass m and moment–of–inertia I moves in the saggital plane under the influence of gravity g. Linear leg–springs are attached to the body via a frictionless pin joint located symmetrically at distance $d/2$ from the center–of–mass. The leg–springs are massless with linear stiffness k, rest length ℓ, and make an angle ψ with respect to the body while in the air. When a foot touches the ground it attaches via a frictionless pin joint, and it detaches when the leg extends to its rest length.

A *pronk* is a gait wherein all legs touch down and lift off from the ground at the same time [Ale84; Gol+99]. Due to symmetries in our model, motion with pitch angle $\theta = 0$ for all time is invariant. Therefore periodic orbits for the *spring–loaded inverted pendulum* model in [Ghi+03] correspond exactly to pronking gaits for our model. Figure 2.13b contains a projection of the guards $G_{(a,r)}$, $G_{(a,f)}$, $G_{(r,g)}$, $G_{(f,g)}$ in (θ, z) coordinates for the transition from the aerial domain D_a to the ground domain D_g through rear stance D_r and front stance D_f. The pronking trajectory is illustrated by a downward–pointing vertical arrow, and a

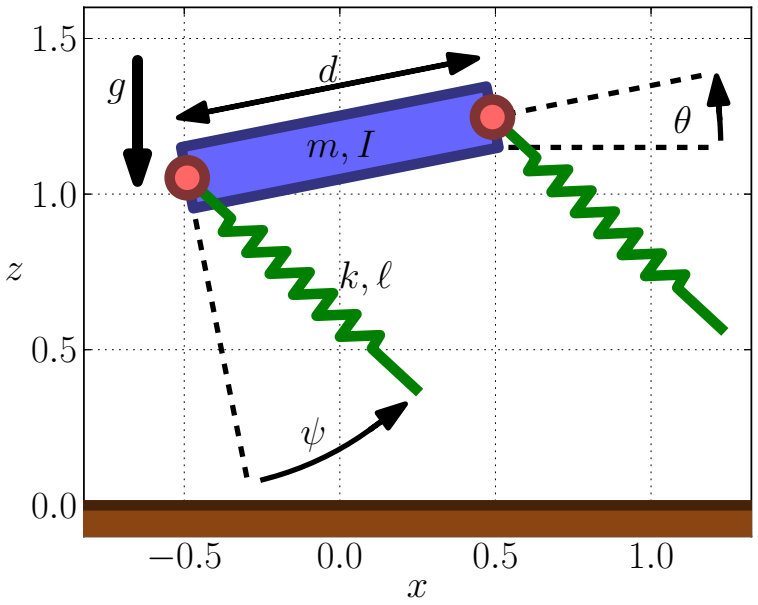

(a) Schematic for the saggital–plane locomotion model with three mechanical degrees of freedom.

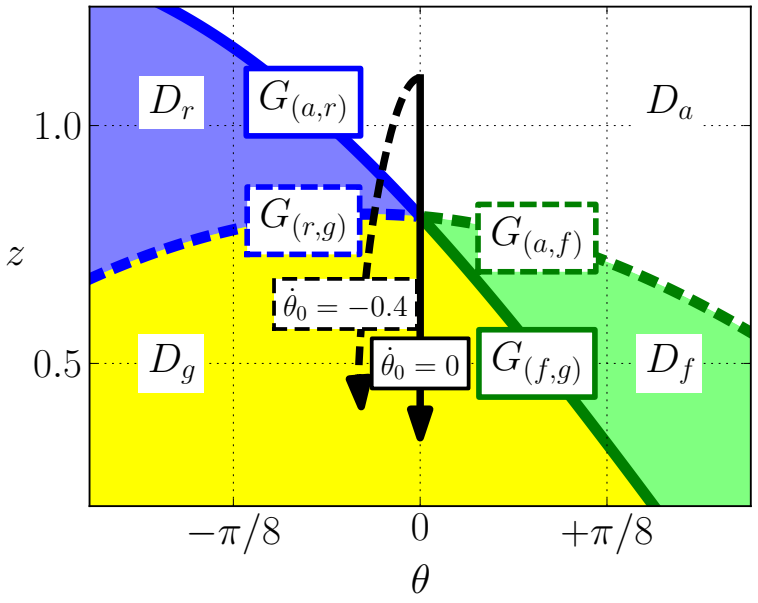

(b) Projection of guards in (θ, z) coordinates for transition from aerial domain D_a to ground domain D_g with parameters $d = \ell = 1$, $\psi = \pi/5$.

Figure 2.13: Schematic and discrete mode diagram for the saggital–plane locomotion model.

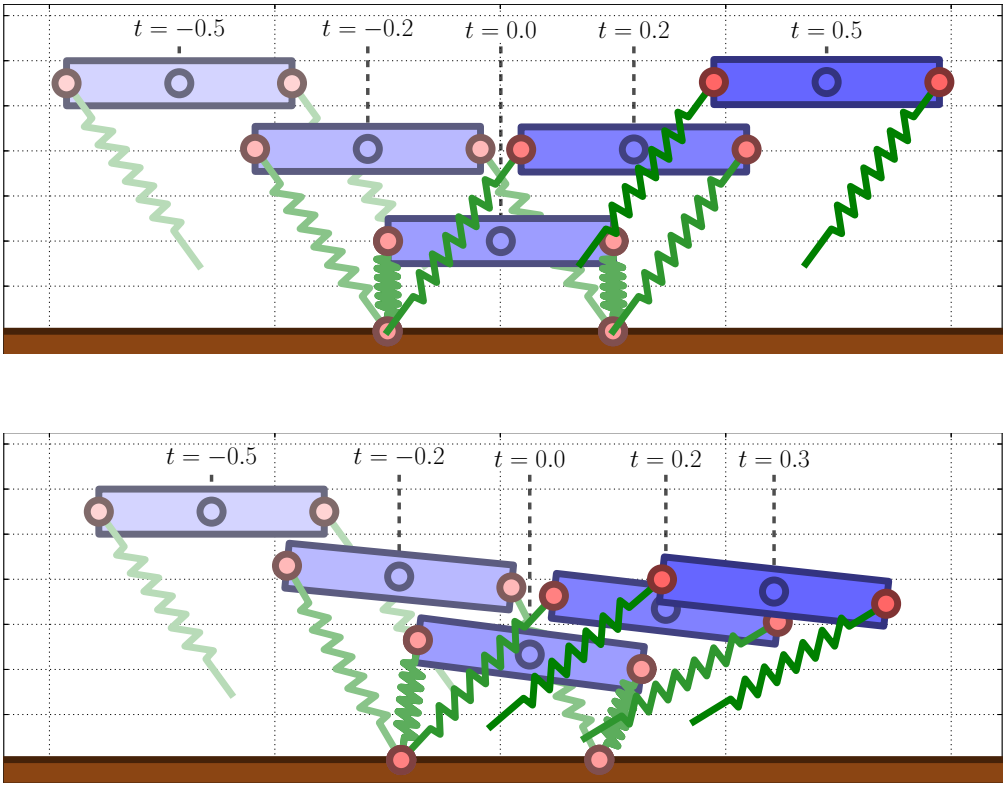

Figure 2.14: Snapshots of *pronk* at discrete transition times with parameters $(m, I, k, \ell, d, g, \psi) = (1, 1, 30, 1, 1, 9.81, \pi/5)$, step size $h = 10^{-3}$, relaxation parameter $\varepsilon = 10^{-2}$: (top) from initial condition $(x_0, z_0, \theta_0, \dot{x}_0, \dot{z}_0, \dot{\theta}_0) = (0, 1.1, 0, 3.4, 0, 0)$; (bottom) same as (top) except $\dot{\theta}_0 = -0.4$.

nearby trajectory initialized with negative rotational velocity is illustrated by a dashed line. Figure 2.14 contains snapshots from these simulations.

The $\dot{\theta}_0 = 0$ trajectory in Figure 2.13b clearly demonstrates the need for a simulation algorithm that allows the intersection of multiple transition surfaces. We emphasize that our state–space metric was necessary to derive a convergent numerical approximation for this execution: since the discrete mode sequence differs for any pair of trajectories arbitrarily close to the $\dot{\theta}_0 = 0$ execution that pass through the interior of D_r and D_f, respectively, a naïve application of the trajectory–space metric in [Tav09] would yield a distance larger than unity between the pair. Consequently no numerical simulation algorithm can be shown to converge to the $\dot{\theta}_0 = 0$ execution using a trajectory–space metric.

Another interesting property of this example is that it is possible to show (by carefully studying the transitions between vector fields through the guards) that the hybrid quotient space $\mathcal{M}$ is a smooth 6–dimensional manifold near the *pronk* execution, and that

the piecewise–defined dynamics yield a continuously–differentiable vector field on this quotient. Since this system is intrinsically smooth, all trajectories are orbitally stable [Lee12, Theorem D.6]. However, this observation argument would not apply if the model included damping or other nonsmooth effects at limb touchdown. In these cases, it may be possible to generalize the piecewise–differentiable flow derived in Chapter 4 to establish orbital stability.

As a final note to practitioners, we remark that our algorithm does not require a specialized mechanism to handle overlapping guards or control inputs: a single code will accurately simulate any orbitally stable execution of the hybrid system under investigation, dramatically simplifying practical implementation.

2.5 Discussion

We developed an algorithm for the numerical simulation of hybrid control systems and proved the uniform convergence of our approximations to executions using a novel metrization of the hybrid control system's state space. The metric and the algorithm impose minimal assumptions on the hybrid system beyond those required to guarantee existence and uniqueness of executions. Beyond their immediate utility, it is our conviction that these tools provide a foundation for formal analysis and computational controller synthesis in a broad class of Cyber–Physical Systems (CPS). For example, Girard and Pappas [GP07] developed a family of *approximate bisimulation* metrics enabling comparison of entire CPS once a trajectory metric is provided for each particular system. We developed a general method to construct metrics on the state space and hence the space of trajectories for hybrid control systems, significantly extending the class of CPS that can be studied in this paradigm. Further, simulation provides a foundation for numerical tools including reachability–based controller synthesis [Din+11] and numerical optimal control [Wes+03]. Current approaches to these problems require a fixed discrete mode sequence, yielding a computational complexity combinatorial in the number of discrete modes. We conjecture that our relaxed state–space metric enables generalizations of these algorithm which avoid combinatorial search by working in our continuous metric space. Finally, Tabuada [Tab07] proposed a control paradigm wherein an embedded system is continually monitored but control effort is updated only when an event specified by a threshold function on the state space is triggered. Implementation of this approach yields a CPS with state–dependent discrete transitions. We provide an algorithm enabling accurate simulation of this closed–loop system, even in systems where multiple events may trigger simultaneously.

Chapter 3

Reduction and Smoothing near Hybrid Periodic Orbits

Rhythmic phenomena are pervasive, appearing in physical situations as diverse as legged locomotion [Hol+06], dexterous manipulation [Bue+94], gene regulation [GP78], and electrical power generation [HR07]. The most natural dynamical models for these systems are piecewise–defined or discontinuous owing to intermittent changes in the mechanical contact state of a locomotor or manipulator, or to rapid switches in protein synthesis or constraint activation in a gene or power network. Such *hybrid* systems generally exhibit dynamical behaviors that are distinct from those of *smooth* systems [Lyg+03]. Restricting our attention to the dynamics near periodic orbits in hybrid dynamical systems, we demonstrate that a class of hybrid models for rhythmic phenomena reduce to classical (smooth) dynamical systems.

Although the results of this chapter do not depend on the phenomenology of the physical system under investigation, a principal application domain for this work is terrestrial locomotion. Numerous architectures have been proposed to explain how animals control their limbs; for steady–state locomotion, most posit a principle of coordination, synergy, symmetry or synchronization, and there is a surfeit of neurophysiological data to support these hypotheses [Gri85; Coh+82; Gol+99; TM05; Li+13]. Taken together, the empirical evidence suggests that the large number of degrees–of–freedom (DOF) available to a locomotor can collapse during regular motion to a low–dimensional dynamical attractor (a *template*) embedded within a higher–dimensional model (an *anchor*) that respects the locomotor's physiology [Hol+06; FK99]. We provide a mathematical framework to model this empirically observed dimensionality reduction in the deterministic setting.

From a modeling viewpoint, a stable hybrid periodic orbit provides a natural abstraction for the dynamics of steady–state legged locomotion. This approach has been widely adopted, generating a variety of models of bipedal [McG90; Gri+02; Sey+03; Col+05] and multi–legged [Ghi+03; SH00b; Kuk+09] locomotion as well as some control–theoretic techniques for composition [KK02], coordination [Hay+12], and stabilization [Wes+03; Car+09; Shi+10] of such models. In certain cases, it has been possible to embed a low–dimensional abstraction

in a higher–dimensional physically–realistic model [PG09; AS11]. Applying these techniques to establish existence of a reduced–order subsystem imposes stringent assumptions on the dynamics of locomotion that are difficult to verify for any particular locomotor. In contrast, the results of this chapter imply that hybrid dynamical systems generically exhibit dimension reduction near periodic orbits solely due to the interaction of the discrete–time switching dynamics with the continuous–time flow.

Under the hypothesis that iterates of the Poincaré map associated with a periodic orbit in a hybrid dynamical system are eventually constant rank, we demonstrate the existence of a constant–dimensional invariant subsystem that attracts all nearby trajectories in finite time regardless of the stability properties of the orbit; this appears as Theorem 3.3.1. Assuming instead that the periodic orbit under investigation is exponentially stable, we show in Theorem 3.4.1 that trajectories *generically* contract superexponentially to a subsystem whose dimension is determined by rank properties of the linearized Poincaré map at a single point. The resulting subsystems possess a special structure that we exploit in Theorem 3.5.1 to construct a topological quotient that removes the hybrid transitions and admits the structure of a smooth manifold, yielding an equivalent smooth dynamical system.

In Section 3.6 we show how these results can be applied to reduce the complexity of hybrid models for mechanical systems and analyze rhythmic hybrid control systems. The example in Section 3.6.1 demonstrates that reduction can occur spontaneously in mechanical systems undergoing plastic impacts. In Section 3.6.2 we present a family of $(3+2n)$–DOF lateral–plane multi–leg models that provably reduce to a common 3–DOF mechanical system independent of the number of limbs, $n \in \mathbb{N}$; this demonstrates model reduction in the mechanical component of the class of neuromechanical models considered in [Hol+06; Kuk+09]. As further applications, we assess structural stability of deadbeat controllers for rhythmic locomotion and manipulation in Section 3.6.3, and derive a normal form for the stability basin of a hybrid oscillator in Section 3.6.4.

3.1 Preliminaries

3.1.1 Linear Algebra [CD91]

Through a standard abuse of notation, we conflate a linear map $A : \mathbb{R}^n \to \mathbb{R}^m$ with its matrix representation $A \in \mathbb{R}^{m\times n}$ in the standard basis. The range $A(\mathbb{R}^n) \subset \mathbb{R}^m$ of a linear map A is a subspace; we let $\operatorname{rank} A$ denote the dimension of this subspace. If $A^n = 0$ then we say A is *nilpotent*. The *spectrum* of a square matrix $A \in \mathbb{R}^{n\times n}$ is denoted

$$\operatorname{spec} A = \{\lambda \in \mathbb{C} : \det(\lambda I - A) = 0\}$$

and the *spectral radius* is denoted by

$$\rho(A) = \max\{|\lambda| : \lambda \in \operatorname{spec} A\}.$$

If $\|\cdot\| : \mathbb{R}^n \to \mathbb{R}$ is a norm, we let $\|\cdot\|_i : \mathbb{R}^{n\times n} \to \mathbb{R}$ denote the corresponding *induced* norm [CD91, Appendix A.6].

3.1.2 Topology [Lee12]

If $(X, \|\cdot\|)$ is a Banach space, we let $B_\delta(x) \subset X$ denote the open ball of radius $\delta > 0$ centered at $x \in X$; For $X = \mathbb{R}^n$, we may emphasize the dimension n by writing $B^n_\delta(0) \subset \mathbb{R}^n$ for the open δ–ball. A subset of a topological space is *precompact* if it is open and its closure is compact. A *neighborhood* of a point $x \in X$ in a topological space X is a connected open subset $U \subset X$ containing x. The *disjoint union* of a collection of sets $\{S_j\}_{j\in J}$ is denoted

$$\coprod_{j\in J} S_j = \bigcup_{j\in J} S_j \times \{j\},$$

a set we endow with the natural piecewise–defined topology. If $\sim \subset D \times D$ is an equivalence relation on the topological space D, then we let $D/\!\sim$ denote the corresponding set of equivalence classes. There is a natural *quotient projection* $\pi : D \to D/\!\sim$ sending $x \in D$ to its equivalence class $[x] \in D/\!\sim$, and we endow $D/\!\sim$ with the (unique) finest topology making π continuous [Lee12, Appendix A]. Any map $R : G \to D$ defined over a subset $G \subset D$ determines an equivalence relation $\sim \subset D \times D$ as the transitive closure of

$$\big\{(x, y) \in D \times D : x \in R^{-1}(y),\ y \in R^{-1}(x),\ \text{or } x = y\big\}.$$

To clarify that the equivalence relation is determined by R we denote the quotient space as

$$D/\!\sim = \frac{D}{G \overset{R}{\sim} R(G)}.$$

3.1.3 Differential Topology [Hir76]

A *C^r n–dimensional manifold M with boundary ∂M* is an n–dimensional topological manifold covered by an *atlas* of *C^r coordinate charts* $\{(U_a, \varphi_a)\}_{a\in\mathcal{A}}$ where $U_a \subset M$ is open, $\varphi_a : U_a \to H^n$ is a homeomorphism, and

$$H^n = \{(y_1, \dots, y_n) \in \mathbb{R}^n : y_n \geq 0\}$$

is the upper half–space; we write $\dim M = n$. The charts are C^r in the sense that $\varphi_a \circ \varphi_b^{-1}$ is a C^r diffeomorphism over $\varphi_b(U_a \cap U_b)$ for all pairs $a, b \in \mathcal{A}$ for which $U_a \cap U_b \neq \emptyset$; if $r = \infty$ we say M is *smooth*. The boundary $\partial M \subset M$ contains those points that are mapped to the plane $\{(y_1, \dots, y_n) \in \mathbb{R}^n : y_n = 0\}$ in some chart. A map $P : M \to N$ is C^r if M and N are C^r manifolds and for every $x \in M$ there is a pair of charts $(U, \varphi), (V, \psi)$ with $x \in U \subset M$ and $P(x) \in V \subset N$ such that the coordinate representation $\widetilde{P} = \psi \circ P \circ \varphi^{-1}$ is a C^r map between subsets of H^n. We let $C^r(M, N)$ denote the normed vector space of C^r maps between M and N endowed with the uniform C^r norm [Hir76, Chapter 2].

Each $x \in M$ has an associated *tangent space* T_xM, and the disjoint union of the tangent spaces is the *tangent bundle*

$$TM = \coprod_{x\in M} T_xM.$$

Note that any element in TM may be regarded as a pair (x, δ) where $x \in M$ and $\delta \in T_x M$, and TM is naturally a smooth $2n$–dimensional manifold. We let $\mathfrak{T}(M)$ denote the set of *smooth vector fields* on M, i.e. smooth maps $F : M \to TM$ for which $\pi \circ F(x) = \mathrm{id}_M$ where $\pi : TM \to M$ is the canonical projection. It is a fundamental result that any $F \in \mathfrak{T}(M)$ determines an ordinary differential equation in every chart on the manifold that may be solved globally to obtain a *maximal flow* $\phi : \mathcal{F} \to M$ where $\mathcal{F} \subset \mathbb{R} \times M$ is the *maximal flow domain* [Lee12, Theorem 9.12].

If $P : M \to N$ is a smooth map between smooth manifolds, then at each $x \in M$ there is an associated linear map

$$DP(x) : T_x M \to T_{P(x)} N$$

called the *pushforward*. Globally, the pushforward is a smooth map

$$DP : TM \to TN;$$

in coordinates, it is the familiar Jacobian matrix. If $M = X \times Y$ is a product manifold, the pushforward naturally decomposes as

$$DP = (D_x P,\, D_y P)$$

corresponding to derivatives taken with respect to X and Y, respectively. The *rank* of a smooth map $P : M \to N$ at a point $x \in M$ is $\operatorname{rank} DP(x)$. If $\operatorname{rank} DP(x) = r$ for all $x \in M$, we simply write $\operatorname{rank} DP \equiv r$. If P is furthermore a homeomorphism onto its image, then P is a *smooth embedding*, and the image $P(M)$ is a *smooth embedded submanifold*. In this case the difference $\dim N - \dim P(M)$ is called the *codimension* of $P(M)$, and any smooth vector field $F \in \mathfrak{T}(M)$ may be pushed forward to a unique smooth vector field

$$DP(F) \in \mathfrak{T}(P(M)).$$

A vector field $F \in \mathfrak{T}(M)$ is *inward–pointing* at $x \in \partial M$ if for any coordinate chart (U, φ) with $x \in U$ the n–th coordinate of $D\varphi(F)$ is positive and *outward–pointing* if it is negative.

3.1.4 Hybrid Differential Topology

For our purposes, it is expedient to define hybrid dynamical systems over a finite disjoint union

$$M = \coprod_{j \in J} M_j = \bigcup_{j \in J} M_j \times \{j\} = \{(x, j) : j \in J, x \in M_j\}$$

where M_j is a finite dimensional connected C^r manifold (possibly with boundary) for each $j \in J$. We endow M with the unique largest topology with respect to which the (canonical) inclusions $M_j \hookrightarrow M$ are continuous [Lee12, Proposition A.25]. This makes M into a *second–countable*, *Hausdorff* topological space which is *locally Euclidean* in the sense that each point $x \in M$ has a neighborhood that is homeomorphic to an open subset of $\mathbb{R}^{n_x}$, some $n_x \in \mathbb{N}$.

Since the dimension is no longer required to be fixed, M is technically not a topological manifold [Lee12, Chapter 1]. However, it is a mild generalization, hence we refer to it as a *hybrid topological manifold*.

For each $j \in J$, M_j has an associated maximal C^r atlas $\mathcal{A}_j$. We construct a maximal C^r hybrid atlas for M by collecting charts from the atlases on the components of M:

$$\mathcal{A} = \{(U \times \{j\}, \varphi \circ \pi_j) : j \in J, (U, \varphi) \in \mathcal{A}_j\}$$

where $\pi_j : M_j \times \{j\} \to M_j$ is the canonical projection. We refer to the pair $(M, \mathcal{A})$ as a C^r *hybrid manifold*, but may suppress the atlas when it is clear from context. We define the *hybrid tangent bundle* as the disjoint union of the component tangent bundles,

$$TM = \coprod_{j \in J} TM_j,$$

and the *hybrid boundary* as the disjoint union of the boundaries,

$$\partial M = \coprod_{j \in J} \partial M_j.$$

Let $M = \coprod_{j \in J} M_j$ and $N = \coprod_{\ell \in L} N_\ell$ be two hybrid manifolds. Note that if a map $R : M \to N$ is continuous, then for each $j \in J$ there exists $\ell \in L$ such that $R(M_j) \subset N_\ell$ and hence $R|_{M_j} : M_j \to N_\ell$. Using this observation, we define differentiability for continuous maps between hybrid manifolds. Namely, a map $R : M \to N$ is called C^r if R is continuous and $R|_{M_j} : M_j \to N$ is C^r for each $j \in J$. In this case the *hybrid pushforward*

$$DR : TM \to TN$$

is the C^r map defined piecewise as

$$DR|_{TM_j} = D(R|_{M_j})$$

for each $j \in J$. A C^r map $F : M \to TM$ is called a *hybrid vector field* if $\pi \circ F = \mathrm{id}_M$ where $\pi : TM \to M$ is the canonical projection, and we let $\mathfrak{T}(M)$ denote the set of hybrid vector fields on M.

3.1.5 Hybrid Dynamical Systems

We now define the class of hybrid systems considered in this chapter. This is a specialization of *hybrid automata* [Lyg+03] that emphasizes the differential–geometric character of hybrid phenomena.

Definition 3.1.1. *A* hybrid dynamical system *is specified by a tuple $H = (D, F, G, R)$ where:*

$D = \coprod_{j \in J} D_j$ *is a smooth hybrid manifold;*

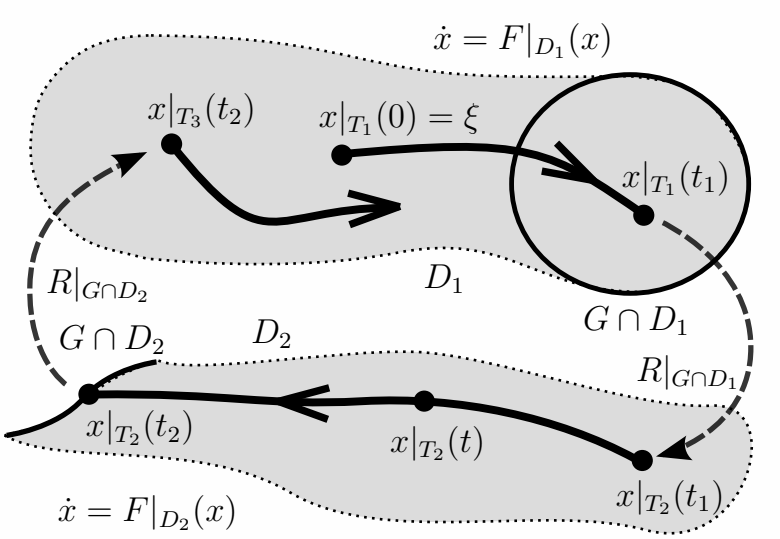

Figure 3.1: Illustration of two–domain hybrid dynamical system $H = (D, F, G, R)$ and execution $x : T \to D$ defined over a hybrid time trajectory $T = T_1 \coprod T_2 \coprod T_3$. In this example, the restrictions $x|_{T_1}, x|_{T_3}$ are confined to D_1, i.e. $x|_{T_1} : T_1 \to D_1$, $x|_{T_3} : T_3 \to D_1$, while $x|_{T_2} : T_2 \to D_2$. Consecutive components of T share a single instant in time, i.e. $T_1 \cap T_2 = \{t_1\}$, $T_2 \cap T_3 = \{t_2\}$, and the corresponding states are related through the reset map by $x|_{T_2}(t_1) = R(x|_{T_1}(t_1))$, $x|_{T_3}(t_2) = R(x|_{T_2}(t_2))$.

$F : D \to TD$ *is a smooth vector field;*

$G \subset \partial D$ *is an open subset of* ∂D*;*

$R : G \to D$ *is a smooth map.*

As in [Lyg+03], we call R *the* reset map *and* G *the* guard. *When we wish to be explicit about the order of smoothness, we will say* H *is* C^r *if* D, F, *and* R *are* C^r *as a manifold, vector field, and map, respectively, for some* $r \in \mathbb{N}$.

Roughly speaking, an *execution* of a hybrid dynamical system is determined from an initial condition in D by following the continuous–time dynamics determined by the vector field F until the trajectory reaches the guard G, at which point the reset map R is applied to obtain a new initial condition; see Figure 3.1 for an illustration. We formalize this using the notion of a *hybrid time trajectory* [Lyg+03].

Definition 3.1.2. *A* hybrid time trajectory *is a disjoint union of intervals* $T = \coprod_{i=1}^{N} T_i$ *such that*

1. $N \in \mathbb{N} \cup \{\infty\}$*;*
2. $T_i \subset \mathbb{R}$ *is an interval for all* $i < N$*, and if* $N < \infty$ *then* $T_N \subset \mathbb{R}$ *is also an interval;*

3. $T_i \cap T_{i+1} = \{t_i\}$ *for all* $i < N$ *(i.e.* $T_i \cap T_{i+1}$ *is nonempty and consists of a single element).*

Remark 3.1.1. *This definition is equivalent to the* hybrid time trajectory *in [Lyg+03]; we emphasize the natural (disjoint–union) topology to simplify the subsequent definition of an* execution*.*

Definition 3.1.3. *An* execution *of a hybrid dynamical system* $H = (D, F, G, R)$ *is a smooth map* $x : T \to D$ *over a hybrid time trajectory* $T = \coprod_{i=1}^{N} T_i$ *satisfying:*

1. $\forall t \in T : \frac{d}{dt}x(t) = F(x(t))$*;*
2. $\forall i < N : x|_{T_i}(t_i) \in G,\ R(x|_{T_i}(t_i)) = x|_{T_{i+1}}(t_i)$ *where* $\{t_i\} = T_i \cap T_{i+1}$*.*

If F is tangent to G at $x \in G$, there is a possible ambiguity in determining a trajectory from x since one may either follow the flow of F on D or apply the reset map to obtain a new initial condition $y = R(x)$.

Assumption 3.1.1. *F is outward–pointing on G.*

Remark 3.1.2. *The use of time–invariant vector fields and reset maps in Definition 3.1.1 is without loss of generality in the following sense. Suppose D is a hybrid manifold, $G \subset \partial D$ is open, and*

$$F : \mathbb{R} \times D \to TD,\ R : \mathbb{R} \times G \to D$$

define a time–varying vector field and reset map, respectively. Define

$$\widetilde{D} = \mathbb{R} \times D,\ \widetilde{G} = \mathbb{R} \times G,$$

and let $\widetilde{F} : \widetilde{D} \to T\widetilde{D}$, $\widetilde{R} : \widetilde{G} \to \widetilde{D}$ *be defined by*

$$\widetilde{F} = \left(\frac{\partial}{\partial t}, F\right) \in \mathfrak{T}(\mathbb{R} \times D),\ \widetilde{R} = (id_{\mathbb{R}}, R) : \mathbb{R} \times G \to \mathbb{R} \times D.$$

Then $\widetilde{H} = (\widetilde{D}, \widetilde{F}, \widetilde{G}, \widetilde{R})$ *is a hybrid dynamical system in the form of Definition 3.1.1.*

3.2 Periodic Orbits and Poincaré Maps

In this chapter, we are principally concerned with *periodic* executions of hybrid dynamical systems, which are nonequilibrium trajectories that intersect themselves; see Figure 3.2 for an illustration.

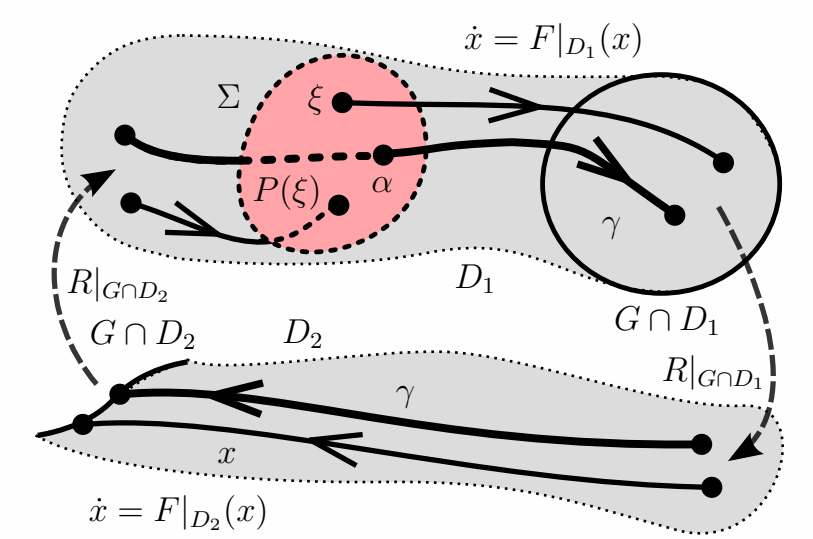

Figure 3.2: Illustration of a periodic orbit γ and Poincaré map $P : U \to \Sigma$ in a two–domain hybrid dynamical system $H = (D, F, G, R)$. The periodic orbit γ intersects the section $\Sigma \subset D_1$ transversally at $\{\alpha\} = \gamma \cap \Sigma$. An initial condition $\xi \in \Sigma$ sufficiently close to α yields an execution $x : T \to D$ that passes through Σ at the point $P(\xi)$. This defines a Poincaré map $P : U \to \Sigma$ over some neighborhood $\alpha \in U \subset \Sigma$. The point α is a fixed point of P, i.e. $P(\alpha) = \alpha$.

Definition 3.2.1. *An execution $\gamma : T \to D$ is* periodic *if there exists $s \in T$, $\tau > 0$ such that $s + \tau \in T$ and*

$$\gamma(s) = \gamma(s + \tau). \tag{3.2.1}$$

If there is no smaller positive number τ such that (3.2.1) holds, then τ is called the period *of γ, and we will say γ is a τ–*periodic orbit*.*

Remark 3.2.1. *The domain T of a periodic orbit may be taken to be the entire real line, $T = \mathbb{R}$, without loss of generality. In the sequel we conflate the execution $\gamma : \mathbb{R} \to D$ with its image $\gamma(\mathbb{R}) \subset D$.*

Motivated by the applications in Section 3.6, we restrict our attention to periodic orbits undergoing *isolated transitions*, i.e. a finite number of discrete transitions that occur at distinct time instants.

Assumption 3.2.1. *Any periodic orbit γ undergoes finitely many isolated discrete transitions each period.*

In addition to excluding *Zeno* periodic orbits [OA11] from our analysis, this assumption enables us to construct Poincaré maps (see [HS74; GH83] for the classical case) associated

with the hybrid periodic orbit γ. Roughly speaking, a *Poincaré map*

$$P : U \to \Sigma$$

is defined over an open subset $U \subset \Sigma$ of an embedded codimension–1 submanifold $\Sigma \subset D$ that intersects the periodic orbit at exactly one point

$$\{\alpha\} = \gamma \cap \Sigma$$

by tracing an execution from $x \in U$ forward in time until it intersects Σ at $P(x)$. The submanifold Σ is referred to as a *Poincaré section*. It is known that this procedure yields a map that is well–defined and smooth near the fixed point $\alpha = P(\alpha)$ [AG58; Gri+02; Ner+02; WA12]. The construction is more delicate than for continuous–time dynamical systems since trajectories of hybrid systems do not necessarily vary continuously with initial conditions; the proof of Lemma 3.2.1, below, contains formal details. Unlike the classical case, Poincaré maps in hybrid systems need not be full rank.

A straightforward application of Sylvester's inequality [CD91, Appendix A.5.3] shows that the rank of the Poincaré map is bounded above by the minimum dimension of all hybrid domains. More precise bounds are pursued elsewhere [WA12], but the following Proposition will suffice for the Applications in Section 3.6.

Proposition 3.2.1. *If $P : U \to \Sigma$ is a Poincaré map associated with a periodic orbit γ, then*

$$\forall x \in U : \operatorname{rank} DP(x) \leq \min_{j \in J} \dim D_j - 1.$$

It is a standard result for continuous–time dynamical systems that the eigenvalues of the linearization of the Poincaré map at its fixed point—commonly called *Floquet multipliers*—do not depend on the choice of Poincaré section [GH83, Section 1.5]. This generalizes to the hybrid setting in the sense that there exist similarity transformations relating the non–nilpotent portion of the Jordan forms for linearizations of Poincaré maps defined over different sections. Note that, since Proposition 3.2.1 implies that zero eigenvalues will generally have different algebraic multiplicity for linearized Poincaré maps obtained from sections located in hybrid domains with different dimensions, we do not expect the nilpotent Jordan blocks for these linear maps to bear any relation to one another.

Lemma 3.2.1. *If $P : U \to \Sigma$, $\widetilde{P} : \widetilde{U} \to \widetilde{\Sigma}$ are Poincaré maps associated with a periodic orbit γ with fixed points $P(\alpha) = \alpha$, $\widetilde{P}(\widetilde{\alpha}) = \widetilde{\alpha}$, then* $\operatorname{spec} DP(\alpha) \setminus \{0\} = \operatorname{spec} D\widetilde{P}(\widetilde{\alpha}) \setminus \{0\}$. *Moreover, with*

$$J = \begin{pmatrix} A & 0 \\ 0 & N \end{pmatrix}, \; \widetilde{J} = \begin{pmatrix} \widetilde{A} & 0 \\ 0 & \widetilde{N} \end{pmatrix}$$

denoting the Jordan canonical forms of $DP(\alpha)$ and $D\widetilde{P}(\widetilde{\alpha})$, where $0 \notin \operatorname{spec} A \cup \operatorname{spec} \widetilde{A}$ and N, $\widetilde{N}$ are nilpotent, we conclude that A is similar to $\widetilde{A}$.

Proof. The periodic orbit undergoes a finite number of transitions $k \in \mathbb{N}$, so we may index the corresponding sequence of domains as[1] $D_1, \dots, D_k$. Without loss of generality, assume the D_j's are distinct[2] and let $\{\alpha_j\} = \gamma \cap G \cap \partial D_j$ be the exit point of γ in D_j. We wish to construct the Poincaré map P_j associated with the periodic orbit over a neighborhood of α_j in G. For $j \in \{1, \dots, k\}$ let:

ϕ_j : $\mathcal{F}_j \to D_j$ be the maximal flow of $F|_{D_j}$ on D_j;

U_j $\subset D_j$ be a neighborhood of $R(\alpha_{j-1})$ over which Lemma 3.A.1 from Appendix 3.A.1 may be applied between $R(\alpha_{j-1}) \in D_j$ and $G \cap \partial D_j$ to obtain a time–to–impact map $\sigma_j : U_j \to \mathbb{R}$;

G_j $\subset G \cap \partial D_j$ be defined as $G_j = R^{-1}(U_{j+1})$;

ρ_j : $G_j \to G_{j+1}$ be defined by $\rho_j(x) = \phi_{j+1}(\sigma_{j+1} \circ R(x), R(x))$.

The Poincaré map defined over G_j is obtained formally by iterating the ρ's around the cycle:

$$P_j = \rho_{j-1} \circ \cdots \circ \rho_1 \circ \rho_k \circ \cdots \circ \rho_j. \tag{3.2.2}$$

The neighborhood $\Sigma_j \subset G_j$ of α_j over which this map is well–defined is determined by pulling G_j backward around the cycle,

$$\Sigma_j = \big(\rho_j^{-1} \circ \cdots \circ \rho_k^{-1} \circ \rho_1^{-1} \circ \cdots \circ \rho_{j-1}^{-1}\big)(G_j),$$

and similarly for any iterate of P_j. Note that $P_j(\alpha_j) = \alpha_j$ is a fixed point of P_j by construction. Without loss of generality we assume[3] $\Sigma, \widetilde{\Sigma} \subset G$ so that $P = P_j$ and $\widetilde{P} = P_i$ for some $i, j \in \{1, \dots, k\}$.

We proceed by showing that, given a chain of generalized eigenvectors associated with a non–zero eigenvalue of $DP_j(\alpha_j)$ for some $j \in \{1, \dots, k\}$, we can construct a chain of generalized eigenvectors associated with $DP_i(\alpha_i)$ for each $i \in \{1, \dots, k\}$. Fix $j \in \{1, \dots, k\}$ and $\lambda \in \operatorname{spec} DP_j(\alpha_j)$ with $\lambda \neq 0$. Suppose $\{x_j^\ell\}_{\ell=1}^m$ is a chain of generalized eigenvectors associated with λ, i.e. $DP_j(\alpha_j)x_j^m = \lambda x_j^m$ and for all $\ell \in \{1, \dots, m-1\}$:

$$x_j^\ell = (DP_j(\alpha_j) - \lambda I)x_j^{\ell+1}. \tag{3.2.3}$$

For all $\ell \in \{1, \dots, m\}$, define $x_{j+1}^\ell = D\rho_j(\alpha_j)x_j^\ell$ and note $D\rho_j(\alpha_j)DP_j(\alpha_j) = DP_{j+1}(\alpha_{j+1})D\rho_j(\alpha_j)$ by (3.2.2). Combining this observation with (3.2.3) yields

$$\begin{aligned} DP_{j+1}(\alpha_{j+1})x_{j+1}^m &= DP_{j+1}(\alpha_{j+1})D\rho_j(\alpha_j)x_j^m \\ &= D\rho_j(\alpha_j)DP_j(\alpha_j)x_j^m \\ &= \lambda D\rho_j(\alpha_j)x_j^m = \lambda x_{j+1}^m, \end{aligned}$$

[1] We regard subscripts modulo k so that $D_k \equiv D_0$.

[2] Otherwise we can find $\{B_j\}_{j=1}^k$ such that $B_j \subset D_j$ is open, $\bigcup_{j=1}^k B_j$ contains γ, and $B_i \cap B_j = \emptyset$ if $i \neq j$, then proceed on $\widetilde{D} = \coprod_{j=1}^k B_j$.

[3] Otherwise we may introduce fictitious guards Σ and/or $\widetilde{\Sigma}$ near γ and repeat the construction.

so that $\lambda \in \operatorname{spec} DP_{j+1}(\alpha_{j+1})$ and for all $\ell \in \{1, \ldots, m-1\}$:

$$\begin{aligned} x_{j+1}^{\ell} &= D\rho_j(\alpha_j) x_j^{\ell} \\ &= D\rho_j(\alpha_j)(DP_j(\alpha_j) - \lambda I) x_j^{\ell+1} \\ &= (DP_{j+1}(\alpha_{j+1}) D\rho_j(\alpha_j) - \lambda D\rho_j(\alpha_j)) x_j^{\ell+1} \\ &= (DP_{j+1}(\alpha_{j+1}) - \lambda I) x_{j+1}^{\ell+1}. \end{aligned}$$

Note that $\left\{x_{j+1}^{\ell}\right\}_{\ell=1}^{m}$ must be linearly independent since they map to the linearly independent collection $\left\{\lambda x_j^{\ell}\right\}_{\ell=1}^{m}$ through the composition of linear maps $D\rho_{j-1}(\alpha_{j-1}) \cdots D\rho_{j+1}(\alpha_{j+1})$. Therefore we conclude $\left\{x_{j+1}^{\ell}\right\}_{\ell=1}^{m}$ is a chain of generalized eigenvectors for $DP_{j+1}(\alpha_{j+1})$ associated with λ. Proceeding inductively, for any $i \in \{1, \ldots, k\}$ we obtain a corresponding chain for $DP_i(\alpha_i)$. Since the subspace associated with a maximal chain of generalized eigenvectors for a linear map is invariant under the linear map, it follows that the non–nilpotent Jordan blocks of $DP_j(\alpha_j)$ must be in one–to–one correspondence with those of $DP_i(\alpha_i)$ for any $i \in \{1, \ldots, k\}$. □

3.3 Exact Reduction

When iterates of the Poincaré map associated with a periodic orbit of a hybrid dynamical system have constant rank, executions initialized nearby converge in finite time to a constant–dimensional subsystem.

Theorem 3.3.1 (Exact Reduction)**.** *Let γ be a periodic orbit that undergoes isolated transitions in a hybrid dynamical system $H = (D, F, G, R)$, $P : U \to \Sigma$ a Poincaré map for γ, $m = \min_j \dim D_j$, and suppose there exists a neighborhood $V \subset U$ of $\{\alpha\} = \gamma \cap U$ and $r \in \mathbb{N}$ such that $\operatorname{rank} DP^m(x) = r$ for all $x \in V$. Then there exists an $(r+1)$–dimensional hybrid embedded submanifold $M \subset D$ and a hybrid open set $W \subset D$ for which $\gamma \subset M \cap W$ and trajectories starting in W contract to M in finite time.*

Proof. We begin in step (i) by applying Lemma 3.B.1 from Appendix 3.B.1 to construct an r–dimensional submanifold S of the Poincaré section Σ that is invariant under the Poincaré map P. Subsequently, in (ii) we flow S forward in time for one cycle, i.e. until it returns to Σ, to obtain for each $j \in J$ an $(r+1)$–dimensional submanifold $M_j \subset D_j$ that contains $\gamma \cap D_j$ and is invariant under F. Finally, in (iii) for each $j \in J$ we construct an open set $W_j \subset D_j$ containing $\gamma \cap D_j$ so that the collection $M = \coprod_{j \in J}$ attracts all trajectories initialized in the hybrid open set $W = \coprod_{j \in J}$ in finite time.

(i) Applying Lemma 3.B.1 from Appendix 3.B.1 to P, there is a neighborhood $V \subset U$ of $\{\alpha\} = \gamma \cap U$ such that $S = P^m(V)$ is an r–dimensional embedded submanifold of $U \subset \Sigma$, $P|_S$ maps S diffeomorphically onto $P(S)$, and $P(S) \cap S$ is an open subset of S. Without loss of generality we assume $U \subset G \cap \partial D_1$ and the periodic orbit γ passes through each domain once per cycle. For notational convenience, for each $j \in J$ we will let $j+1 \in J$ denote

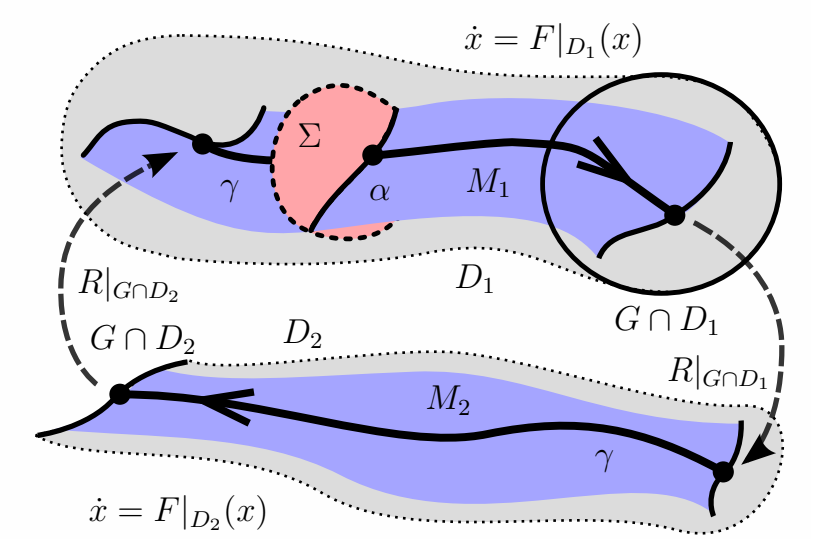

Figure 3.3: Applying Theorem 3.3.1 (Exact Reduction) to a hybrid dynamical system $H = (D, F, G, R)$ containing a periodic orbit γ with associated Poincaré map $P : U \to \Sigma$ yields an invariant subsystem $M = \coprod_{j\in J} M_j$. Nearby trajectories contract to M in finite time.

the subsequent domain visited by γ (i.e. we identify J with an additive monoid of integers modulo $|J|$). Set

$$\{\alpha_1\} = \gamma \cap G \cap \partial D_1,$$

let $U_2 \subset D_2$ be a neighborhood of $R(\alpha_1)$ over which Lemma 3.A.1 from Appendix 3.A.1 may be applied to construct a time–to–impact map $\sigma_2 : U_2 \to \mathbb{R}$, let $G_1 = R^{-1}(U_2)$ be a neighborhood of α_1 in $G \cap \partial D_1$, and let $\phi_1 : \mathcal{F}_1 \to D_1$ the maximal flow of $F|_{D_1}$ on D_1. Proceed inductively forward around the cycle to construct, for each $j \in J$: the exit point

$$\{\alpha_j\} = \gamma \cap G \cap \partial D_j;$$

time–to–impact map $\sigma_j : U_j \to \mathbb{R}$ over a neighborhood $U_j \subset D_j$ containing $R(\gamma_{j-1})$; a neighborhood

$$G_j = R^{-1}(U_{j+1}) \subset G \cap \partial D_j$$

containing α_j; and the maximal flow $\phi_j : \mathcal{F}_j \to D_j$ of $F|_{D_j}$ on D_j.

(ii) By flowing S forward through one cycle, for each $j \in J$ we will construct a submanifold $M_j \subset D_j$ that is diffeomorphic to $[0, 1] \times \mathbb{R}^r$. Observe that, since $P|_S$ is a diffeomorphism, with $S_1 = S \cap G_1$ we have that the restriction $R|_{S_1}$ is a diffeomorphism onto its image and $F|_{R(S_1)}$ is nowhere tangent to $R(S_1)$. Let $M_2 \subset D_2$ be the embedded submanifold obtained by flowing $R(S_1)$ to $G\cap\partial D_2$, and let $S_2 = M_2\cap G_2$; observe that S_2 is diffeomorphic to S_1, M_2 is diffeomorphic to $[0, 1]\times S_2$, and $F|_{D_2}$ is tangent to M_2. Proceed inductively forward around the cycle to construct, for each $j \in J$, an embedded submanifold $S_j \subset G_j$ diffeomorphic to

S_1 and a submanifold $M_j \subset D_j$ diffeomorphic to $[0,1] \times S_j$ such that $F|_{D_j}$ is tangent to M_j. Note that S_1 is diffeomorphic to the r–dimensional manifold $\mathbb{R}^r$, so $\dim M_j = r+1$ for each $j \in J$. The subsystem

$$M = \coprod_{j \in J} M_j \subset D$$

contains γ, is invariant under the continuous flow by construction, and is invariant under the reset map in the sense that

$$R^{-1}(M) \cap M \subset G \cap M$$

is open.

(iii) Finally, let

$$W_1 = \phi_j^{-1}(\mathbb{R} \times V) \subset D_1$$

be the open set that flows into V, where $S = P^m(V)$ was defined in step (i). Let

$$W_{|J|} = \phi_{|J|}^{-1}(R^{-1}(W_1)) \subset D_{|J|}$$

be the open set that flows into W_1 where $|J|$ denotes the number of elements in J. Proceed inductively backward around the cycle to construct, for each $j \in J$, an open set $W_j \subset D_j$ that flows into S in finite time. Then the hybrid open set

$$W = \coprod_{j \in J} W_j \subset D$$

contains γ and all executions initialized in W flow into $S \subset M$ in finite time. □

Since M is invariant under the continuous dynamics (i.e. $F|_M$ is tangent to M) and the discrete dynamics (i.e. $R(G \cap M) \subset M$), it determines a hybrid subsystem that governs the stability of γ in H.

Corollary 3.3.1. *The collection*

$$H|_M = (M, F|_M, G \cap M, R|_{G \cap M})$$

is a hybrid dynamical system with periodic orbit γ.

See Figure 3.4 for an illustration of this subsystem.

Corollary 3.3.2. *The periodic orbit γ is Lyapunov (resp. asymptotically, exponentially) stable in H if and only if γ is Lyapunov (resp. asymptotically, exponentially) stable in $H|_M$.*

When the rank at the fixed point $\alpha = P(\alpha)$ achieves the upper bound stipulated by Proposition 3.2.1, the following Corollary ensures that DP^m is constant rank (and hence Theorem 3.3.1 may be applied). This is important since it is possible to compute a lower bound for rank $DP^m(\alpha)$ via numerical simulation [Bur+13a].

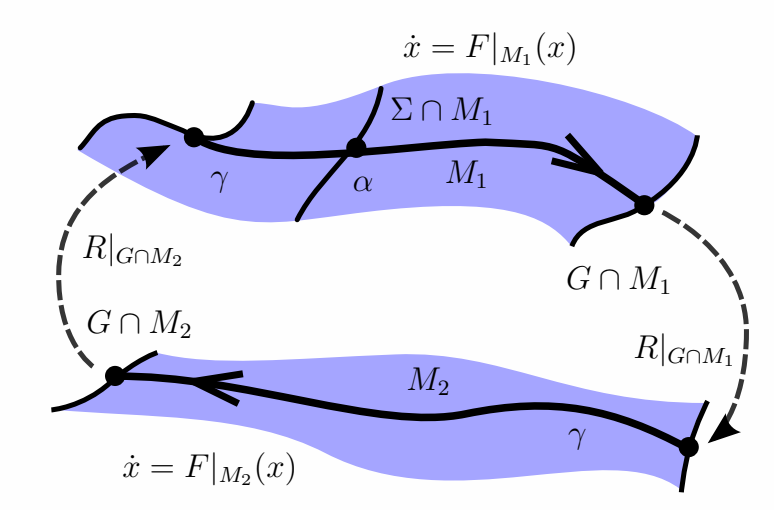

Figure 3.4: The subsystem obtained by applying Theorem 3.3.1 near a periodic orbit γ may be extracted to yield a hybrid dynamical system $H|_M = (M, F|_M, G \cap M, R|_{G\cap M})$.

Corollary 3.3.3. *If $DP^m(\alpha)$ achieves the upper bound specified by Proposition 3.2.1, i.e.*

$$\operatorname{rank} DP^m(\alpha) = \min_{j\in J} \dim D_j - 1 = m - 1,$$

then there exists an open set $V \subset U$ containing α such that $\operatorname{rank} DP^m(x) = m - 1$ for all $x \in V$. Thus the hypotheses of Theorem 3.3.1 are satisfied with $r = m - 1$.

If the Poincaré map attains the same constant rank r for two subsequent iterates, it is not necessary to continue up to iterate $m = \min_j \dim D_j$ before checking the hypotheses of Theorem 3.3.1.

Corollary 3.3.4. *If there exists a neighborhood $W \subset U$ of α and $k, r \in \mathbb{N}$ such that*

$$\forall x \in W : \operatorname{rank}\ DP^k(x) = r \text{ and } \operatorname{rank}\ DP^{k+1}(\alpha) = \operatorname{rank}\ DP^k(\alpha),$$

then there exists a neighborhood $V \subset W$ of α such that

$$\operatorname{rank}\ DP^m(x) = r$$

for all $x \in V$. Thus the hypotheses of Theorem 3.3.1 are satisfied with $r = \operatorname{rank}\ DP^k(\alpha)$.

Proof. We know $\operatorname{rank} DP^m(\alpha) = r$ since k bounds the *ascent* of $DP(\alpha)$ [CD91, §4.3], so $\operatorname{rank} DP^m \geq r$ near α. But by Sylvester's inequality we have

$$\operatorname{rank} DP^m(x) \leq \min\{\operatorname{rank} DP^{m-k}(P^k(x)), \operatorname{rank} DP^k(x)\}$$

for all x near α. Therefore $\operatorname{rank} DP^m \equiv r$ near α. □

The choice of Poincaré section in Theorem 3.3.1 is irrelevant in the sense that the Poincaré map $\widetilde{P} : \widetilde{U} \to \widetilde{\Sigma}$ defined over any other Poincaré section $\widetilde{\Sigma}$ will be constant–rank in a neighborhood $\widetilde{V} \subset \widetilde{U}$ of its fixed point $\{\widetilde{\alpha}\} = \gamma \cap \widetilde{\Sigma}$, as the following Corollary shows; this follows directly from Lemma 4 in [Bur+11a].

Corollary 3.3.5. *Under the hypotheses of Theorem 3.3.1, if $\widetilde{P} : \widetilde{U} \to \widetilde{\Sigma}$ is any other Poincaré map for γ with fixed point $\widetilde{\alpha} = \widetilde{P}(\widetilde{\alpha})$, then there exists an open subset $\widetilde{V} \subset \widetilde{U}$ containing $\widetilde{\alpha}$ such that*

$$\forall x \in \widetilde{V} : \operatorname{rank} D\widetilde{P}^m(x) = r.$$

Thus the hypotheses of Theorem 3.3.1 are satisfied for $\widetilde{P}$ with $r = \operatorname{rank}\, D\widetilde{P}^m(\alpha)$.

3.4 Approximate Reduction

Restricting our attention to exponentially stable periodic orbits, we find that a hybrid system generically contracts superexponentially to a constant–dimensional subsystem near a periodic orbit.

Theorem 3.4.1 (Approximate Reduction)**.** *Let γ be an exponentially stable periodic orbit undergoing isolated transitions in a hybrid dynamical system $H = (D, F, G, R)$, $P : U \to \Sigma$ a Poincaré map for γ with fixed point $\{\alpha\} = \gamma \cap \Sigma$, $m = \min_j \dim D_j$, and $r = \operatorname{rank} DP^m(\alpha)$. Then there exists an $(r+1)$–dimensional hybrid embedded submanifold $M \subset D$ such that for any $\varepsilon > 0$ there exists a hybrid open set $W^\varepsilon \subset D$ for which $\gamma \subset M \cap W^\varepsilon$ and the distance from trajectories starting in W^ε to M contracts by ε each cycle.*

Proof. We begin with an overview of the proof strategy. First (i), for each $j \in J$ we construct a Poincaré map P_j over a Poincaré section $\Sigma_j \subset G \cap \partial D_j$ and apply Lemma 3.B.2 from Appendix 3.B.2 to obtain a change–of–coordinates in which P_j splits into two components: a linear map that only depends on the first r coordinates and a nonlinear map whose linearization is nilpotent at the fixed point of P_j. Second (ii), for each $j \in J$ we construct an r–dimensional submanifold $S_j \subset \Sigma_j$ such that $R|_{S_j}$ is a diffeomorphism near the fixed point of P_j. We subsequently flow the image $R(S_j)$ forward until it impacts the guard to construct an $(r+1)$–dimensional submanifold $M_{j+1} \subset D_{j+1}$ that contains $\gamma \cap D_{j+1}$ and is invariant under F. Third (iii), for each $j \in J$ we apply Lemma 3.B.3 from Appendix 3.B.3 to construct a distance metric on an open set $W_j \subset D_j$ containing $\gamma \cap D_j$ with respect to which executions contract superexponentially toward M_j.

(i) Without loss of generality we assume $U \subset G \cap \partial D_1$ the periodic orbit γ passes through each domain once per cycle. As in the proof of Theorem 3.3.1, for each $j \in J$ we will let $j+1 \in J$ denote the subsequent domain visited by γ (i.e. we identify J with an additive monoid of integers modulo $|J|$). For each $j \in J$ let $P_j : U_j \to \Sigma_j$ be a Poincaré map for γ defined over

$$U_j \subset \Sigma_j \subset G \cap \partial D_j,$$

and let

$$\{\alpha_j\} = \gamma \cap G \cap \partial D_j$$

be the exit point of γ in D_j. By a straightforward application of Sylvester's inequality [CD91, Appendix A.5.4], we find $\operatorname{rank} DP_j^m(\alpha_j) = r$ for all $j \in J$. Applying Lemma 3.B.2 from Appendix 3.B.2 implies that for each $j \in J$ there exists an open set $V_j \subset U$ containing α_j and a C^1 diffeomorphism $\varphi_j : V_j \to \mathbb{R}^{n_j-1}$ where $n_j = \dim D_j$ such that $\varphi_j(\alpha_j) = 0$ and the coordinate representation

$$\widetilde{P}_j = \varphi_j \circ P_j \circ \varphi_j^{-1}$$

of P_j has the form

$$\widetilde{P}_j(z_j, \zeta_j) = (A_j z_j,\ S_j(z_j, \zeta_j))$$

where $z_j \in \mathbb{R}^r$, $\zeta_j \in \mathbb{R}^{n_j-1-r}$, $A_j \in \mathbb{R}^{r\times r}$ is invertible, $S_j(0,0) = 0$, and $D_{\zeta_j} S_j(0,0)$ is nilpotent. For each $j \in J$, let $\Pi_j : V_j \to G$ be a smooth map defined as follows. Given $x \in V_j$, write $(z_x, \zeta_x) = \varphi_j(x) \in \mathbb{R}^r \times \mathbb{R}^{n_j-r-1}$ and let $\Pi_j(x) = \varphi_j^{-1}(z_x, 0)$.

(ii) Fix $j \in J$ and let

$$N_j = \varphi_j^{-1}(\mathbb{R}^r \times \{0\}) \subset V_j,$$

which is an r–dimensional embedded submanifold tangent to the non–nilpotent eigendirections of $DP_j^m(\alpha_j)$. Observe that

$$\operatorname{rank} DR|_{G\cap N_j}(\alpha_j) = r = \dim N_j,$$

hence by the Inverse Function Theorem [Lee12, Theorem C.34] there is a neighborhood $S_j \subset N_j$ containing α_j such that $R|_{S_j} : S_j \to D$ is a diffeomorphism onto its image $R(S_j) \subset D_{j+1}$. Furthermore, since $\operatorname{rank} DP_j^m(\alpha_j) = r$, the vector field is transverse to $R(S_j)$ at α_j, i.e.

$$F(R(\alpha_j)) \notin T_{R(\alpha_j)} R(S_j),$$

and we assume S_j was chosen small enough so that F is transverse along all of $R(S_j)$. Let $M_{j+1} \subset D_{j+1}$ be the embedded submanifold obtained by flowing $R(S_j)$ forward to G; note that M_{j+1} is diffeomorphic to $[0,1] \times \mathbb{R}^r$. Observe that

$$M = \coprod_{j\in J} M_j$$

is invariant under the continuous flow (i.e. $F|_M$ is tangent to M) and approximately invariant under the reset map in the sense that $DR|_{G\cap M}$ is tangent to M on γ: for all $j \in J$ and $\delta \in T_{\alpha_j}(G \cap M)$ we have

$$DR|_{G\cap M}(\alpha_j)\delta \in T_{R(\alpha_j)} M.$$

Observe that $R \circ \Pi_j|_{G\cap M_j} : G \cap M_j \to M_{j+1}$ is a diffeomorphism onto its image.

(iii) Fix $\varepsilon > 0$ and apply the construction in the proof of Lemma 3.B.3 from Appendix 3.B.3 to obtain a radius $\delta > 0$ and for each $j \in J$ a norm

$$\|\cdot\|_j^\varepsilon : \mathbb{R}^{n_j-1} \to \mathbb{R}$$

such that the nonlinearity

$$\widetilde{P}_j(z_j, \zeta_j) - (A_j z_j, 0)$$

contracts exponentially fast with rate ε on $B_\delta^{n_j-1}(0) \subset \mathbb{R}^{n_j-1}$ as measured by $\|\cdot\|_j^\varepsilon$. For each $j \in J$ define

$$V_j^\varepsilon = \varphi_j^{-1}(B_\delta^{n_j-1}(0)) \subset G \cap \partial D_j,$$

let $\phi_j : \mathcal{F}_j \to D_j$ denote the maximal flow of $F|_{D_j}$ on D_j, and let

$$W_j^\varepsilon = \phi_j^{-1}(\mathbb{R} \times V_j^\varepsilon) \subset D_j$$

be the (open) set of points that flow into V_j^ε. Since ϕ_j is the flow of a smooth vector field transverse to V_j^ε, any $x \in W_j^\varepsilon$ can be written uniquely as $x = \phi_j(t_x, v_x)$ for some $t_x \leq 0$ and $v_x \in V_j^\varepsilon$. Using this representation, we endow W_j^ε with a distance metric $d_j^\varepsilon : W_j^\varepsilon \times W_j^\varepsilon \to \mathbb{R}$ by defining

$$d_j^\varepsilon(x, y) = |t_x - t_y| + \|\varphi_j(v_x) - \varphi_j(v_y)\|_j^\varepsilon.$$

Observe that the exponential contraction of $\widetilde{P}_j$ at rate ε in $\|\cdot\|_j^\varepsilon$ to $\varphi_j(M_j \cap G)$ implies exponential contraction of executions initialized in W_j^ε at rate ε to M in d_j^ε.

Finally, let $W^\varepsilon = \coprod_{j \in J} W_j^\varepsilon$ and $M^\varepsilon = M \cap W^\varepsilon$. Define a smooth hybrid map $\Pi^\varepsilon : G \cap W^\varepsilon \to G$ piecewise for each $j \in J$ by observing that $G \cap W_j^\varepsilon \subset V_j$ and letting $\Pi^\varepsilon(x) = \Pi_j(x)$ for all $x \in G \cap W_j^\varepsilon$. □

Corollary 3.4.1. *Letting $M^\varepsilon = M \cap W^\varepsilon$, the collection $H|_{M^\varepsilon} = (M^\varepsilon, F|_{M^\varepsilon}, G \cap M^\varepsilon, R \circ \Pi^\varepsilon|_{G \cap M^\varepsilon})$ is a C^1 hybrid dynamical system with periodic orbit γ, where $\Pi^\varepsilon : G \cap W^\varepsilon \to G$ is the smooth hybrid map constructed in the proof of Theorem 3.4.1.*

Although the submanifold $M \subset D$ is invariant under the continuous dynamics of H in the sense that $F|_M$ is tangent to M, the reset map must be modified to ensure M is invariant under the discrete dynamics. However, since $DR|_{G \cap M^\varepsilon} = D(R \cap \Pi^\varepsilon)|_{G \cap M^\varepsilon}$, the map Π does not affect R to first order.

Remark 3.4.1. *We emphasize that hypothesis on the rank of the Poincaré map $P : U \to \Sigma$ in Theorem 3.4.1 (*$\operatorname{rank} DP^m(\alpha) = r$ *at the point $\{\alpha\} = \gamma \cap \Sigma$) is weaker than the hypothesis in Theorem 3.3.1 (*$\operatorname{rank} DP^m(x) = r$ *for all x in an open set $V \subset U$). In particular, approximating the rank over an uncountably infinite set typically involves estimates on higher–order derivatives of P^m.*

If the rank is constant for two subsequent iterates of the linearized Poincaré map, then the rank is constant for all subsequent iterates, including iterate $m = \min_j \dim D_j$.

Corollary 3.4.2. *If there exist $k \in \mathbb{N}$ such that* $\operatorname{rank}\ DP^k(\alpha) = \operatorname{rank}\ DP^{k+1}(\alpha)$, *then*

$$\operatorname{rank}\ DP^m(\alpha) = \operatorname{rank}\ DP^k(\alpha).$$

Thus the hypotheses of Theorem 3.4.1 are satisfied with $r = \operatorname{rank}\ DP^k(\alpha)$.

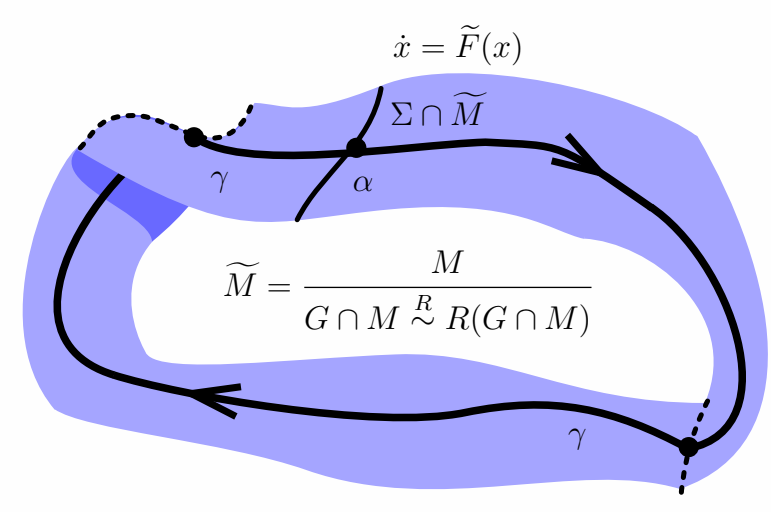

Figure 3.5: The hybrid subsystem $H|_M$ obtained by Corollary 3.3.1 to Theorem 3.3.1 (Exact Reduction) may be smoothed via Theorem 3.5.1 (Smoothing) to yield a continuous-time dynamical system $(\widetilde{M}, \widetilde{F})$.

3.5 Smoothing

The subsystems yielded by Theorems 3.3.1 and 3.4.1 on *exact* and *approximate* reduction share important properties: the constituent manifolds have the same dimension; the reset map is a hybrid diffeomorphism between disjoint portions of the boundary; and the vector field points inward along the range of the reset map. Under these conditions, we can globally *smooth* the hybrid transitions using techniques from differential topology to obtain a single continuous–time dynamical system. Executions of the hybrid (sub)system are preserved as integral curves of the continuous–time system. This provides a smooth n–dimensional generalization of the *hybrifold* construction in [Sim+05], the *phase space* constructed in [Sch98] to analyze mechanical impact, as well as the change–of–coordinates constructed in [De10, §3.1.1] to simplify analysis of juggling.

Theorem 3.5.1 (Smoothing)**.** *Let $H = (M, F, G, R)$ be a hybrid dynamical system with $M = \coprod_{j \in J} M_j$. Suppose $\dim M_j = n$ for all $j \in J$, $R(G) \subset \partial M$, $\partial M = G \coprod R(G)$, R is a hybrid diffeomorphism onto its image, and F is inward–pointing along $R(G)$. Then the topological quotient*

$$\widetilde{M} = \frac{M}{G \overset{R}{\sim} R(G)}$$

may be endowed with the structure of a smooth manifold such that:

1. *the quotient projection $\pi : M \to \widetilde{M}$ restricts to a smooth embedding for each $j \in J$:*

$$\pi|_{M_j} : M_j \to \widetilde{M};$$

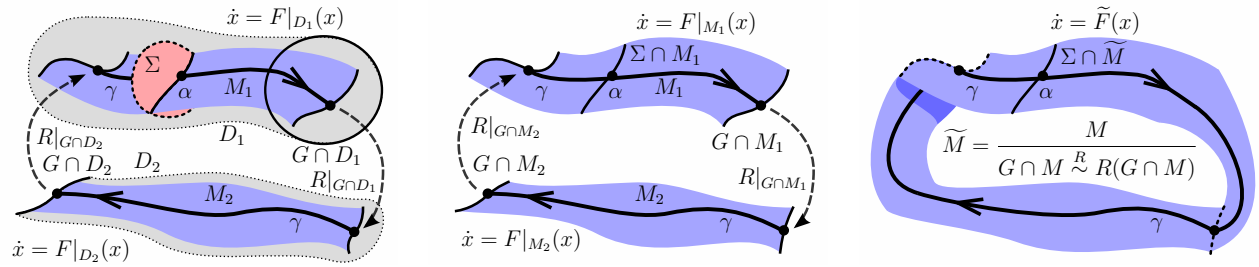

(a) $H = (D, F, G, R)$ (b) $H|_M = (M, F|_M, G \cap M, R|_{G\cap M})$ (c) $(\widetilde{M}, \widetilde{F})$

Figure 3.6: *Reduction to and smoothing of a hybrid subsystem.* (a) Applying Theorem 3.3.1 (Exact Reduction) to a hybrid dynamical system $H = (D, F, G, R)$ containing a periodic orbit γ with associated Poincaré map $P : U \to \Sigma$ yields an invariant subsystem $M = \coprod_{j\in J} M_j$; nearby trajectories contract to M in finite time. (b) The subsystem may be extracted to yield a hybrid dynamical system $H|_M$. (c) The hybrid system $H|_M$ may subsequently be smoothed via Theorem 3.5.1 (Smoothing) to yield a continuous-time dynamical system $(\widetilde{M}, \widetilde{F})$. Application of Theorem 3.5.1 to the subsystem yielded by Theorem 3.4.1 (Approximate Reduction) is illustrated by replacing $H|_M$ in (b) by $H|_{M^\varepsilon}$.

2. *there is a smooth vector field* $\widetilde{F} \in \mathfrak{T}(\widetilde{M})$ *such that any execution* $x : T \to M$ *of* H *descends to an integral curve of* $\widetilde{F}$ *on* $\widetilde{M}$ *via* $\pi : M \to \widetilde{M}$*:*

$$\forall t \in T : \frac{d}{dt}\pi \circ x(t) = \widetilde{F}(\pi \circ x(t)).$$

Proof. Let $S \subset G \cap M_i$ be a connected component in some domain $i \in J$, and let $k \in J$ be the index for which $R(S) \subset M_k$. The hypotheses of this Theorem together with Assumption 3.1.1 ensure Lemma 3.A.2 from Appendix 3.A.2 may be applied to attach M_i to M_k to yield a new smooth manifold $\widetilde{M}_{ik}$. The hybrid system defined over the domain

$$\coprod\left\{\widetilde{M}_{ik}\right\} \cup \{M_j : j \in J \setminus \{i, k\}\}$$

and guard $G \setminus S$ satisfies the hypotheses of this Theorem, hence we may inductively attach domains on each connected component that remains in $G \setminus S$. This yields a smooth manifold $\widetilde{M}$ and vector field $\widetilde{F} \in \mathfrak{T}(\widetilde{M})$ with the required properties. □

Remark 3.5.1. *As illustrated in Figure 3.6, Theorem 3.5.1 is applicable to the subsystems* $H|_M$, $H|_{M^\varepsilon}$ *that emerge as a consequence of the Corollaries to Theorems 3.3.1 and 3.4.1, respectively. Thus a class of hybrid models for periodic phenomena may be reduced (exactly or approximately) to smooth dynamical systems.*

3.6 Applications

The Theorems of Section 3.1.5 apply directly to autonomous hybrid dynamical systems; in Section 3.6.1 we demonstrate that reduction to a smooth subsystem can occur spontaneously in a mechanical system undergoing intermittent impacts. The results are also applicable to systems with control inputs; in Section 3.6.2 we synthesize a state–feedback control law that reduces a family of multi–leg models for lateral–plane locomotion to a common low–dimensional subsystem, and in Section 3.6.3 we analyze the structural stability of event–triggered deadbeat control laws for locomotion. Finally, the reduction of hybrid dynamics to a smooth subsystem provides a route through which tools from classical dynamical systems theory can be generalized to the hybrid setting; in Section 3.6.4 we extend a normal form for limit cycles.

3.6.1 Spontaneous Reduction in a Vertical Hopper

In this section, we apply Theorem 3.3.1 (Exact Reduction) to the *vertical hopper* example shown in Figure 3.7. This system evolves through an *aerial* mode and a *ground* mode. In the aerial mode, the lower mass moves freely at or above the ground height. Transition to the ground mode occurs when the lower mass reaches the ground height with negative velocity, where it undergoes a perfectly plastic impact (i.e. its velocity is instantaneously set to zero). In the ground mode, the lower mass remains stationary. Transition to the aerial mode occurs when the aerial mode force allows the mass to lift off. We now formulate this model in the hybrid dynamical system framework of Definition 3.1.1.

The aerial mode D_a (see Figure 3.7 for notation) consists of

$$(y, \dot{y}, x, \dot{x}) \in D_a = T\mathbb{R} \times T\mathbb{R}_{\geq 0},$$

and the vector field $F|_{D_a}$ is given by $\mu\ddot{y} = k(\ell - (y - x)) - \mu g$, $m\ddot{x} = -k(\ell - (y - x)) - b\dot{x} - mg$. The boundary

$$\partial D_a = \{(y, \dot{y}, x, \dot{x}) \in D_a : x = 0\}$$

contains the states where the lower mass has just impacted the ground, and a hybrid transition occurs on the subset

$$G_a = \{(y, \dot{y}, 0, \dot{x}) \in \partial D_a : \dot{x} < 0\}$$

of the boundary D_a where the lower mass has negative velocity. The state is reinitialized in the ground mode via $R|_{G_a} : G_a \to D_g$ defined by

$$R|_{G_a}(y, \dot{y}, 0, \dot{x}) = (y, \dot{y}).$$

In the ground mode

$$D_g = \{(y, \dot{y}) \in T\mathbb{R} : -k(\ell - y) \leq mg\},$$

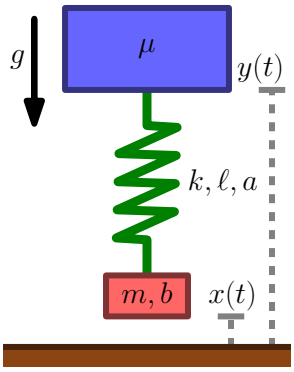

Figure 3.7: *Schematic of vertical hopper from Section 3.6.1.* Two masses m and μ, constrained to move vertically above a ground plane in a gravitational field with magnitude g, are connected by a linear spring with stiffness k and nominal length ℓ. The lower mass experiences viscous drag proportional to velocity with constant b when it is in the air, and impacts plastically with the ground (i.e. it is not permitted to penetrate the ground and its velocity is instantaneously set to zero whenever a collision occurs). When the lower mass is in contact with the ground, the spring stiffness is multiplied by a constant $a > 1$.

the boundary consists of the set of configurations where the force in the aerial mode allows the lower mass to lift off,

$$\partial D_g = \{(y, \dot{y}) \in D_g : -k(\ell - y) = mg\},$$

and the vector field $F|_{D_g}$ is given by

$$\mu\ddot{y} = ak(\ell - y) - \mu g.$$

A hybrid transition occurs when the forces balance and will instantaneously increase to pull the mass off the ground,

$$G_g = \{(y, \dot{y}) \in \partial D_g : \dot{y}(t) > 0\},$$

and the state is reset via $R|_{G_g} : G_g \to D_a$ defined by

$$R|_{G_g}(y, \dot{y}) = (y, \dot{y}, 0, 0).$$

This defines a hybrid dynamical system (D, F, G, R) where

$$D = D_a \coprod D_g,\ F \in \mathfrak{T}(D),\ G = G_a \coprod G_g,\ R : G \to D.$$

With parameters

$$(m, \mu, k, b, \ell, a, g) = (1, 3, 10, 5, 2, 2, 2),$$

numerical simulations suggest the vertical hopper possesses a stable periodic orbit

$$\gamma = (y^*, \dot{y}^*, x^*, \dot{x}^*)$$

to which nearby trajectories $(y, \dot{y}, x, \dot{x})$ converge asymptotically. Choosing a Poincaré section Σ in the ground domain D_g at mid-stance,

$$\Sigma = \{(y, \dot{y}) : \dot{y} = 0\} \subset D_g,$$

we find numerically[4] using parameter values given in the caption of Figure 3.7 that the hopper possesses a stable periodic orbit γ that intersects the Poincaré section at $\gamma \cap \Sigma = \{\alpha\}$ where

$$\alpha = (y, \dot{y}) \approx (0.94, 0.00).$$

Using finite differences, we determine that the linearization DP of the associated scalar–valued Poincaré map $P : \Sigma \to \Sigma$ has eigenvalue $\operatorname{spec} DP(\alpha) \approx 0.57$ at the fixed point $P(\alpha) = \alpha$. The rank of the Poincaré map P attains the upper bound of Proposition 3.2.1, hence Corollary 3.3.3 implies the rank hypothesis of Theorem 3.3.1 (Exact Reduction) is satisfied. Thus the dynamics of the hopper collapse to a one degree–of–freedom mechanical system after a single hop. Geometrically, the portion of the reduced subsystem in each domain is diffeomorphic to $[0, 1] \times \mathbb{R}$. Algebraically, the constraint that activates when the lower mass impacts the ground transfers to the aerial mode where no such physical constraint exists: the lower mass state $(x, \dot{x})$ is uniquely determined by the upper mass state $(y, \dot{y})$ for all future times.

3.6.2 Reducing a $(3 + 2n)$ DOF Polyped to a 3 DOF LLS

A primary motivation for the present work is analysis of legged locomotion. Several approaches have been proposed for embedding lower–dimensional dynamics in legged robot systems, notably *hybrid zero dynamics* [Wes+03] and *active embedding* [AS11]. Complementing these engineering approaches and predating them, the *templates and anchors hypotheses* (TAH) [FK99] conjectures that animal locomotion behaviors arise through reduction of the *anchor* dynamics governing the nervous system and body [Hol+06] to lower–dimensional *template* dynamics that encode a specific behavior [SH00b; Ghi+03]. One well–studied template is the Lateral Leg Spring (LLS) [SH00b] model for sprawled posture running, which has been shown to match how cockroaches run and begin to recover from perturbations [JF02]. Higher–dimensional neuromechanical variants of the model have been shown to reduce states associated with the nervous system [Hol+06]. In this section, we focus on reduction in the mechanical dynamics of limbs. Specifically, we synthesize a state–feedback control law under which the underactuated lateral–plane polyped illustrated in Figure 3.8a exactly reduces to the Lateral Leg–Spring (LLS) [SH00b] model in Figure 3.8b. With n limbs, the polyped

[4] For numerical simulations, we use a recently–developed algorithm [Bur+13a] with step size $h = 1 \times 10^{-2}$ and relaxation parameter $\epsilon = 1 \times 10^{-10}$.

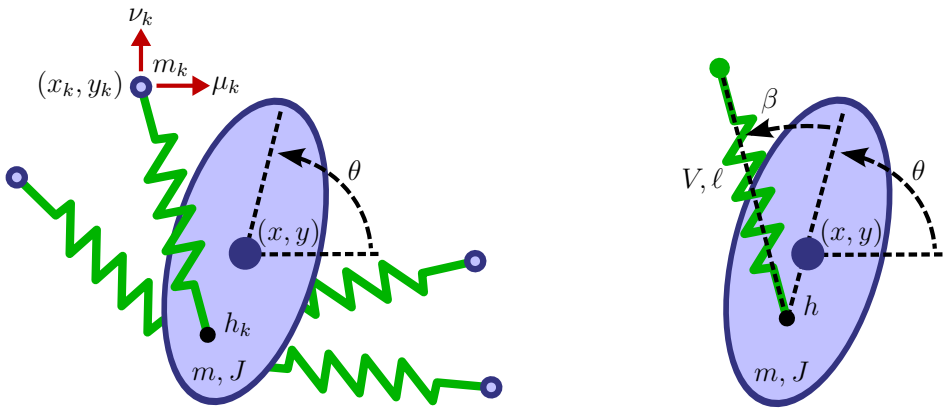

(a) polyped with $n = 4$ legs; leg $\#k$ is annotated (b) Lateral Leg–Spring (LLS) [SH00b]

Figure 3.8: Schematics for lateral–plane locomotion models described in Section 3.6.2.

possesses $(3 + 2n)$ degrees–of–freedom (DOF); the LLS has 3 DOF. This example serves a dual purpose: first, it demonstrates how our theoretical results can be applied to reduce an arbitrary number of DOF in a locomotion model; second, it suggests a mechanism that legged robot controllers could exploit to *anchor* a desired *template*.

Before we proceed with describing the reduction procedure in detail, we give an overview of the approach and the connection with Theorem 3.3.1. We begin in Section 3.6.2 by describing the dynamics of the LLS template and polyped anchor. Then in Section 3.6.2 we construct a smooth state feedback law that ensures that trajectories of the polyped body exactly match those of the LLS; we accomplish this by simply ensuring the net *wrench* [Mur+94] comprised of generalized forces and torques acting on the polyped body matches that of the LLS for all time. Subsequently, in Section 3.6.2 we modify the feedback law to further ensure the states associated with the polyped's limbs reduce after a single stride via Theorem 3.3.1. Finally, in Section 3.6.2 we discuss the effect of perturbations on the closed–loop reduced–order system.

Dynamics of Lateral Leg–Spring (LLS) and n–leg polyped

The LLS is an energy–conserving lateral–plane model for locomotion comprised of a massless leg–spring with elastic potential V affixed at hip position h to an inertial body with two translational (x, y) and one rotational (θ) DOF. The system is initialized at the start of a stride by orienting the leg at a fixed angle β with respect to the body at rest length ℓ and touching the foot down such that the leg will instantaneously contract. The step ends once the leg extends to its rest length by touching the foot down on the opposite side of the body; subsequent steps are defined inductively. In certain parameter regimes, the model possesses a periodic running gait [SH00b].

The underactuated hybrid control system illustrated in Figure 3.8a extends neurome-

chanical models previously proposed to study multi–legged locomotion [Hol+06; Kuk+09] by introducing masses into $n \geq 4$ feet connected by massless limbs affixed at hip locations $\{h_k\}_{k=1}^n$ on the inertial body. We assume that each foot can attach or detach from the substrate at any time, and the transition from *swing* to *stance* entails a plastic impact that annihilates the kinetic energy in a foot. We assume that each limb k is fully–actuated; for simplicity we assume the inputs act along the Cartesian coordinates and do not saturate so that any $(\mu_k, \nu_k) \in \mathbb{R}^2$ is feasible at any limb configuration. We let

$$q_0 = (x, y, \theta) \in Q_0 = \mathbb{R}^2 \times S^1$$

denote the position and orientation of the body, and for each $k \in \{1, \ldots, n\}$ we let

$$q_k = (x_k, y_k) \in Q_k \in \mathbb{R}^2$$

denote the position of the k–th foot. The configuration space of the polyped is the $(n+1)$–fold product

$$\prod_{k=0}^{n} Q_k.$$

The n–leg polyped's dynamics thus have the form

$$M\ddot{q}_0 = \sum_{k=1}^{n} (-\mu_k, -\nu_k, 0)\,\mathrm{Ad}_{g_k}, \;\; m_k \ddot{q}_k = (\mu_k, \nu_k) \tag{3.6.1}$$

where $M = \mathrm{diag}(m, m, J) \in \mathbb{R}^{3\times 3}$ is the mass distribution of the body and $\mathrm{Ad}_{g_k} \in \mathbb{R}^{3\times 3}$ transforms a wrench applied at the k–th hip to an equivalent wrench applied at the body center–of–mass [Mur+94, §5.1].

Embedding LLS in polyped

For any subset $K \subset \{1, \ldots, n\}$ of limbs, let

$$\sum_{k\in K} (-\mu_k, -\nu_k, 0)\,\mathrm{Ad}_{g_k} \in T^*Q_0 \tag{3.6.2}$$

denote the net wrench [Mur+94] on the body resulting from actuating legs in K. Then so long as no two hips are coincident, any desired wrench may be imposed on the body by appropriate choice of inputs to the limbs in K. In the next section we describe a limb coordination procedure that ensures there will be a subset $K(t) \subset \{1, \ldots, n\}$ of limbs in stance that can impose the LLS's wrench and cancel the reaction wrench from actuating other limbs at any time t.

Reducing polyped to LLS

We construct a smooth state feedback control law yielding a closed–loop Poincaré map $P_A : U_A \to \Sigma_A$ for the polyped that splits as $P_A : U_T \times U_N \to \Sigma_T \times \Sigma_N$ such that

$$P_A(z, \zeta) = (P_T(z), P_N(z)) \tag{3.6.3}$$

where $P_T : U_T \to \Sigma_T$ is a Poincaré map for the LLS and $P_N : U_T \to \Sigma_N$ is a smooth map. In the form (3.6.3) it is clear that since P_T is a diffeomorphism near the fixed point $\alpha = P_T(\alpha)$, all iterates of P_A have constant rank equal to rank $DP_T(\alpha) = \dim \Sigma_T$ near α, and therefore Theorem 3.3.1 applies.

Partition the $n \geq 4$ limbs into two disjoint sets

$$\text{swing} \coprod \text{stance},$$

ensuring $|\text{swing}|$, $|\text{stance}| \geq 2$. Initialize at the beginning of a step at time t with LLS and polyped body state $(q_0(t), \dot{q}_0(t))$ and polyped limb states $\{(q_k(t), \dot{q}_k(t))\}_{k=1}^n$ by attaching stance limbs and detaching swing limbs from the ground. Note that the termination time τ for the LLS step depends smoothly on the initial condition $(q_0(t), \dot{q}_0(t))$. For each $k \in$ swing choosing constant inputs

$$(\mu_k,\ \nu_k) = 2((x(\tau), y(\tau)) + r(\theta(\tau))\bar{q}_k - q_k(t) - \tau\dot{q}_k(t))/\tau^2 \tag{3.6.4}$$

ensures that the limb will reach a fixed location $\bar{q}_k$ in the body frame of reference at time τ. For each $k \in$ stance choose inputs (μ_k, ν_k) to cancel the reaction wrench from the swing limbs and impose the LLS acceleration on the polyped body. At time $t + \tau$, exchange the stance and swing limb sets and proceed as with the previous step from the new initial condition. After two steps, it is clear that the positions and velocities of the polyped's n limbs are uniquely determined by the body initial condition $(q_0(t), \dot{q}_0(t))$. Therefore the polyped's Poincaré map has the form of (3.6.3), so Theorem 3.3.1 implies the polyped anchor reduces exactly to the LLS template after a single stride.

Qualitative description of reduction

The active embedding described in Section 3.6.2 ensures the polyped body motion is always identical to that of the LLS, regardless of the state of the limbs. The limb posture control in Section 3.6.2 guarantees the limb states are determined by the LLS body state after two steps, and furthermore synchronizes touchdown and liftoff events with those of the LLS.

Effect of perturbations and parameter variations

The qualitative description in the preceding section makes it clear that, following a sufficiently small perturbation or parameter variation, the closed–loop polyped will continue to track and ultimately reduce to an LLS that experiences the corresponding disturbance.

Note that this conclusion requires that the polyped maintains the same control architecture exploited above to obtain the product decomposition in (3.6.3). In particular, the controller must maintain observability of the full state and controllability of the limbs. We study the effect of more general perturbations in the next section.

3.6.3 Deadbeat Control of Rhythmic Hybrid Systems

Generalizing the example from the previous section, we now consider a system wherein a finitely–parameterized control input updates when an execution passes through a distinguished subset of state space. This form control in rhythmic hybrid systems dates back (at least) to Raibert's hoppers [Rai86] and Koditschek's jugglers [Bue+94], and has received recent interest [Car+09; Rem+10]. We model this with a hybrid system $H = (D, F, G, R)$ whose vector field and reset map depend on a control input that takes values in a smooth boundaryless manifold Θ. The value of the control input may be updated whenever an execution passes through the guard G, but it does not change in response to the continuous flow. Suppose for some $\theta \in \Theta$ that H possesses a periodic orbit γ, let

$$P : U \times \Theta \to \Sigma$$

be a Poincaré map associated with γ where $U \subset \Sigma \subset G$, and let $\{\alpha\} = \gamma \cap \Sigma$. In this section we study deadbeat control of the discrete–time nonlinear control system

$$x_{i+1} = P(x_i, \theta_i) \tag{3.6.5}$$

and the discrete–time linear control system obtained by linearizing P about the fixed point $\alpha = P(\alpha, \theta)$,

$$\delta x_{i+1} = D_x P(\alpha, \theta)\delta x_i + D_\theta P(\alpha, \theta)\delta\theta_i. \tag{3.6.6}$$

The control architecture we present is well–known for linear and nonlinear maps arising in locomotion [Car+09]; the novelty of this section lies in the connection to *exact* and *approximate* reduction via Theorems 3.3.1 and 3.4.1.

Exact reduction over one cycle

As studied in [Car+09], an application of the Implicit Function Theorem [Lee12, Theorem C.40] shows that if $\operatorname{rank} D_\theta P(\alpha, \theta) = \dim \Sigma$ then there exists a neighborhood $V \subset U$ of α and a smooth feedback law $\psi : V \to \Theta$ such that

$$\forall x \in V : P(x, \psi(x)) = \alpha,$$

i.e. ψ is a *deadbeat* control law for (3.6.5). Since ψ is smooth, the closed–loop Poincaré map $P_\psi : V \to \Sigma$ defined by

$$\forall x \in V : P_\psi(x) = P(x, \psi(x))$$

satisfies the hypotheses of Theorem 3.3.1 (Exact Reduction) with rank $r = 0$, so the invariant hybrid subsystem yielded by the Theorem is simply the periodic orbit γ.

In practice it may be desirable to reduce fewer than $\dim \Sigma$ coordinates. If there exists a smooth function $h : \Sigma \to \mathbb{R}^d$ that satisfies

$$h \circ P(\alpha, \theta) = 0 \text{ and } \operatorname{rank} D_\theta h \circ P(\alpha, \theta) = d,$$

then the preceding construction yields a closed–loop system that reduces via Theorem 3.3.1 to the embedded d–dimensional submanifold $h^{-1}(0)$ near α.

Exact reduction over multiple cycles

If $\operatorname{rank} D_\theta P(\alpha, \theta) < \dim \Sigma$, as noted in [Car+09] it may be possible to construct a deadbeat control law by applying inputs over multiple cycles. Specifically, let $P_0 = P$ and for each $\ell \in \mathbb{N}$ define $P_\ell : U_\ell \times \Theta^\ell \to \Sigma$ by

$$P_\ell(x, (\theta_1, \ldots, \theta_\ell)) = P(P_{\ell-1}(x, (\theta_1, \ldots, \theta_{\ell-1})), \theta_\ell) \tag{3.6.7}$$

for all $(x, (\theta_1, \ldots, \theta_\ell)) \in U_\ell \times \Theta^\ell$ where $U_\ell \subset U$ is a neighborhood of α sufficiently small to ensure (3.6.7) is well–defined. Then if there exists $k \in \mathbb{N}$ such that

$$\operatorname{rank} D_{(\theta_1, \ldots, \theta_k)} P_k(\alpha, (\theta, \ldots, \theta)) = \dim \Sigma, \tag{3.6.8}$$

the construction from the previous paragraph yields a smooth k–step feedback law

$$\psi_k : V_k \to \Theta^k$$

such that the closed–loop hybrid system reduces via Theorem 3.3.1 to the periodic orbit γ after k cycles. We conclude this section by noting that [Car+09] contains an example that performs exact reduction after two cycles, and for which reduction in fewer cycles is impossible.

Approximate reduction

Since (3.6.8) is equivalent to controllability [CD91, Chapter 8d.5] of the linear control system (3.6.6), it is worthwhile to consider the linear control problemAny stabilizable subspace S [CD91, Chapter 8d.7] of (3.6.6) can be rendered attracting in a finite number of steps $k \in \mathbb{N}$ with linear state feedback

$$\delta\theta_i = \Psi \delta x_i$$

where Ψ is a fixed matrix [O'R81]. Applying this linear feedback law to the nonlinear system (3.6.5) yields a closed–loop Poincaré map P_Ψ such that the rangespace of the k–th iterate of its linearization is contained in S,

$$D_x P_\Psi^k(\alpha)\left(\mathbb{R}^{\dim \Sigma}\right) \subset S.$$

Therefore Theorem 3.4.1 (Approximate Reduction) yields an invariant hybrid subsystem, tangent to S on Σ, that attracts nearby trajectories superexponentially. Thus, although feedback laws for the nonlinear control system (3.6.5) constructed above can be computed using the procedure described in [Car+09] to achieve exact reduction to the target subsystem, if approximate reduction suffices in practice then one may simply apply the linear deadbeat controller computed for (3.6.6).

Structural stability of deadbeat control

Suppose the preceding development is applied to a model that differs from that used to construct the feedback law $\psi \in C^\infty(V, \Theta)$. We study the *structural stability* [GH83, Section 1.7] of attracting invariant sets arising in this class of systems by applying the Theorems of Section 3.1.5. If the models differ by a small smooth deformation (as would occur if there was a small perturbation in model parameters), one interpretation of this change is that some

$$\widetilde{\psi} \in B_\varepsilon(\psi) \subset C^\infty(V, \Theta)$$

is applied to the model for which ψ is deadbeat, where $\varepsilon > 0$ bounds the error. For all $\varepsilon > 0$ sufficiently small, $\widetilde{\psi}$ yields a perturbed closed–loop Poincaré map $\widetilde{P} : V \to \Sigma$ possessing a unique fixed point $\widetilde{\alpha} \in V$, and $\widetilde{\alpha}$ is an exponentially stable fixed point of the perturbed system.

We conclude by noting that it is possible for the structure of the hybrid dynamics to constrain the achievable perturbations. For instance, if one domain of the hybrid system has lower dimension than that in which the Poincaré map is constructed, then zero is always a Floquet multiplier regardless of the applied feedback; in this case Theorem 3.4.1 (Approximate Reduction) implies the existence of a proper submanifold of the Poincaré section Σ to which trajectories contract superexponentially in the presence of any (sufficiently small) smooth perturbation to the closed–loop dynamics.

3.6.4 Hybrid Floquet Coordinates

When a hybrid system reduces to a smooth dynamical system near a periodic orbit via Theorem 3.3.1 (Exact Reduction), we can generalize the *Floquet normal form* [Flo83; Guc75; Rev09; RG12] using Theorem 3.5.1 (Smoothing). Broadly, this demonstrates how the Theorems of Section 3.1.5 can be applied to generalize constructions from classical dynamical systems theory to the hybrid setting. More concretely, this provides a theoretical framework that justifies application of the empirical approach developed in [Rev09; RG12] to estimate low–dimensional invariant dynamics in data collected from physical locomotors.

Consider a hybrid dynamical system $H = (D, F, G, R)$ with τ–periodic orbit γ that satisfies the hypotheses of Theorem 3.3.1. Let $M \subset D$ be the $(r+1)$–dimensional invariant hybrid subsystem yielded by the Theorem, and $W \subset D$ a hybrid open set containing γ that contracts to M in finite time. Let $(\widetilde{M}, \widetilde{F})$ denote the smooth dynamical system obtained by

applying Theorem 3.5.1. Under a genericity condition[5] there exists a neighborhood $U \subset \widetilde{M}$ of γ and a smooth chart $\varphi : U \to \mathbb{R}^r \times S^1$ such that the coordinate representation of the vector field has the form

$$D\varphi \circ \widetilde{F} \circ D\varphi^{-1}(z, \theta) = \begin{pmatrix} \dot{z} \\ \dot{\theta} \end{pmatrix} = \begin{pmatrix} A(\theta)z \\ 2\pi/\tau \end{pmatrix} \tag{3.6.9}$$

where $z \in \mathbb{R}^r$ and $\theta \in S^1$. In these coordinates, each $\theta \in S^1$ determines an embedded submanifold

$$\widetilde{N}_\theta = \mathbb{R}^r \times \{\theta\} \subset \mathbb{R}^r \times S^1$$

that is mapped to itself after flowing forward in time by τ; for this reason, the submanifolds $\widetilde{N}_\theta$ are referred to as *isochrons* [Guc75]. Each $x \in \widetilde{N}_\theta$ may be assigned the *phase* $\theta \in S^1$; if γ is stable, then as $t \to \infty$ the trajectory initialized at x will asymptotically converge to the trajectory initialized at $(0, \theta)$.

The isochrons may be pulled back to any precompact hybrid open set $V \subset W$ containing γ in the original hybrid system as follows. The proof of Theorem 3.3.1 implies there exists a finite time $t < \infty$ such that every execution initialized in V is defined over the time interval $[0, t]$ and reaches M before time t; without loss of generality, we take this time to be a multiple $k\tau$ of the period of γ for some $k \in \mathbb{N}$. Let $\psi : V \to \widetilde{M}$ denote the map that flows an initial condition $x \in V$ forward by t time units and then applies the quotient projection $\pi : M \to \widetilde{M}$ obtained from Theorem 3.5.1 to yield the point $\psi(x) \in \widetilde{M}$. Then the constructions in the proof of Theorem 3.3.1 imply that ψ is a smooth map in the sense defined in Section 3.1.4, i.e. it is continuous and $\psi|_{V \cap D_j}$ is smooth for each $j \in J$. Now for any $\theta \in S^1$ the set

$$N_\theta = \psi^{-1}(U)$$

is mapped into $\widetilde{N}_\theta$ after $k\tau$ units of time; we thus refer to $N_\theta \subset D$ as a *hybrid isochron*. We conclude by noting that N_θ will generally not be a smooth (hybrid) submanifold.

3.7 Discussion

Generically near an exponentially stable periodic orbit in a hybrid dynamical system, trajectories contract superexponentially to a subsystem containing the orbit. Under a non–degeneracy condition on the rank of any Poincaré map associated with the orbit, this contraction occurs in finite time regardless of the stability of the orbit. Hybrid transitions may be removed from the resulting subsystem, yielding an equivalent smooth dynamical system. Thus the dynamics near stable hybrid periodic orbits are generally obtained by extending the behavior of a smooth system in transverse coordinates that decay superexponentially. Although the applications presented in Section 3.6 focused on terrestrial locomotion [Hol+06],

[5] Either the periodic orbit is exponentially stable or it is *hyperbolic* and the associated *Floquet multipliers* do not satisfy any *Diophantine equation* [GH83, Chapter 3.3].

we emphasize that the theoretical results in this chapter do not depend on the phenomenology of the physical system under investigation, and are hence equally suited to study rhythmic hybrid control systems appearing in robotic manipulation [Bue+94], biochemistry [GP78], and electrical systems [HR07].

In addition to providing a canonical form for the dynamics near hybrid periodic orbits, the results of this chapter suggest a mechanism by which a many–legged locomotor or a multi–fingered manipulator may collapse a large number of mechanical degrees–of–freedom to produce a low–dimensional coordinated motion. This provides a link between disparate lines of research: formal analysis of hybrid periodic orbits; design of robots for rhythmic locomotion and manipulation tasks; and scientific probing of neuromechanical control architectures in humans and animals. Our theoretical results show that hybrid models of rhythmic phenomena generically reduce dimensionality, and our applications demonstrate that this reduction may be deliberately designed into an engineered system. We furthermore speculate that evolution may have exploited this reduction in developing its spectacularly dexterous agents.

3.A Continuous–Time Dynamical Systems

Definition 3.A.1. *A* continuous–time dynamical system *is a pair* (M, F) *where:*

M *is a smooth manifold with boundary* ∂M*;*

F *is a smooth vector field on* M*, i.e.* $F \in \mathfrak{T}(M)$*.*

3.A.1 Time–to–Impact

When a trajectory passes transversely through an embedded submanifold, the time required for nearby trajectories to pass through the manifold depends smoothly on the initial condition [HS74, Chapter 11.2]. This provides the prototype used in the proofs of Theorems 3.3.1 and 3.4.1 for the dynamics near the portion of a hybrid periodic orbit in one domain of a hybrid system.

Lemma 3.A.1. *Let* (M, F) *be a smooth dynamical system,* $\phi : \mathcal{F} \to M$ *the maximal flow associated with* F*, and* $G \subset M$ *a smooth codimension–1 embedded submanifold. If there exists* $x \in M$ *and* $t \in \mathcal{F}^x$ *such that* $\phi(t, x) \in G$ *and* $F(\phi(t, x)) \notin T_x G$*, then there is a neighborhood* $U \subset M$ *containing* x *and a smooth map* $\sigma : U \to \mathbb{R}$ *so that* $\sigma(x) = t$ *and* $\phi(\sigma(y), y) \in G$ *for all* $y \in U$*;* σ *is called the* time–to–impact *map.*

Proof. Near $\phi(t, x)$, G is the zero section of a constant–rank map $h : M \to \mathbb{R}$ where $Dh(\phi(t, x)) \neq 0$. Define $g : \mathcal{F} \to \mathbb{R}$ by $g(s, y) = (h \circ \phi)(s, y)$. Then since F is transverse to G at $\phi(t, x)$,

$$\frac{\partial g}{\partial t}(t, x) = Dh(F(\phi(t, x))) \neq 0.$$

By the Implicit Function Theorem *see* Theorem C.40 in [Lee12] there exists a neighborhood U of x and a smooth map $\sigma : U \to \mathbb{R}$ so that $\sigma(x) = t$ and $g(\sigma(y), y) = 0$ for all $y \in U$, i.e. $\phi(\sigma(y), y) \in G$. □

Remark 3.A.1. *This lemma is applicable when* $G \subset \partial M$*.*

3.A.2 Smoothing Flows

Two continuous–time dynamical systems can be smoothly attached to one another along their boundaries to obtain a new continuous–time system [Hir76, Theorem 8.2.1]. Distinct hybrid domains were attached to one another using this construction in Section 3.1.5.

Lemma 3.A.2. *Suppose* $(M_1, F_1), (M_2, F_2)$ *are* n*–dimensional continuous–time dynamical systems, there exists a diffeomorphism* $R : \partial M_1 \to \partial M_2$*,* F_1 *is outward–pointing along* ∂M_1*, and* F_2 *is inward–pointing along* ∂M_2*. Then the topological quotient*

$$\widetilde{M} = \frac{M_1 \coprod M_2}{\partial M_1 \overset{R}{\sim} \partial M_2}$$

can be endowed with the structure of a smooth manifold such that for $j \in \{1,2\}$:

1. *the quotient projections $\pi_j : M_j \to \widetilde{M}$ are smooth embeddings; and*
2. *there is a smooth vector field $\widetilde{F} \in \mathfrak{T}(\widetilde{M})$ that restricts to $D\pi_j(F_j)$ on $\pi(M_j) \subset \widetilde{M}$.*

Proof. Let $\phi_j : \mathcal{F}_j \to M_j$ be the maximal flow associated with F_j on M_j. Then there is a neighborhood $\widetilde{U}_j \subset \mathcal{F}_j$ of $\{0\} \times M_j$ on which the flow is defined, and with $U_j = \widetilde{U}_j \cap (\mathbb{R} \times \partial M_j)$, transversality of F_j along ∂M_j implies $\phi_j : U_j \to M_j$ is an embedding which is the identity on $\{0\} \times \partial M_j$. Since F_1 is outward–pointing and F_2 is inward–pointing, the neighborhoods are one–sided and without loss of generality we may assume for $j = 1, 2$ that there exist continuous positive functions $\delta_j : \partial M_j \to [0, \infty)$ such that $U_1 = \{(-\delta_1(x), 0] : x \in \partial M_1\}$ and $U_2 = \{[0, \delta_2(x)) : x \in \partial M_2\}$. Therefore $U = \frac{U_1 \coprod U_2}{\partial M_1 \simeq \partial M_2}$ inherits a smooth structure from its product structure, i.e. the fibers $U^x = (-\delta_1(x), \delta_2(\varphi(x))) \times \{x\}$ are smooth curves for $x \in \partial M_1$ and both $\{0\} \times \partial M_1 \hookrightarrow U$ and $\{0\} \times \varphi^{-1}(\partial M_2) \hookrightarrow U$ are smooth embeddings; let $\varphi : U \to \mathbb{R}^n$ denote the chart. Note in addition that by construction the constant vector field $\frac{\partial}{\partial t} \in \mathfrak{T}(U_j)$ pushes forward to $F_j|_{\phi_j(U_j) \cap M_j} \in \mathfrak{T}(\phi_j(U_j) \cap M_j)$, since $(D\phi_j)\frac{\partial}{\partial t} = F_j$.

We construct the smooth structure on $\widetilde{M} = \frac{M_1 \coprod M_2}{\partial M_1 \simeq \partial M_2}$ by covering M with interior charts from the M_j's together with U. Note that since $\phi_j|_{U_j} : U_j \to M_j$ is a smooth embedding, the interior charts on M_j are smoothly compatible with the product chart on U, and the natural quotient projections $\pi_j : M_j \hookrightarrow \widetilde{M}$ are smooth embeddings. Finally, $(D\pi_1)F_1 = (D\pi_2)F_2$ along $\pi_1(\partial M_1)$ by construction, whence the vector field $\widetilde{F} \in \mathfrak{T}(\widetilde{M})$ which restricts to F_j on M_j, $j = 1, 2$, is well–defined and smooth. □

Remark 3.A.2. *The smooth structure constructed in Lemma 3.A.2 is unique up to diffeomorphism [Hir76, Theorem 2.1 in Chapter 8].*

3.B Discrete–time Dynamical Systems

Definition 3.B.1. *A* discrete–time dynamical system *is a pair* (Σ, P) *where:*

Σ *is a smooth manifold without boundary;*

P *is a smooth endomorphism of* Σ*, i.e.* $P : \Sigma \to \Sigma$*.*

In studying hybrid dynamical systems, we encounter smooth maps $P : \Sigma \to \Sigma$ that are noninvertible. Viewing iteration of P as determining a discrete–time dynamical system, we wish to study the behavior of these iterates near a fixed point $\alpha = P(\alpha)$. Note that if P has constant rank equal to $k < n = \dim \Sigma$, then its image $P(\Sigma) \subset \Sigma$ is an embedded k–dimensional submanifold near α by the Rank Theorem [Lee12, Theorem 4.12]. With an eye toward model reduction, one might hope that the composition $(P \circ P) : \Sigma \to P(\Sigma)$ is also constant–rank, but this is not generally true[6].

In this section we provide three results that introduce regularity into iterates of a noninvertible map $P : \Sigma \to \Sigma$ on an n–dimensional manifold Σ near a fixed point $P(\alpha) = \alpha$. If the rank of DP is strictly bounded above by $m \in \mathbb{N}$ and if P^m, the m–th iterate of P, has constant rank equal to $r \in \mathbb{N}$ near the fixed point α, then P reduces to a diffeomorphism over an r–dimensional invariant submanifold after m iterations; this result is given in Section 3.B.1. Even if DP^m is not constant rank, as long as α is exponentially stable then P can be approximated by a diffeomorphism on a submanifold whose dimension equals rank $DP^m(\alpha)$; this is the subject of Section 3.B.2. A bound on the error in this approximation is provided in Section 3.B.3.

3.B.1 Exact Reduction

If the rank of $P : \Sigma \to \Sigma$ is strictly bounded above by $m \in \mathbb{N}$ and the derivative of the m–th iterate of P has constant rank near a fixed point, then the range of P is locally an embedded submanifold, and P restricts to a diffeomorphism over that submanifold. This originally appeared without proof as Lemma 3 in [Bur+11a].

Lemma 3.B.1. *Let* (Σ, P) *be an* n*–dimensional discrete–time dynamical system with* $P(\alpha) = \alpha$ *for some* $\alpha \in \Sigma$*. Suppose the rank of* P *is strictly bounded above by* $m \in \mathbb{N}$ *and there exists a neighborhood* $W \subset \Sigma$ *of* α *such that* $\operatorname{rank} DP^m(x) = r$ *for all* $x \in W$*. Then there is a neighborhood* $V \subset \Sigma$ *containing* α *such that* $P^m(V)$ *is an* r*–dimensional embedded submanifold near* α *and there is a neighborhood* $U \subset P^m(V)$ *containing* α *that* P *maps diffeomorphically onto* $P(U) \subset P^m(V)$*.*

In the proof of Lemma 3.B.1, we make use of a fact from linear algebra obtained by passing to the Jordan canonical form.

Proposition 3.B.1. *If* $A \in \mathbb{R}^{n \times n}$ *and* $\operatorname{rank} A < m$*, then* $\operatorname{rank}(A^{2m}) = \operatorname{rank}(A^m)$*.*

[6] Consider the map $P : \mathbb{R}^2 \to \mathbb{R}^2$ defined by $P(x, y) = (x^2, x)$.

Proof. (of Lemma 3.B.1) By the Rank Theorem [Lee12, Theorem 4.12], there is a neighborhood $V \subset \Sigma$ of α for which $S = P^m(V)$ is an r–dimensional embedded submanifold and by Proposition 3.B.1 we have

$$\begin{aligned}\operatorname{rank}(DP^m|_S)(\alpha) &= \operatorname{rank} D(P^m \circ P^m)(\alpha) \\ &= \operatorname{rank} DP^m(\alpha).\end{aligned}$$

Therefore $DP^m|_S : T_\alpha S \to T_\alpha S$ is a bijection, so by the Inverse Function Theorem [Lee12, Theorem C.34], there is a neighborhood $W \subset S$ containing α so that $P^m(W) \subset S$ and $P^m|_W : W \to P^m(W)$ is a diffeomorphism.

We now show that W is invariant under P in a neighborhood of α. By continuity of P, there is a neighborhood $L \subset V$ containing α for which $P(L) \subset V$ and $P^m(L) \subset W$. The set $U = P^m(L)$ is a neighborhood of α in S. Further, we have

$$P(U) = P \circ P^m(L) = P^m \circ P(L) \subset S.$$

The restriction $P^m|_U : U \to P^m(U)$ is a diffeomorphism since $U \subset W$, whence $P|_U$ is a diffeomorphism onto its image $P(U) \subset S$. □

3.B.2 Approximate Reduction

Now suppose that iterates of P are not constant rank but $\alpha = P(\alpha)$ is exponentially stable, meaning that the *spectral radius* $\rho(DP(\alpha)) = \max\{|\lambda| : \lambda \in \operatorname{spec} DP(\alpha)\}$ satisfies $\rho(DP(\alpha)) < 1$. We show that P may be approximated by a diffeomorphism defined on a submanifold whose dimension equals the number of non–zero eigenvalues of $DP(\alpha)$. The technical result we desire was originally established by Hartman [Har60][7]. We apply Hartman's Theorem to construct a C^1 change–of–coordinates that exactly linearizes all eigendirections corresponding to non–zero eigenvalues of $DP(\alpha)$.

Lemma 3.B.2. *Let (Σ, P) be an n–dimensional discrete–time dynamical system. Suppose $\alpha = P(\alpha)$ is an exponentially stable fixed point and let r be the number of non–zero eigenvalues of $DP(\alpha)$. Then there is a neighborhood $U \subset \Sigma$ of α and a C^1 diffeomorphism $\varphi : U \to \mathbb{R}^n$ such that $\varphi(\alpha) = 0$ and the coordinate representation $\widetilde{P} = \varphi \circ P \circ \varphi^{-1}$ of P has the form*

$$\widetilde{P}(z, \zeta) = (Az,\ N(z, \zeta))$$

where $z \in \mathbb{R}^r$, $\zeta \in \mathbb{R}^{n-r}$, $A \in \mathbb{R}^{r \times r}$ is invertible, $N : \varphi(U) \to \mathbb{R}^{n-r}$ is C^1, $N(0,0) = 0$, and $D_\zeta N(0,0)$ is nilpotent.

[7] The statement in [Har60] only considered invertible contractions. However, as noted in [AG94], the proof in [Har60] of the result we require does not make use of invertibility and the conclusion is still valid if zero is an eigenvalue of the linearization. For details we refer to [Abb04].

Proof. Let (U_0, φ_0) be a smooth chart for Σ with $\alpha \in U_0$ and $\varphi_0(\alpha) = 0$. We begin by verifying that the hypotheses of Theorem 3.C.1 from Appendix 3.C are satisfied for the map $P_0 : \varphi_0(U_0) \to \mathbb{R}^n$ defined by $P_0 = \varphi_0 \circ P \circ \varphi_0^{-1}$. Let $\lambda \in \operatorname{spec} DP_0(0)$ be the eigenvalue with largest magnitude, and $\ell \in \mathbb{N}$ its algebraic multiplicity. Applying the linear change–of–coordinates that puts $DP_0(0)$ into Jordan canonical form, we assume

$$DP_0(0) = \begin{pmatrix} A & 0 \\ 0 & B \end{pmatrix}$$

where $B \in \mathbb{R}^{\ell \times \ell}$ and $\operatorname{spec} B = \{\lambda\}$. Now in the notation of Theorem 3.C.1 from Appendix 3.C,

$$P_0(x, y) = (Ax + X(x, y), By + Y(x, y))$$

where $x \in \mathbb{R}^{n-\ell}$, $y \in \mathbb{R}^\ell$, and X, Y are smooth and $X(0,0) = 0$, $Y(0,0) = 0$; note that $m = 0$ (there is no z coordinate) at this step. Because X and Y are smooth on the neighborhood U_0 of the origin, their derivatives are uniformly Lipschitz and Hölder continuous on a precompact open subset of U_0.

Theorem 3.C.1 from Appendix 3.C implies there exists a neighborhood $U_1 \subset \mathbb{R}^n$ of the origin and a C^1 diffeomorphism $\varphi_1 : U_1 \to \mathbb{R}^n$ for which the map $P_1 : \varphi_1(U_1) \to \mathbb{R}^n$ defined by $P_1 = \varphi_1 \circ P_0 \circ \varphi_1^{-1}$ has the form (after reversing the order of the coordinates)

$$P_1(z_1, \zeta_1) = (A_1 z_1,\ N_1(z_1, \zeta_1))$$

where $z_1 \in \mathbb{R}^{r_1}$, $r_1 > 0$, $\zeta_1 \in \mathbb{R}^{n-r_1}$ and $A_1 \in \mathbb{R}^{r_1 \times r_1}$ is invertible. Observe that the map P_1 satisfies the hypotheses of Theorem 3.C.1 from Appendix 3.C. Therefore we may inductively apply the Theorem to construct a sequence of coordinate charts $\{(U_k, \varphi_k)\}_{k=1}^K$ and corresponding maps $\{P_k\}_{k=1}^K$ such that for all $k \in \{1, \dots, K\}$

$$P_k(z_k, \zeta_k) = (A_k z_k,\ N_k(z_k, \zeta_k))$$

where $z_k \in \mathbb{R}^{r_k}$, $\zeta_k \in \mathbb{R}^{n-r_k}$, $A_k \in \mathbb{R}^{r_k \times r_k}$ is invertible, and $r_k > r_{k-1}$ (note that $r_0 = 0$). The sequence terminates at a finite $K < \infty$ with $r_K = r = \operatorname{rank} DP^n(\alpha)$. Therefore in the C^1 chart (U, φ) given by $\varphi = \varphi_K \circ \cdots \circ \varphi_0$ and $U = \varphi^{-1}(\mathbb{R}^n)$, the coordinate representation $\widetilde{P} = \varphi \circ P \circ \varphi^{-1}$ of P has the form

$$\widetilde{P}(z, \zeta) = (Az,\ N(z, \zeta))$$

where $z \in \mathbb{R}^r$, $\zeta \in \mathbb{R}^{n-r}$ and $A \in \mathbb{R}^{r \times r}$ is invertible. Since A is invertible and $\operatorname{rank} D\widetilde{P}^n(\alpha) = r$, $D_\zeta N(0,0)$ is nilpotent. □

3.B.3 Superstability

Finally, we recall that if all eigenvalues of the linearization of a map at a fixed point are zero—a so–called "superstable" fixed point [WA12]—then the map contracts superexponentially;[8] this is a straightforward consequence of Ostrowski's Theorem [Ort90, p. 8.1.7].

[8] The map need not be nilpotent simply because its linearization is; consider the map $P : \mathbb{R} \to \mathbb{R}$ defined by $P(x) = x^2$.

Lemma 3.B.3. *Let $P : \mathbb{R}^n \to \mathbb{R}^n$ be a C^1 map with $P(0) = 0$, $\operatorname{spec} DP(0) = \{0\}$. Then for every $\varepsilon > 0$ and norm $\|\cdot\| : \mathbb{R}^n \to \mathbb{R}$ there exists $\delta, C > 0$ such that*

$$\forall x \in B_\delta(0), k \in \mathbb{N} : \left\|P^k(x)\right\| \leq C\varepsilon^k \|x\|.$$

The proof of Lemma 3.B.3 relies on the following elementary fact regarding induced norms [Ort90, p. 1.3.6].

Proposition 3.B.2 (1.3.6 in [Ort90])**.** *Given $\varepsilon > 0$ and $A \in \mathbb{R}^{n\times n}$, there exists a norm $\|\cdot\| : \mathbb{R}^n \to \mathbb{R}$ such that $\|A\|_i \leq \rho(A) + \varepsilon$, where $\|\cdot\|_i : \mathbb{R}^{n\times n} \to \mathbb{R}$ is the operator norm induced by $\|\cdot\|$ and $\rho(A)$ is the spectral radius of A.*

Proof. (of Lemma 3.B.3) Given $\varepsilon > 0$, choose the norm $\|\cdot\| : \mathbb{R}^n \to \mathbb{R}$ obtained by applying Proposition 3.B.2 to $DP(0)$ so that $\|DP(0)\|_i \leq \frac{1}{2}\varepsilon$. Since DP is continuous, there exists a $\delta > 0$ such that

$$\forall x \in B_\delta(0) : \|DP(x) - DP(0)\|_i < \frac{1}{2}\varepsilon.$$

Whence we find for $\|x\| < \delta$ that

$$\begin{aligned}\|DP(x)\|_i &= \|DP(x) - DP(0) + DP(0)\|_i \\ &\leq \|DP(x) - DP(0)\|_i + \|DP(0)\|_i \leq \varepsilon.\end{aligned}$$

Combined with 8.1.4 in [Ort90] (a generalization of the Mean Value Theorem to vector–valued functions), we find for all $x \in B_\delta(0)$,

$$\|P(x)\| \leq \sup_{s\in[0,1]} \|DP(sx)\|_i \|x\| \leq \varepsilon\|x\|.$$

Iterating, for all $k \in \mathbb{N}$ and $\|x\| < \delta$ we have $\left\|P^k(x)\right\| \leq \varepsilon^k\|x\|$. Since all norms on finite–dimensional vector spaces are equivalent, the desired result follows immediately. □

Remark 3.B.1. *Let (Σ, P) be an n–dimensional discrete–time dynamical system that satisfies the hypotheses of Lemma 3.B.2 near $\alpha = P(\alpha)$. Then P has a coordinate representation $\widetilde{P}(z, \zeta) = (Az, N(z, \zeta))$ in a neighborhood of α where A is an invertible matrix, $N(0, 0) = 0$, and $\operatorname{spec} D_\zeta N(0, 0) = \{0\}$. Therefore given $\varepsilon > 0$ we can apply Lemma 3.B.3 to the nonlinearity $\widetilde{P}(z, \zeta) - (Az, 0) = (0, N(z, \zeta))$ to find $\delta, C > 0$ such that for all $(z, \zeta) \in B_\delta(0)$ and $k \in \mathbb{N}$:*

$$\left\|\widetilde{P}^k(z, \zeta) - \left(A^k z, 0\right)\right\| \leq C\varepsilon^k\|(z, \zeta)\|.$$

We conclude that P is arbitrarily well–approximated near α by a diffeomorphism on a submanifold whose dimension equals $\operatorname{rank} DP^n(\alpha)$.

3.C C^1 Linearization of a Noninvertible Map

The technical result we desire was originally established by Hartman in the course of proving that an invertible contraction is C^1–conjugate to its linearization[9]. The original statement in [Har60] only considered invertible contractions. However, as noted in [AG94], the proof in [Har60] of the result we require does not make use of invertibility and the conclusion is still valid if zero is an eigenvalue of the linearization. For details we refer the reader to [Abb04], which also contains a generalization to *hyperbolic* periodic orbits whose eigenvalues satisfy genericity conditions.

Theorem 3.C.1 (Induction Assertion in [Har60])**.** *Let $U \subset \mathbb{R}^n$ be a neighborhood of the origin and $P : U \to \mathbb{R}^n$ a C^1 map of the form*

$$P(x, y, z) = (Ax + X(x, y, z),\ By + Y(x, y, z),\ Cz)$$

such that

$$DP(0) = \begin{pmatrix} A & 0 & 0 \\ 0 & B & 0 \\ 0 & 0 & C \end{pmatrix}$$

where:

1. *$x \in \mathbb{R}^k$, $y \in \mathbb{R}^\ell$, $z \in \mathbb{R}^m$ and $k + \ell + m = n$;*
2. *$A \in \mathbb{R}^{k\times k}$, $B \in \mathbb{R}^{\ell\times\ell}$, and $C \in \mathbb{R}^{m\times m}$;*
3. *$X : \mathbb{R}^n \to \mathbb{R}^k$ and $Y : \mathbb{R}^n \to \mathbb{R}^\ell$ are C^1;*
4. *D_xX, D_yX, D_xY, and D_yY are uniformly Lipschitz continuous in (x, y);*
5. *D_zX and D_zY are uniformly Hölder continuous in z;*

Suppose all the eigenvalues of B have the same magnitude, that the eigenvalues of A have smaller magnitude and those of C have larger magnitude than those of B, and all eigenvalues of $DP(0)$ lie inside the unit disc:

$$\forall b, \beta \in \operatorname{spec} B : |b| = |\beta|;$$
$$\forall a \in \operatorname{spec} A, b \in \operatorname{spec} B, c \in \operatorname{spec} C : 0 \le |a| < |b| < |c| < 1.$$

Then there is a neighborhood of the origin $V \subset \mathbb{R}^n$ and a C^1 diffeomorphism $\varphi : V \to \mathbb{R}^n$ of the form

$$\varphi(x, y, z) = (x + \varphi_X(z),\ y + \varphi_Y(x, y, z),\ z)$$

[9]Readers may be more familiar with the Hartman–Grobman Theorem *see* [GH83, Theorem 1.4.1] or [Sas99, Theorem 7.8]hich states that the phase portrait near an exponentially stable fixed point of a discrete–time dynamical system is *topologically* conjugate to its linearization.

for which $D\varphi(0) = I$ *and for all* $(u, v, w) \in \varphi(V)$ *we have*

$$(\varphi \circ P \circ \varphi^{-1})(u, v, w) = (Au + U(u, v, w),\ Bv,\ Cw)$$

where:

1. $U : \varphi(V) \to \mathbb{R}^k$ *is* C^1*;*
2. $D_u U$ *is uniformly Lipschitz continuous in* (u, v, w)*;*
3. $D_v U$ *and* $D_w U$ *are uniformly Lipschitz continuous in* u*;*
4. $D_v U$ *and* $D_w U$ *are uniformly Hölder continuous in* (v, w)*.*

Remark 3.C.1. *Theorem 3.C.1 may be applied inductively to exactly linearize all eigendirections corresponding to non–zero eigenvalues via a* C^1 *change–of–coordinates; this is the content of Lemma 3.B.2 in Section 3.B.2.*

Chapter 4

Piecewise–Differentiable Flow through Overlapping Guards

Legged animals with four, six, and more limbs exhibit gaits with near–simultaneous touchdown of two or more legs [Ale84; Gol+99; Hol+06]. The appearance of such simultaneous contact gaits in terrestrial locomotion across unrelated species suggests they confer some inherent advantage. Locomotion is commonly modeled as a hybrid dynamical oscillator [Lyg+03] that undergoes discontinuous hybrid transitions when legs touch down [Rai86; KK02; Gri+02; Col+05; Hol+06; Rem+10]. Although analytical tools exist to study orbits that pass transversely through non–intersecting switching surfaces (e.g. to assess stability [AG58; Gri+02] and compute first–order variations [HP00; WA12]), general hybrid systems that admit simultaneous discrete transitions can easily accept executions that are neither unique nor orbitally stable [Lyg+03]. Analysis of trajectories passing through overlapping guards has generally been limited to two transversally–intersecting surfaces of discontinuity [Iva98; DL11; DB+08; Biz+13]. Extensions to arbitrary numbers of guards has been restricted to the case of pure phase oscillators [MS90].

We study a class of discontinuous vector fields that arise in biomechanics [Hol+06] and neuroscience [Biz+13]. Under the conditions that (i) the vector field's discontinuities are locally confined to a finite number of smooth submanifolds and (ii) the vector field is "transverse" to these surfaces in an appropriate sense, we show that the vector field yields a well–defined flow that is Lipschitz continuous and piecewise–differentiable. The definition of piecewise–differentiability we use (introduced only recently [Bar+95; Roc03; Sch12]) implies that although the flow is not classically differentiable, nevertheless it admits a first–order approximation (the so–called *Bouligand derivative* [Sch12, Chapter 3]). We exploit this first–order approximation to infer existence of piecewise–differentiable impact maps and assess structural stability of the flow.

4.1 Preliminaries

4.1.1 Topology [Fol99]

If $U \subset X$ is a subset of a topological space, then $\operatorname{Int} U \subset X$ denotes its *interior* and ∂U denotes its *boundary*. Let $f : X \to Y$ be a map between topological spaces. If $U \subset X$ then $f|_U : U \to Y$ denotes the *restriction*. If $V \subset Y$ then $f^{-1}(V) = \{x \in X : f(x) \in V\}$ denotes the *pre–image of* V *under* f.

4.1.2 Differential Topology [Lee12]

Given C^r manifolds D, N, we let $C^r(D, N)$ denote the set of C^r functions from D to N. $H \subset D$ is a C^r *codimension-k submanifold* of the d-dimensional manifold D if every $x \in H$ has a neighborhood $U \subset D$ over which there exists a C^r diffeomorphism $h : U \to \mathbb{R}^d$ such that

$$H \cap U = h^{-1}\big(\{y \in \mathbb{R}^d : y_{k+1} = \cdots = y_d = 0\}\big).$$

If $f \in C^r(D, N)$ then at every $x \in D$ there exists an induced linear map $Df(x) : T_xD \to T_{f(x)}N$ called the *pushforward* (in coordinates, $Df(x)$ is the Jacobian linearization of f at $x \in D$). When $N = \mathbb{R}$, we will invoke the standard identification $T_yN \simeq \mathbb{R}$ for all $y \in N$ and regard $Df(x)$ as a linear map from T_xD into $\mathbb{R}$ for every $x \in D$. If $U \subset D$ and $f : U \to N$ is a map, then a map $\widetilde{f} : D \to N$ is a C^r *extension of* f if $\widetilde{f}$ is C^r and $\widetilde{f}|_U = f$.

4.1.3 Non–Smooth Dynamical Systems [Fil88]

A (possibly discontinuous or non–differentiable) map $F : D \to TD$ is a *vector field* if $\pi \circ F = \mathrm{id}_D$ where $\pi : TD \to D$ is the natural projection and id_D is the identity map on D. A vector field may, under appropriate conditions, yield an associated *flow* $\phi : \mathcal{F} \to D$ defined over an open subset $\mathcal{F} \subset \mathbb{R} \times D$ called a *flow domain*; in this case for every $x \in D$ the set $\mathcal{F}^x = \mathcal{F} \cap (\mathbb{R} \times \{x\})$ is an open interval containing the origin, the restriction $\phi|_{\mathcal{F}^x} : \mathcal{F}^x \to D$ is absolutely continuous, and the derivative with respect to time is $D_t\phi(t, x) = F(\phi(t, x))$ for almost every $t \in \mathcal{F}^x$. A flow is *maximal* if it cannot be extended to a larger flow domain. An *integral curve* for F is an absolutely continuous function $\xi : I \to D$ over an open interval $I \subset \mathbb{R}$ such that $\dot{\xi}(t) = F(\xi(t))$ for almost all $t \in I$; it is *maximal* if it cannot be extended to an integral curve on a larger open interval.

4.1.4 Piecewise Differentiable Functions [Sch12]

Let $r \in \mathbb{N} \cup \{\infty\}$ and $D \subset \mathbb{R}^d$ be open. A continuous function $f : D \to \mathbb{R}^n$ is called *piecewise–C^r* if near every $x \in D$ there exists an open set $U \subset D$ containing x and a finite collection $\{f_j : U \to \mathbb{R}^n\}_{j \in \mathcal{J}}$ of C^r–functions such that for all $x \in U$ we have $f(x) \in \{f_j(x)\}_{j \in \mathcal{J}}$. The functions $\{f_j\}_{j \in \mathcal{J}}$ are called *selection functions* for $f|_U$, and f is said to be a *continuous selection* of $\{f_j\}_{j \in \mathcal{J}}$. A selection function f_j is said to be *active* at $x \in U$ if $f(x) = f_j(x)$.

We let $PC^r(D, \mathbb{R}^n)$ denote the set of piecewise–C^r functions from D to $\mathbb{R}^n$. Note that PC^r is closed under composition and pointwise maximum or minimum of a finite collection of functions. Piecewise–differentiable functions possess a useful but non–classical derivative $Df : TD \to T\mathbb{R}^n$ called the *Bouligand derivative* (or B–derivative) [Sch12, Chapter 3]; this is the content of Lemma 4.1.3 in [Sch12]. We let $Df(x; v)$ denote the B–derivative of f evaluated along the tangent vector $v \in T_xD$. The B–derivative is positively homogeneous, i.e. $\forall v \in T_xD, \lambda \geq 0 : Df(x; \lambda v) = \lambda Df(x; v)$.

4.2 Local and Global Flow

4.2.1 Event–Selected Vector Fields Discontinuities

To simplify the statement of our definitions and results, we fix notation of some objects in $\mathbb{R}^n$: $+\mathbb{1} \in \mathbb{R}^n$ denotes the vector of all ones and $-\mathbb{1}$ its negative; e_j is the j–th standard Euclidean basis vector; $B_n = \{-1, +1\}^n \subset \mathbb{R}^n$ is the set of corners of the n-dimensional cube.

The flow of a discontinuous vector field $F : D \to TD$ over an open domain $D \subset \mathbb{R}^d$ can exhibit pathological behaviors ranging from nondeterminism to orbital instability. We will investigate local properties of the flow when the discontinuities are confined to a finite collection of smooth submanifolds through which the flow passes transversally, as formalized in the following definitions.

Definition 4.2.1. *Given a vector field $F : D \to TD$ over an open domain $D \subset \mathbb{R}^d$ and a function $h \in C^r(U, \mathbb{R})$ defined on an open subset $U \subset D$, we say that h* is an event function for F on U *if there exists a positive constant $f > 0$ such that $Dh(x)F(x) \geq f$ for all $x \in U$. A codimension–1 embedded submanifold $\Sigma \subset U$ for which $h|_\Sigma$ is constant is referred to as a* local section for F.

Note that if h is an event function for F on a set containing $\rho \in D$ then necessarily $Dh(\rho) \neq 0$.

We will show that vector fields that are differentiable everywhere except a finite collection of local sections give rise to a well–defined flow that is piecewise–differentiable. This class of *event–selected* vector fields is defined formally as follows.

Definition 4.2.2. *Given a vector field $F : D \to TD$ over an open domain $D \subset \mathbb{R}^d$, $\rho \in D$, we say that F* is event–selected C^r at ρ *if there exists an open set $U \subset D$ containing ρ and a collection $\{h_j\}_{j=1}^n \subset C^r(U, \mathbb{R})$ such that:*

1. *(event functions) h_j is an event function for F on U for all $j \in \{1, \ldots, n\}$;*
2. *(C^r extension) for all $b \in \{-1, +1\}^n = B_n$, with $D_b = \{x \in U : b_j(h_j(x) - h_j(\rho)) \geq 0\}$, $F|_{\operatorname{Int} D_b}$ admits a C^r extension $F_b : U \to TU$.*

(Note that for any $b \in B_n$ such that $\operatorname{Int} D_b = \emptyset$ the latter condition is satisfied vacuously.) We let $EC^r(D)$ denote the set of vector fields that are event–selected C^r at every $x \in D$.

For an illustration of an event–selected C^r vector field in the plane $D = \mathbb{R}^2$, refer to Figure 4.2.

4.2.2 Construction of the Piecewise–Differentiable Flow

The following constructions will be used to state and prove results throughout the chapter. Suppose $F : D \to TD$ is event–selected C^r at $\rho \in D$. By definition there exists a neighborhood $\rho \in U \subset D$ and associated event functions $\{h_j\}_{j=1}^n \subset C^r(U, \mathbb{R})$ that divide U into regions $\{D_b\}_{b\in B_n}$ by defined by $D_b := \{x \in U : (h_j(x) - h_j(\rho))b_j \geq 0\}$. The boundary of each D_b is contained in the collection of event surfaces $\{H_j\}_{j=1}^n$ defined for each $j \in \{1, \ldots, n\}$ by $H_j := \{x \in U : h_j(x) = h_j(\rho)\}$. For each $j \in \{1, \ldots, n\}$ and $b \in B_n$, we refer to the surface H_j as an *exit boundary in positive time* for D_b if $h_j(D_b) \subset (-\infty, 0]$; we refer to H_j as an *exit boundary in negative time* if $h_j(D_b) \subset [0, +\infty)$. In addition, the definition of event–selected C^r implies that there is a collection of C^r vector fields $\{F_b : U \to TU\}_{b\in B_n} \subset C^r(U, TU)$ such that $F|_{\operatorname{Int} D_b} = F_b|_{\operatorname{Int} D_b}$ for all $b \in B_n$.

Budgeted time–to–boundary

For each $b \in B_n$ with $\operatorname{Int} D_b \neq \emptyset$, let $\phi_b : \mathcal{F}_b \to U$ be a flow for F_b over a flow domain $\mathcal{F}_b \subset \mathbb{R} \times U$ containing $(0, \rho)$; recall that $\phi_b \in C^r(\mathcal{F}_b, U)$ since $F_b \in C^r(U, TU)$. Each $H \in \{H_j\}_{j=1}^n$ is a local section for F, and therefore a local section for F_b as well. This implies $F_b(\rho)$ is transverse to H (more precisely, $F_b(\rho) \notin T_\rho H$), thus the Implicit Function Theorem [Lee12, Theorem C.40] implies there exists a C^r "time–to–impact" map $\tau_b^H : U_b^H \to \mathbb{R}$ defined on an open set $U_b^H \subset D$ containing ρ such that

$$\forall x \in U_b^H : (\tau_b^H(x), x) \in \mathcal{F}_b \text{ and } \phi_b(\tau_b^H(x), x) \in H. \tag{4.2.1}$$

The collection of maps $\left\{\tau_b^H\right\}_{b\in B_n}$ are jointly defined over the open set $U_b := \bigcap_{j=1}^n U_b^{H_j}$. Any $x \in U_b$ can be taken to any $H \in \{H_j\}_{j=1}^n$ by flowing with the vector field F_b for time $\tau_b^H(x) \in \mathbb{R}$.

We now define functions $\tau_b^+, \tau_b^- : \mathbb{R} \times U_b \to \mathbb{R}$ that specify the time required to flow to the exit boundary of D_b in forward or backward time, respectively, without exceeding a given time budget:

$$\begin{aligned}
\forall (t, x) \in \mathbb{R} \times U_b : \tau_b^+(t, x) &= \max\left\{0, \min\left(\{t\} \cup \left\{\tau_b^{H_j}(x) : b_j < 0\right\}_{j=1}^n\right)\right\}, \\
\forall (t, x) \in \mathbb{R} \times U_b : \tau_b^-(t, x) &= \min\left\{0, \max\left(\{t\} \cup \left\{\tau_b^{H_j}(x) : b_j > 0\right\}_{j=1}^n\right)\right\}.
\end{aligned} \tag{4.2.2}$$

Since τ_b^+, τ_b^- are obtained via pointwise minimum and maximum of a finite collection of C^r functions, we conclude $\tau_b^+, \tau_b^- \in PC^r(\mathbb{R} \times U_b, \mathbb{R})$. See Figure 4.1 for an illustration of the component functions of τ_b^+ in a planar vector field.

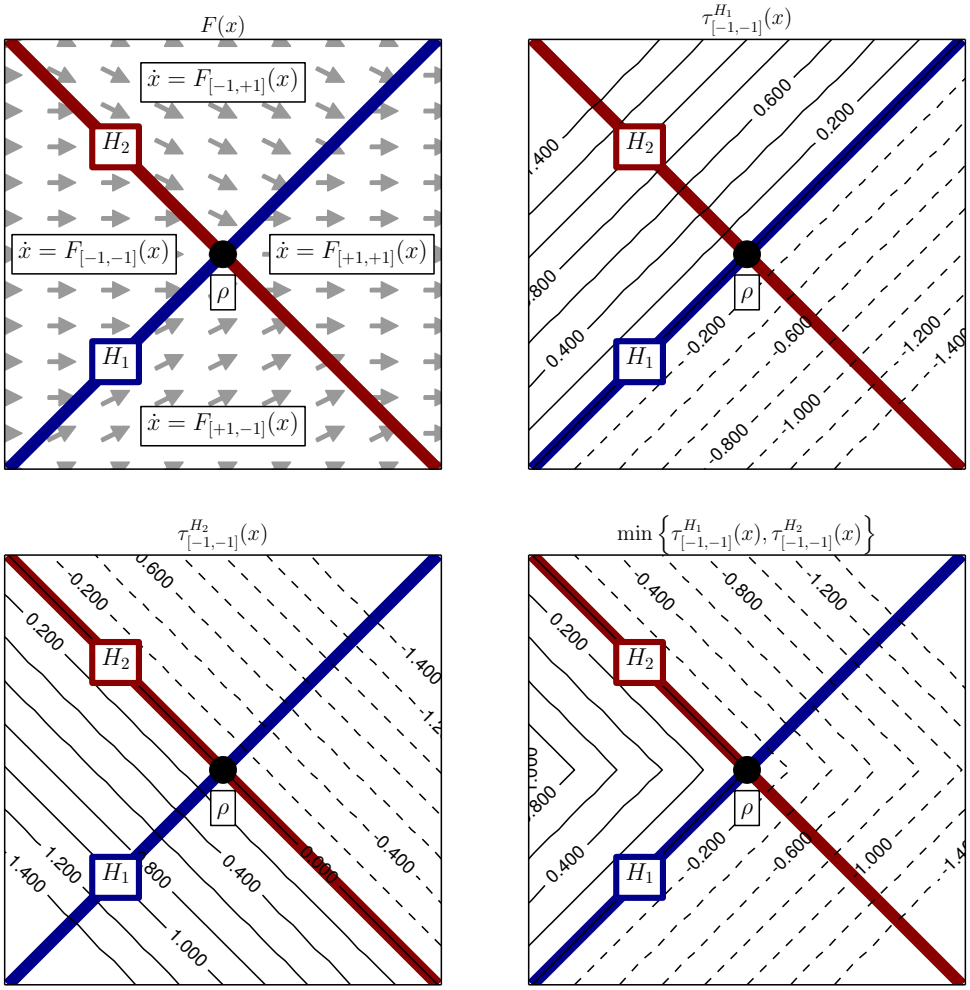

Figure 4.1: Illustration of a vector field $F : D \to TD$ that is event–selected C^r near $\rho \in D = \mathbb{R}^2$. The functions $\left\{\tau^{H_j}_{[-1,-1]}\right\}_{j=1}^{2}$ specify the time required to flow via the vector field $F_{[-1,-1]}$ to the surface H_j. The pointwise minimum $\min\left\{\tau^{H_j}_{[-1,-1]}(x)\right\}_{j=1}^{2}$ is used in the definition of $\tau^{+}_{[-1,-1]}$ in (4.2.2).

Flow–to–boundary

By composing the flow ϕ_b with the budgeted time–to–boundary functions τ_b^+, τ_b^-, we now construct functions that flow points up to the exit boundary of D_b in forward or backward time over domains

$$\mathcal{V}_b^+ = \left\{(t,x) \in \mathbb{R} \times U_b : (\tau_b^+(t,x), x) \in \mathcal{F}_b\right\},$$
$$\mathcal{V}_b^- = \left\{(t,x) \in \mathbb{R} \times U_b : (\tau_b^-(t,x), x) \in \mathcal{F}_b\right\}.$$

(Note that $\mathcal{V}_b^+, \mathcal{V}_b^-$ are open since τ_b^+, τ_b^- are continuous and nonempty since $(0,\rho) \in \mathcal{V}_b^+, \mathcal{V}_b^-$.) For each $b \in B_n$ define the functions $\zeta_b^+ : \mathcal{V}^+ \to D, \zeta_b^- : \mathcal{V}^- \to D$ by

$$\begin{aligned}\forall (t,x) \in \mathcal{V}_b^+ : \zeta_b^+(t,x) &= \phi_b\big(\tau_b^+(t,x), x\big),\\ \forall (t,x) \in \mathcal{V}_b^- : \zeta_b^-(t,x) &= \phi_b\big(\tau_b^-(t,x), x\big).\end{aligned}$$

Clearly $\zeta_b^+ \in PC^r(\mathcal{V}_b^+, D)$ and $\zeta_b^- \in PC^r(\mathcal{V}_b^-, D)$ since they are obtained by composing PC^r functions [Sch12, §4.1]. Loosely speaking, the function ζ_b^+ coincides with ϕ_b for pairs (t,x) that do not cross the forward–time exit boundary of D_b. Yet unlike ϕ_b, it is the identity (stationary) flow over the remainder of its domain. More precisely, for $t < 0$ and for values of

$$t > t_b^+ := \min\Big\{\tau_b^{H_j}(x) : b_j < 0\Big\}_{j=1}^n,$$

the function $\tau_b^+(t,x)$ is constant (and hence the derivative with respect to time $D_t\zeta_b^+(t,x) = 0$), while for $t \in (0, t_b^+)$ we have $\zeta_b^+(t,x) = \phi_b(t,x)$ (and hence $D_t\zeta_b^+(t,x) = F_b(\phi_b(t,x))$).

Now fix $x \in D_b$, choose $b' \in B_n \setminus b$, and for $t \in \mathbb{R}$ define

$$t_{b'}^+(t) := \min\Big\{\tau_{b'}^{H_j}\big(\zeta_b^+(t,x)\big) : {b'}_j < 0\Big\}_{j=1}^n.$$

Applying the conclusions from the preceding paragraph, with $t' \in \mathbb{R}$ the composition

$$\zeta_{b'}^+(t', \zeta_b^+(t,x))$$

is classically differentiable with respect to both t' and t almost everywhere. Furthermore, we can deduce that the derivative of the composition with respect to t is $F_b(\phi_b(t,x))$ when $t \in \big(0, t_b^+\big)$ and zero where it is otherwise defined; similarly, the derivative with respect to t' is $F_{b'}\big(\phi_{b'}(t', \zeta_b^+(t,x)\big)$ when $t' \in \big(0, t_{b'}^+(t)\big)$ and zero where it is otherwise defined. If we impose the relationship $t' := t - \tau_b^+(t,x)$, we have $t' = 0$ for any $t \in (0, t_b^+)$. The composition

$$\zeta_{b'}^+(t - \tau_b^+(t,x), \zeta_b^+(t,x))$$

follows the flow for F_b from x toward (but never passing) the exit boundary of D_b, then follows the flow of $F_{b'}$ from $\zeta_b^+(t,x)$ toward the exit boundary of $D_{b'}$.

Combining budgeted time–to–boundary with flow–to–boundary

Define $\varphi_b^+ : \mathcal{V}_b^+ \to \mathbb{R} \times D$, $\varphi_b^- : \mathcal{V}_b^- \to \mathbb{R} \times D$ by

$$\begin{aligned}\forall (t,x) \in \mathcal{V}_b^+ : \varphi_b^+(t,x) &= \big(t - \tau_b^+(t,x), \zeta_b^+(t,x)\big) = \big(t - \tau_b^+(t,x), \phi_b\big(\tau_b^+(t,x), x\big)\big),\\ \forall (t,x) \in \mathcal{V}_b^- : \varphi_b^-(t,x) &= \big(t - \tau_b^-(t,x), \zeta_b^-(t,x)\big) = \big(t - \tau_b^-(t,x), \phi_b\big(\tau_b^-(t,x), x\big)\big).\end{aligned} \tag{4.2.3}$$

Clearly $\varphi_b^+ \in PC^r(\mathcal{V}_b^+, \mathbb{R}\times D)$ and $\varphi_b^- \in PC^r(\mathcal{V}_b^-, \mathbb{R}\times D)$. Intuitively, the second component of the φ_b^+, φ_b^- functions flow according to F_b up to exit boundaries of D_b in forward or backward time, respectively, while the first component deducts the flow time $t - \tau_b^\pm(t,x)$ from the total time budget t. These functions satisfy an invariance property:

$$\begin{aligned}\forall (t,x) \in \big(\mathcal{V}_b^+ \cap (-\infty, 0] \times U_b\big) : \varphi_b^+(t,x) &= (t,x),\\ \forall (t,x) \in \big(\mathcal{V}_b^- \cap [0, +\infty) \times U_b\big) : \varphi_b^-(t,x) &= (t,x).\end{aligned} \tag{4.2.4}$$

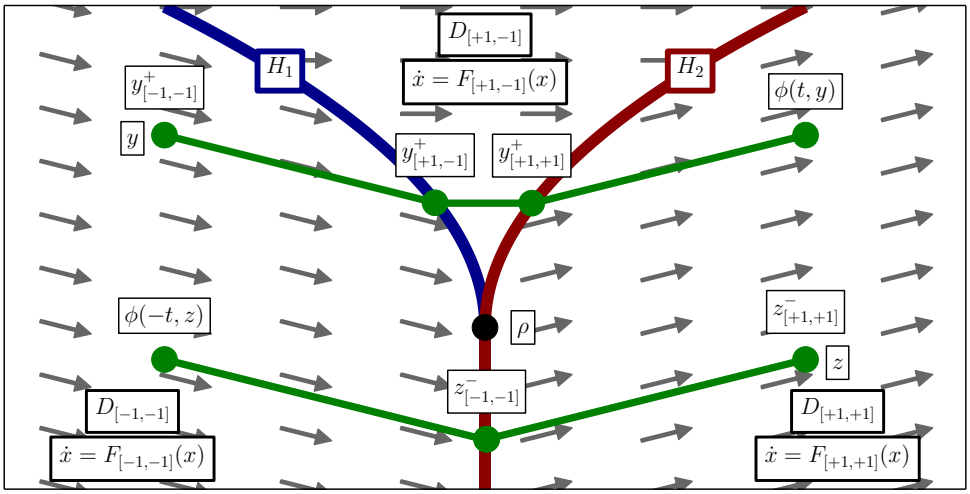

Figure 4.2: Illustration of a vector field $F : D \to TD$ that is event–selected C^r near $\rho \in D = \mathbb{R}^2$. The vector field is discontinuous across the C^r codimension–1 submanifolds $H_1, H_2 \subset D$. For each $b \in B_n = \{[-1,-1],[+1,-1],[-1,+1],[+1,+1]\}$, if $\operatorname{Int} D_b \neq \emptyset$ then the vector field restricts as $F|_{\operatorname{Int} D_b} = F_b|_{\operatorname{Int} D_b}$ where $F_b : U_b \to TU_b$ is a smooth vector field over a neighborhood $\rho \in U_b \subset D$. An initial condition $y \in D_{[-1,-1]}$ flows in forward time to $\phi(t,y) \in D_{[+1,+1]}$ through $y^+_{[+1,-1]} \in H_1$ and $y^+_{[+1,+1]} \in H_2$. An initial condition $z \in D_{[+1,+1]}$ flows in backward time to $\phi(-t,y) \in D_{[-1,-1]}$ through $z^-_{[-1,-1]} \in H_1 \cap H_2$.

Obtaining flow via composition

Consider now the formal composition

$$\phi = \pi_2 \circ \left(\prod_{b=-\mathbb{1}}^{+\mathbb{1}} \varphi_b^+ \right) \circ \left(\prod_{b=+\mathbb{1}}^{-\mathbb{1}} \varphi_b^- \right) \tag{4.2.5}$$

where $\pi_2 : \mathbb{R} \times D \to D$ is the canonical projection and $\prod_{b=-\mathbb{1}}^{+\mathbb{1}}$ denotes composition in lexicographic order (similarly $\prod_{b=+\mathbb{1}}^{-\mathbb{1}}$ denotes composition in reverse lexicographic order). The set $\phi^{-1}(D) \subset \mathbb{R} \times D$ is open (since ϕ is continuous) and nonempty (since combining (4.2.4) and (4.2.5) implies $\phi(0,\rho) = \rho$). Therefore there exist open neighborhoods $0 \in J \subset \mathbb{R}$, $\rho \in V \subset D$ such that $\mathcal{F} = J \times V \subset \phi^{-1}(D)$. Clearly $\phi \in PC^r(\mathcal{F}, D)$ since it is obtained by composing PC^r functions.

Lemma 4.2.1. *If the vector field $F : D \to TD$ is event–selected C^r at $\rho \in D$, then $\phi \in PC^r(\mathcal{F}, D)$ defined by (4.2.5) is differentiable with respect to time for almost all $(t,x) \in \mathcal{F}$ and*

$$D_t\phi(t,x) = F(\phi(t,x)). \tag{4.2.6}$$

Proof. Choose $x \in D$ such that $(0, x) \in \mathcal{F}$. We will show that $\phi|_{\mathcal{F}^x}$ is classically differentiable for almost all times $t \in \mathcal{F}^x$. Let $t^- = \inf \mathcal{F}^x$, $t^+ = \sup \mathcal{F}^x$ so that $0 \in \mathcal{F}^x = (t^-, t^+)$. We construct a partition of $[0, t^+)$ as follows. For each $b \in B_n$, let $(t_b^+, x_b^+) = \big(\prod_{a<b} \varphi_a^+\big)(t^+, x)$ where the composition is over all $a \in B_n$ that occur before b lexicographically; refer to Figure 4.2 for an illustration of the sequence $\{y_b\}_{b \in B_n}$ generated by an initial condition $y \in D_{-\mathbb{1}}$. Note that $\big\{t^+ - t_b^+\big\}_{b \in B_n}$ is (lexicographically) non–increasing and $t^+ - t_{+\mathbb{1}}^+ + \tau_{+\mathbb{1}}^+(t_{+\mathbb{1}}^+, x_{+\mathbb{1}}^+) = t^+$. Defining the interval

$$J_b = [t^+ - t_b^+, t^+ - t_b^+ + \tau_b^+(t_b^+, x_b^+)],$$

we have $[0, t^+) \subset \bigcup_{b \in B_n} J_b^+$ and $\operatorname{Int} J_a^+ \cap \operatorname{Int} J_b^+ = \emptyset$ for all $a \in B_n \setminus \{b\}$. Observe that

$$\forall t \in \operatorname{Int} J_b^+ : \phi(t, x) = \pi_2 \circ \varphi_b^+(t - (t^+ - t_b^+), x_b^+) \in \operatorname{Int} D_b,$$

where the condition is vacuously satisfied if $\operatorname{Int} J_b^+ = \emptyset$. Therefore for all $t \in \operatorname{Int} J_b^+$, the piecewise–differentiable function ϕ is classically differentiable with respect to time at (t, x) and we have

$$\begin{aligned} D_t\phi(t, x) &= D\pi_2 \, D_t\varphi_b^+(t - (t^+ - t_b^+), x_b^+) \\ &= F_b(\pi_2 \circ \varphi_b^+(t - (t^+ - t_b^+), x_b^+)) \\ &= F(\pi_2 \circ \varphi_b^+(t - (t^+ - t_b^+), x_b^+)) \\ &= F(\phi(t, x)). \end{aligned}$$

Applying an analogous argument in backward time, we conclude that $D_t\phi(t, x) = F(\phi(t, x))$ for almost all $t \in (t^-, t^+) = \mathcal{F}^x$. Since $(0, x) \in \mathcal{F}$ was arbitrary, the Lemma follows. □

4.2.3 Piecewise–Differentiable Flow

We now show that the piecewise–differentiable function $\phi \in PC^r(\mathcal{F}, D)$ defined in (4.2.5) is in fact a flow for the discontinuous vector field F. See Figure 4.2 for an illustration of this flow.

Theorem 4.2.1. *Suppose the vector field $F : D \to TD$ is event–selected C^r at $\rho \in D$. Then there exists a flow $\phi : \mathcal{F} \to D$ for F over a flow domain $\mathcal{F} \subset \mathbb{R} \times D$ containing $(0, \rho)$ such that $\phi \in PC^r(\mathcal{F}, D)$ and*

$$\forall (t, x) \in \mathcal{F} : \phi(t, x) = x + \int_0^t F(\phi(s, x)) \, ds. \tag{4.2.7}$$

Proof. We claim that $\phi \in PC^r(\mathcal{F}, D)$ from (4.2.5) satisfies (4.2.7). Applying the fundamental theorem of calculus [Sch12, Proposition 3.1.1] in conjunction with Lemma 4.2.1 and positive–

homogeneity of the derivative (4.2.6), we find

$$\begin{aligned}\phi(t,x) &= \phi(0,x) + \int_0^1 D\phi(tu,x;t,0)du \\ &= x + \int_0^t D\phi(s,x;t,0)\frac{1}{t}ds \\ &= x + \int_0^t D_t\phi(s,x)ds \\ &= x + \int_0^t F(\phi(s,x))ds.\end{aligned}$$

□

If the vector field $F : D \to TD$ is event–selected C^r at every point in the domain D, we may stitch together the local flows obtained from Theorem 4.2.1 to obtain a global flow.

Corollary 4.2.1. *If $F \in EC^r(D)$, then there exists a unique maximal flow $\phi \in PC^r(\mathcal{F}, D)$ for F. This flow has the following properties:*

(a) For each $x \in D$, the curve $\phi^x : \mathcal{F}^x \to D$ is the unique maximal integral curve of F starting at x.

(b) If $s \in \mathcal{F}^x$, then $\mathcal{F}^{\phi(s,x)} = \mathcal{F}^x - s = \{t - s : t \in \mathcal{F}^x\}$.

(c) For each $t \in \mathbb{R}$, the set $D_t = \{x \in D : (t,x) \in \mathcal{F}\}$ is open in D and $\phi_t : D_t \to D_{-t}$ is a piecewise–C^r homeomorphism with inverse ϕ_{-t}.

Proof. This follows from a straightforward modification of the analogous Theorem 9.12 in [Lee12] (simply replace all occurrences of the word "smooth" with "PC^r"). We recapitulate the argument in Appendix 4.A. □

If a vector field is event–selected C^r at every point along an integral curve, the following Lemma shows that it is actually C^r at all but a finite number of points along the curve.

Lemma 4.2.2. *Suppose the vector field $F : D \to TD$ is event–selected C^r at every point along an integral curve $\xi : I \to D$ for F over a compact interval $I \subset \mathbb{R}$. Then there exists a finite subset $\delta \subset \xi(I)$ such that F is C^r on $\xi(I) \setminus \delta$.*

Proof. Let $\delta \subset \xi(I)$ be the set of points where F fails to be C^r. If $|\delta| = \infty$, then since $\xi(I)$ is compact there exists an accumulation point $\alpha \in \xi(I)$. Since F is event–selected C^r at α, there exists $\varepsilon > 0$ such that F is C^r at every point in the set $(B_\varepsilon(\alpha) \cap \xi(I)) \setminus \{\alpha\}$, but this violates the existence of an accumulation point $\alpha \in \delta$. Therefore $|\delta| < \infty$. □

Remark 4.2.1. *One of the major values of Theorem 4.2.1 lies in the fact that piecewise–differentiable functions possess a useful but non–classical first–order approximation called the* Bouligand derivative *as described in Section 4.1.4. This Bouligand derivative (or B–derivative) is weaker than the classical (Fréchet) derivative, but significantly stronger than the directional derivative. The B–derivative of the composition (4.2.5) can be computed by applying the chain rule [Sch12, Theorem 3.1.1].*

4.3 Time–to–Impact and Poincaré Maps

4.3.1 Piecewise–Differentiable Time–to–Impact Map

Theorem 4.3.1. *Suppose the vector field $F : D \to TD$ is event–selected C^r at $\rho \in D$. If $\sigma \in C^r(U, \mathbb{R})$ is an event function for F on an open neighborhood $\rho \in U \subset D$, then there exists an open neighborhood $\rho \in V \subset D$ and piecewise–differentiable function $\mu \in PC^r(V, \mathbb{R})$ such that*

$$\forall x \in V : \sigma \circ \phi(\mu(x), x) = \sigma(\rho) \tag{4.3.1}$$

where $\phi \in PC^r(\mathcal{F}, D)$ is a flow for F and $(0, \rho) \in \mathcal{F}$.

Proof. Theorem 4.2.1 ensures the existence of a flow $\phi \in PC^r(\mathcal{F}, D)$ such that $\mathcal{F} \subset \mathbb{R} \times D$ contains $(0, \rho)$. Let $\alpha = \sigma \circ \phi$, and note that there exist open neighborhoods $0 \in T \subset \mathbb{R}$, $\rho \in W \subset D$ such that $\alpha \in PC^r(T \times W, \mathbb{R})$. We aim to apply an Implicit Function Theorem to show that the equation $\alpha(s, x) = \sigma(\rho)$ has a unique piecewise–differentiable solution $s = \mu(x)$ near $(0, \rho)$.

Specializing Definition 16 in [RS97], a sufficient condition for α to be *completely coherently oriented* with respect to its first argument at $(0, \rho)$ is that the (scalar) derivatives $D\alpha_j(0, \rho; 1, 0)$ of all essentially active selection functions $\{\alpha_j : j \in I^e(\alpha, (0, \rho))\}$ have the same sign. Lemma 4.2.1 implies the time derivatives of all essentially active selection functions for ϕ at $(0, \rho)$ are contained in the collection $\{F_b(\rho) : b \in B_n, D_b \neq \emptyset\}$ where $\{F_b : b \in B_n\}$ are the C^r vector fields that define F near ρ. Since σ is an event function for F, there exists $f > 0$ such that

$$\forall b \in B_n : D\sigma(\rho)F_b(\rho) \geq f > 0.$$

This implies α is completely coherently oriented with respect to time at $(0, \rho)$. Therefore we may apply Corollary 20 in [RS97] to obtain an open neighborhood $0 \in V \subset \mathbb{R}$ and a piecewise–differentiable function $\mu \in PC^r(V, \mathbb{R})$ such that (4.3.1) holds. □

Corollary 4.3.1. *Suppose the vector field $F : D \to TD$ is event–selected C^r at every point along an integral curve $\xi : [0, t] \to D$ for F. If $\sigma \in C^r(U, \mathbb{R})$ is an event function for F on an open set $U \subset D$ containing $\xi(t)$, then there exists an open neighborhood $\xi(0) \in V \subset D$ and piecewise–differentiable function $\mu \in PC^r(V, \mathbb{R})$ that satisfies (4.3.1).*

Proof. Corollary 4.2.1 ensures the existence of a flow $\phi \in PC^r(\mathcal{F}, D)$ such that $\mathcal{F} \subset \mathbb{R} \times D$ contains $[0, t] \times \{\xi(0)\}$. Let $\widetilde{\mu} \in PC^r(\widetilde{V}, \mathbb{R})$ be the impact time function for σ obtained by

applying Corollary 4.3.1 at $\xi(t) = \phi(t, \xi(0))$. Then with $V = \left\{x \in D : \phi(t,x) \in \widetilde{V}\right\}$, noting that V is nonempty since $\xi(0) \in V$ and open since ϕ is continuous, the function $\mu : V \to \mathbb{R}$ defined by $\mu(x) = t + \widetilde{\mu} \circ \phi(t,x)$ is piecewise–C^r and satisfies (4.3.1). □

Theorem 4.3.1 enables us to easily derive a canonical form for the flow near an event–selected vector field discontinuity.

Corollary 4.3.2. *Suppose the vector field $F : D \to TD$ is event–selected C^r at $\rho \in D$, and let $\phi : \mathcal{F} \to D$ be the flow obtained from Theorem 4.2.1. Then there exists a piecewise–differentiable homeomorphism $\psi : V \to W$ between neighborhoods $\rho \in V \subset D$, $0 \in W \subset \mathbb{R}^d$ such that*

$$\forall x \in V, t \in \mathcal{F}^x : \psi \circ \phi(t,x) = \psi(x) + te_1$$

where $e_1 \in \mathbb{R}^d$ is the first standard Euclidean basis vector.

Proof. Let $\sigma \in C^r(U, \mathbb{R})$ be an event function for F on a neighborhood $\rho \in U \subset D$ that is linear[1]. Theorem 4.3.1 implies there exists a piecewise–differentiable time–to–impact map $\mu \in PC^r(V, \mathbb{R})$ on a neighborhood $\rho \in V \subset D$ such that

$$\forall x \in V : \sigma \circ \phi(\mu(x), x) = \sigma(\rho),$$

i.e. $\phi(\mu(x), x)$ lies in the codimension–1 subspace $\Sigma = \sigma^{-1}(\sigma(\rho))$. Define $\psi : V \to \mathbb{R} \times \Sigma$ by

$$\forall x \in V : \psi(x) = (-\mu(x), \phi(\mu(x), x)).$$

Clearly $\psi \in PC^r(V, \mathbb{R} \times \Sigma)$ and hence ψ is continuous. Furthermore, it is clear that ψ is injective since (i) $\pi_\Sigma \psi(x) = \pi_\Sigma \psi(y)$ implies x and y lie along the same integral curve, and (ii) distinct points along an integral curve pass through Σ at distinct times. It follows from Brouwer's Open Mapping Theorem [Bro11a; Hat02] that the image $W = \psi(V)$ is an open subset of $\mathbb{R}^d$. This implies ψ is a homeomorphism between V and W. With $\iota : \mathbb{R} \times \Sigma \to \mathbb{R} \times D$ denoting the canonical inclusion, the inverse of $\psi \in PC^r(V, W)$ is $\phi \circ \iota|_W \in PC^r(W, V)$, thus ψ is a PC^r homeomorphism. Finally, using the semi–group property of the flow ϕ and the fact that $\mu \circ \phi(t,x) = \mu(x) - t$ for all $x \in V, t \in \mathcal{F}^x$,

$$\begin{aligned}
\forall x \in V,\ t \in \mathcal{F}^x : \psi \circ \phi(t,x) &= (-\mu \circ \phi(t,x), \phi(\mu \circ \phi(t,x), \phi(t,x))) \\
&= (t - \mu(x), \phi(\mu(x) - t, \phi(t,x))) \\
&= (t - \mu(x), \phi(\mu(x), x)) \\
&= \psi(x) + te_1.
\end{aligned}$$

□

Thus the flow is conjugate via a piecewise–differentiable homeomorphism to a *flowbox* [HS74, §11.2], [Lee12, Theorem 9.22].

[1] Existence of a linear event function is always guaranteed. For instance, take the linear approximation at ρ of any nonlinear event function for F

4.3.2 Piecewise–Differentiable Poincaré Map

Definition 4.3.1. *An integral curve $\gamma : \mathbb{R} \to D$ is a* periodic orbit *for the vector field $F : D \to TD$ if there exists $t > 0$ such that $\gamma(t) = \gamma(0)$ and $D_t\gamma(s) \neq 0$ for all $s \in [0, t]$. The minimal $t > 0$ for which $\gamma(t) = \gamma(0)$ is referred to as the* period *of γ, and we say that γ is a t–periodic orbit for F.*

We now apply Theorem 4.3.1 in the important case where the integral curve is a periodic orbit to construct a piecewise–differentiable Poincaré map. Suppose the vector field $F : D \to TD$ is event–selected C^r at every point along a t–periodic orbit γ for F. Then given a local section $\Sigma \subset D$ for F that intersects γ at $\{\alpha\} = \gamma \cap \Sigma$, Corollary 4.3.1 implies there exists a piecewise–differentiable impact time function $\mu \in PC^r(V, \mathbb{R})$ defined over an open neighborhood $\alpha \in V$ such that $\mu(\alpha) = t$. With $V \cap \Sigma$, we let $\psi : V \to \Sigma$ be the piecewise–differentiable map defined by

$$\forall x \in V : \psi(x) = \phi(\mu(x), x). \tag{4.3.2}$$

Theorem 4.3.2. *Suppose the vector field $F : D \to TD$ is event–selected C^r at every point along a periodic orbit γ for F. Then given a local section $\Sigma \subset D$ for F that intersects γ at $\{\alpha\} = \gamma \cap \Sigma$, there exists an open neighborhood $\alpha \in V \subset D$ such that the impact map (4.3.2) restricts to a piecewise–differentiable (Poincaré) map $P \in PC^r(S, \Sigma)$ on $S = V \cap \Sigma$.*

Proof. Without loss of generality assume $\gamma(0) \in \Sigma$. Let T be the period of γ, apply Theorem 4.3.1 to $\gamma|_{[0,T]}$ to obtain an open set $V \subset D$ containing $\gamma(0)$ and a piecewise–C^r impact time map $\mu \in PC^r(V, \mathbb{R})$, and define $\psi : V \to \Sigma$ as in (4.3.2). Then with $S = V \cap \Sigma$, the restriction $P = \psi|_S$ is a piecewise–C^r Poincaré map for γ. □

Since the Poincaré map $P : S \to \Sigma$ yielded by Theorem 4.3.2 is piecewise–differentiable, it admits a first–order approximation (its Bouligand derivative) $DP : TS \to T\Sigma$ that can be used to assess local exponential stability of the fixed point $P(\alpha) = \alpha$. This topic will be investigated in more detail in Section 4.5.1.

4.4 Perturbed Flow

In this section we study how the flow associated with an event–selected C^r vector field varies under perturbations to both the smooth vector field components and the event functions.

4.4.1 Perturbation of Vector Fields

Suppose $F : D \to TD$ is event–selected C^r at $\rho \in D$ with respect to the components of $h \in C^r(D, \mathbb{R}^n)$. Then by Definition 4.2.2 there exists $U \subset D$ containing ρ such that for each $b \in B_n$ either $\operatorname{Int} D_b = \emptyset$ or $D_b \subset U$ and $F|_{\operatorname{Int} D_b}$ admits a C^r extension $F_b : U \to TU$. We note that F is determined on U up to a set of measure zero from h and the

function $\widehat{F} \in C^r\big(\coprod_{b\in B_n} U, \coprod_{b\in B_n} TU\big)$ defined by $\widehat{F}|_{\{b\}\times U} = F_b|_U$. Note that we regard $C^r\big(\coprod_{b\in B_n} U, \coprod_{b\in B_n} TU\big)$ as a vector space under pointwise addition of tangent vectors and the norm

$$\left\|\widehat{F}\right\|_{C^r} = \sum_{b\in B_n} \left\|\widehat{F}|_{\{b\}\times U}\right\|_{C^r}. \tag{4.4.1}$$

Thus in the sequel we consider perturbations to event–selected C^r vector fields in the space $C^r\big(\coprod_{b\in B_n} U, \coprod_{b\in B_n} TU\big)$.

Theorem 4.4.1. *Let $F \in C^r\big(\coprod_{b\in B_n} D, \coprod_{b\in B_n} TD\big)$, $h \in C^r(D, \mathbb{R}^n)$ determine an event–selected C^r vector field at $\rho \in D$, $r \geq 2$. Then for all $\varepsilon > 0$ there exists $\delta > 0$ such that for all $\widetilde{F} \in B_\delta^{C^r}(F)$:*

(a) pairing h with the perturbed vector field $\widetilde{F}$ determines an event–selected C^r vector field at ρ;

(b) the perturbed flow $\widetilde{\phi} : \widetilde{\mathcal{F}} \to D$ obtained by applying Theorem 4.2.1 to this perturbed vector field satisfies $\widetilde{\phi} \in B_\varepsilon^{C^0}(\phi)$ on $\widetilde{\mathcal{F}} \cap \mathcal{F}$ and $(0, \rho) \in \widetilde{\mathcal{F}} \cap \mathcal{F}$;

Proof of Theorem 4.4.1. Claim (a) follows directly from from continuity of the F_b's. We claim that (b) follows from [Fil88, Theorem 1 in §8 of Chapter 2], which we reproduce as Theorem 4.B.1 in Appendix 4.B. Given any $G \in C^r(\coprod_{b\in B_n} D, \coprod_{b\in B_n} TD)$ for which (G, h) determines an event–selected C^r vector field, define a set–valued map $\overline{G} : D \to 2^{TD}$ as follows:

$$\forall x \in D : \overline{G}(x) = \big\{G|_{\{b\}\times D}(x) : b \in B_n,\ x \in D_b\big\}. \tag{4.4.2}$$

It is straightforward to verify that solutions to the differential inclusion $\dot{x} \in \overline{G}(x)$ coincide with those of the differential equation $\dot{x} = G(x)$ since the derivatives of the (absolutely continuous) solution functions agree almost everywhere. Furthermore, the map $\overline{G}$ satisfies Assumption 4.B.1 over the domain of the flow for G. Claim (b) then follows by applying Theorem 4.B.1 to $\overline{F}$ determined from F by (4.4.2) and $\overline{\widetilde{F}}$ determined from $\widetilde{F} \in B_\delta^{C^r}(F)$ by (4.4.2). □

4.4.2 Perturbation of Event Functions

It is a well–known fact that the solution of n equations in n unknowns generically varies continuously with variations in the equations. This observation provides a basis for studying structural stability of the flow associated with event–selected C^r vector fields when there are exactly $n = d = \dim D$ event functions, since for a collection of event functions $\{h_j\}_{j=1}^d \subset C^r(D, \mathbb{R})$ whose composite $h \in C^r(D, \mathbb{R}^d)$ satisfies $\det Dh(\rho) \neq 0$, the existence of a unique intersection point $\widetilde{\rho}$ and the set of possible transition sequences undertaken by nearby trajectories are unaffected by a sufficiently small perturbation $\widetilde{h}$ of h. We now combine this observation with the previous Theorem.

Theorem 4.4.2. *Let $F \in C^r\big(\coprod_{b\in B_n} D, \coprod_{b\in B_n} TD\big)$, $h \in C^r(D,\mathbb{R}^d)$ determine an event–selected C^r vector field at $\rho \in D$ and suppose $Dh(\rho)$ is invertible and $r \geq 1$. Then for all $\varepsilon > 0$ sufficiently small there exists $\delta > 0$ such that for all $\widetilde{F} \in B_\delta^{C^r}(F)$, $\widetilde{h} \in B_\delta^{C^r}(h)$:*

(a) there exists a unique $\widetilde{\rho} \in B_\delta(\rho)$ such that $\widetilde{h}(\widetilde{\rho}) = 0$ and $\widetilde{h}(x) \neq 0$ for all $x \in B_\delta(\rho)\setminus\{\widetilde{\rho}\}$;

(b) pairing $\widetilde{h}$ with the perturbed vector field $\widetilde{F}$ determines an event–selected C^r vector field at $\widetilde{\rho}$;

(c) the perturbed flow yielded by Theorem 4.2.1, $\widetilde{\phi} : \widetilde{\mathcal{F}} \to D$, satisfies $\widetilde{\phi} \in B_\varepsilon^{C^0}(\phi)$ on $\widetilde{\mathcal{F}} \cap \mathcal{F} \neq \emptyset$;

Proof of Theorem 4.4.2. Smooth dependence of the intersection point follows from the Implicit Function Theorem [Zei95, Theorem 4.E] since C^r functions over compact domains comprise a Banach space [Hir76, Chapter 2.1]. Specifically, if $h \in C^r(D,\mathbb{R}^n)$ satisfies $h(\rho) = 0$ for some $\rho \in D$ and $Dh(\rho)$ is invertible[2], then there exists $\alpha, \beta > 0$ and $\widetilde{\rho} \in C^r(B_\alpha(h), B_\beta(\rho))$ such that for all $\widetilde{h} \in B_\alpha(h)$ the point $\widetilde{\rho}(\widetilde{h})$ is the unique zero of $\widetilde{h}$ on $B_\beta(\rho)$, i.e. $\widetilde{h}(\widetilde{\rho}(\widetilde{h})) = 0$ and for all $x \in B_\beta(\rho) \setminus \left\{\widetilde{\rho}(\widetilde{h})\right\}$ we have $\widetilde{h}(x) \neq 0$. This establishes (a); (b) follows from continuity.

For any $\delta' > 0$, we can choose $\delta > 0$ sufficiently small to ensure that $\widetilde{F} \in B_\delta^{C^r}(F)$, $\widetilde{h} \in B_\delta^{C^r}(h)$ implies $D\widetilde{h}^{-1} \circ \widetilde{F} \in B_{\delta'}^{C^r}(Dh^{-1} \circ F)$; let $\widetilde{F}' = D\widetilde{h}^{-1} \circ \widetilde{F}$, $F' = Dh^{-1} \circ F$. With $\widetilde{\phi}' : \widetilde{\mathcal{F}}' \to \mathbb{R}^d$, $\phi' : \mathcal{F}' \to \mathbb{R}^d$ denoting the flows for $\widetilde{F}'$, F', Theorem 4.4.1 implies that $\delta' > 0$ can be chosen sufficiently small to ensure $\widetilde{\varphi} \in B_{\varepsilon'}^{C^0}(\varphi)$ for any $\varepsilon' > 0$. Since $\widetilde{\phi} = \widetilde{h} \circ \widetilde{\varphi} \circ \widetilde{h}^{-1}$, $\phi = h \circ \phi \circ h$, we conclude that $\delta > 0$ can be chosen sufficiently small to ensure $\widetilde{\phi} \in B_\varepsilon^{C^0}(\phi)$ on $\widetilde{\mathcal{F}} \cap \mathcal{F}$. This establishes (c). □

4.5 Applications

In this section, we apply the theoretical results from Sections 4.2, 4.3, and 4.4 to derive conditions for stability, optimality, and controllability of rhythmic phenomena in piecewise–differentiable flows. In the sequel, we will assume given an event–selected C^r vector field $F \in EC^r(D)$ over an open domain $D \subset \mathbb{R}^d$ possessing a periodic orbit $\gamma : \mathbb{R} \to D$. Theorem 4.2.1 and Corollary 4.2.1 together yield a maximal flow $\phi \in PC^r(\mathcal{F}, D)$ for F. Theorem 4.3.2 yields a Poincaré map $P \in PC^r(S, \Sigma)$ over any local section $\Sigma \subset D$ that intersects the periodic orbit at $\{\alpha\} = \gamma \cap \Sigma$.

4.5.1 Stability

The Bouligand derivative $DP : TS \to T\Sigma$ of the piecewise–differentiable Poincaré map $P : S \to \Sigma$ yielded by Theorem 4.3.2 can be used to assess local exponential stability of

[2]Note that necessarily $n = \dim D$.

the fixed point $P(\alpha) = \alpha$, as the following Corollary shows; this generalizes Proposition 3 in [Iva98] to stability of fixed points for arbitrary PC^r functions.

Corollary 4.5.1. *Suppose $P \in PC^r(S, \Sigma)$ has a fixed point $P(\alpha) = \alpha$ and DP is a contraction over tangent vectors near α, i.e. there exists $c \in (0, 1)$, $\delta > 0$, and $\|\cdot\| : \mathbb{R}^{d-1} \times \mathbb{R}^{d-1} \to \mathbb{R}$ such that*

$$\forall x \in B_\delta(\alpha) \subset S \cap \Sigma,\ v \in T_x\Sigma : \|DP(x; v)\| \leq c\|v\|.$$

Then γ is an exponentially stable periodic orbit.

Proof. By the fundamental theorem of calculus [Sch12, Proposition 3.1.1],

$$\begin{aligned}\forall x, y \in \overline{B_\delta(\alpha)} : \|P(x) - P(y)\| &\leq \int_0^1 \|DP(y + s(x - y); x - y)\| ds \\ &\leq c\|x - y\|.\end{aligned}$$

We conclude that P is a contraction over the compact ball $\overline{B_\delta(\alpha)}$, whence its unique fixed point $P(\alpha) = \alpha$ is exponentially stable [Ban22] [Lee12, Lemma C.35]. □

Remark 4.5.1. *Near α, the Poincaré map P is a continuous selection of a finite collection of C^r functions, $\{P_j\}_{j \in \mathcal{J}}$. The maximum of the local Lipschitz constants of these selection functions provides a Lipschitz constant for P near α [Sch12, Corollary 4.1.1]. Since each selection function P_j is continuously differentiable, the supremum of the induced norm of its (Fréchet) derivative provides a local Lipschitz constant for P_j. By shrinking the neighborhood under consideration, continuity implies this supremum can be made arbitrarily close to the induced norm of the derivative at α. Thus if $\max\{\|DP_j(\alpha)\|\}_{j \in \mathcal{J}} < 1$, the contraction hypothesis of Corollary 4.5.1 is satisfied on a neighborhood of α, whence the Poincaré map P is a contraction near α. The condition $\max\{\|DP_j(\alpha)\|\}_{j \in \mathcal{J}} < 1$ is exactly the hypothesis for stability in [Iva98, Proposition 3].*

4.5.2 Optimality

In this section, we consider the finite–dimensional non–smooth optimization problem

$$\min_{z \in Z} J(z) \tag{4.5.1}$$

where $Z \subset \mathbb{R}^m$ is open and $J \in PC^r(Z, \mathbb{R})$. We transcribe several variants of this problem into the canonical form (4.5.1) before proceeding to discuss a solution strategy.

Suppose that we are given a *loss function* $L \in C^r(D, \mathbb{R})$, whose value we seek to minimize after following the flow for a specified amount of time. For instance, given $t \in \mathbb{R}$ we may wish to solve the problem

$$\min_{x \in D} L \circ \phi(t, x).$$

Letting $J \in PC^r(Z, \mathbb{R})$ be defined by $J(z) = L \circ \phi(t, z)$ for all $z \in Z = D$, we obtain the equivalent problem (4.5.1). Alternately, we may wish to restrict to the Poincaré section Σ to solve the problem

$$\min_{x \in S} L \circ P(x).$$

Letting $J \in PC^r(Z, \mathbb{R})$ be defined by $J(z) = L \circ P(z)$ for all $z \in Z = S$, we obtain the equivalent problem (4.5.1). It is also straightforward to: incorporate a cost that accumulates along the state trajectory; include the final time as a decision variable [Pol97, §4.1.2]; optimize over a subset of the state variables; or accommodate parameters (and hence finitely–parameterized control inputs).

The non–smooth problem in (4.5.1) has been studied extensively, yielding analytical conditions for optimality [BTZ82; Cha89] and "bundle–method" algorithms [Kiw85; SZ92; Lem+95] applicable under more general hypotheses than we have imposed in (4.5.1). In particular, regardless of which problem formulation we adopted above, near any $z \in Z$ we may effectively (if laboriously) enumerate the selection functions $\{J_j\}_{j \in \mathcal{J}}$ for J and compute their derivatives $\left\{D^k J_j : j \in \mathcal{J}, k \in \{1, \ldots, r\}\right\}$ up to order r. Thus in the vernacular of [WF86] we seek to solve a *composite non–smooth problem*. This extra structure leads to second–order algorithms that significantly outperform the more general "bundle–method" [WF86; Fle00].

4.5.3 Controllability

Suppose that the domain D splits as $D = X \times \Theta$ where $X \subset \mathbb{R}^m$ and $\Theta \subset \mathbb{R}^\ell$ are open sets. Suppose further that with the induced splitting $F = (F_X, F_\Theta) : X \times \Theta \to TX \times T\Theta$ we have

$$\forall (x, \theta) \in X \times \Theta : F_\Theta(x, \theta) = 0. \tag{4.5.2}$$

The interpretation is that $\theta \in \Theta$ is a *parameter* whose value affects the vector field but is not itself affected by the continuous–time dynamics. Note that (4.5.2) implies that the induced splitting $\gamma = (\gamma_X, \gamma_\Theta) : \mathbb{R} \to X \times \Theta$ satisfies

$$\forall t \in \mathbb{R} : \gamma_\Theta(t) = \gamma_\Theta(0); \tag{4.5.3}$$

we let $\eta = \gamma_\Theta(0)$ denote the parameter value associated with the periodic orbit γ, and let $(\zeta, \eta) = \alpha$.

Suppose now that the parameter may be adjusted whenever the system trajectory passes through the Poincaré section Σ, and for simplicity assume the section splits as $\Sigma = \Sigma_X \times \Theta$. With $S_X = S \cap \Sigma_X$, we let

$$P = (P_X, P_\Theta) : S_X \times \Theta \to \Sigma_X \times \Theta \tag{4.5.4}$$

denote the induced splitting of the Poincaré map; note that (4.5.3) implies that $P_\Theta(x, \theta) = \theta$ for all $(x, \theta) \in S_X \times \Theta$. We may regard P_X as defining a discrete–time control system

$$x_{i+1} = P_X(x_i, \theta_i). \tag{4.5.5}$$

As in Section 3.6.3, we seek to apply an Implicit Function Theorem to assess deadbeat controllability of (4.5.5) near the fixed point $P(\zeta, \eta) = (\zeta, \eta)$. Unlike the case considered in Section 3.6.3, the map P_X is non–smooth. However, since P_X is piecewise–differentiable, we may adapt an Implicit Function Theorem due to Scholtes to obtain a sufficient condition for deadbeat controllability via piecewise–differentiable state feedback.

Corollary 4.5.2. *Let $P_X \in PC^r(S_X \times \Theta, \Sigma_X)$ be given in (4.5.4), and let $\{P_{X,j}\}_{j\in\mathcal{J}} \subset C^r(S_X \times \Theta, \Sigma_X)$ be selection functions for P_X near (ζ, η). If the matrices $\{D_\theta P_{X,j}(\zeta, \eta) : j \in \mathcal{J}\}$ have the same nonvanishing determinant sign and the piecewise–linear equation*

$$DP_X(x, \theta; u, v) - w = 0 \tag{4.5.6}$$

has a unique solution $v(u, w)$ for every $u \in \mathbb{R}^m$ and $w \in \mathbb{R}^\ell$, then there exist neighborhoods $\zeta \in U \subset \mathbb{R}^m$, $\eta \in V \subset \mathbb{R}^\ell$ and a piecewise–differentiable function $\psi \in PC^r(U, V)$ such that

$$\forall x \in U : P_X(x, \psi(x)) = \zeta,$$

i.e. ψ is a 1–step deadbeat control law for (4.5.5).

Proof. This is a straightforward specialization of [Sch12, Theorem 4.2.3]. □

Remark 4.5.2. *The condition that (4.5.6) have a unique solution is equivalent to the condition that P_X be* completely coherently oriented *with respect to θ at (ζ, η); see Definition 16 and Theorem 18 in [RS97]. This provides a straightforward (though laborious) computational procedure to check the hypotheses on this Corollary.*

4.6 Discussion

Piecewise–smooth vector fields whose discontinuities are locally confined to a finite collection of local sections generate Lipschitz continuous global flows. These flows possess a non–classical (Bouligand) derivative that can be used to: assess stability of Poincaré maps; implement scalable algorithms to solve non–smooth optimization problems; and determine deadbeat controllability near a periodic orbit. This significantly broadens the class of non–smooth dynamics that can be studied with tractable analytical and computational techniques. In particular, the tools we derived for stability, optimality, and controllability are suitable for non–smooth dynamics arising in multi–legged biomechanics [Hol+06] and neuron populations [Biz+13], and hence provide a foundation for dynamical modeling of neuromechanical systems.

4.A Global Piecewise–Differentiable Flow

Lemma 4.A.1 (Translation Lemma)**.** *Let $D \subset \mathbb{R}^d$ be open, $F \in EC^r(D)$, $J \subset \mathbb{R}$ be an interval, and $\xi : J \to D$ an integral curve for F. For any $b \in \mathbb{R}$, the curve $\widehat{\xi} : \widehat{J} \to D$ defined by $\widehat{\xi}(t) = \xi(t+b)$ is also an integral curve for F, where $\widehat{J} = \{t : t + b \in J\}$.*

Proof. Clearly $\widehat{\xi} \in PC^r(\widehat{J}, D)$, whence the fundamental theorem of calculus [Sch12, Proposition 3.1.1] in conjunction with Lemma 4.2.1 implies $\widehat{\xi}$ is an integral curve for F. □

Theorem 4.A.1 (Fundamental Theorem on Flows)**.** *If $F \in EC^r(D)$, then there exists a unique maximal flow $\phi \in PC^r(\mathcal{F}, D)$ for F. This flow has the following properties:*

(a) For each $x \in D$, the curve $\phi^x : \mathcal{F}^x \to D$ is the unique maximal integral curve of F starting at x.

(b) If $s \in \mathcal{F}^x$, then $\mathcal{F}^{\phi(s,x)} = \mathcal{F}^x - s = \{t - s : t \in \mathcal{F}^x\}$.

(c) For each $t \in \mathbb{R}$, the set $D_t = \{x \in D : (t, x) \in \mathcal{F}\}$ is open in D and $\phi_t : D_t \to D_{-t}$ is a piecewise–C^r homeomorphism with inverse ϕ_{-t}.

Proof. This proof is a straightforward adaptation of the proof of Theorem 9.12 in [Lee12].

Theorem 4.2.1 shows that there exists an integral curve for F starting at each point $x \in D$. Suppose $\xi, \widetilde{\xi} : J \to D$ are two integral curves for F defined on the same open interval J such that $\xi(t_0) = \widetilde{\xi}(t_0)$ for some $t_0 \in J$. Let $S = \left\{s \in J : \xi(s) = \widetilde{\xi}(s)\right\}$. Clearly $S \neq \emptyset$ since $t_0 \in S$, and S is closed in J by continuity of integral curves. On the other hand, suppose $t_1 \in S$. Applying Theorem 4.2.1 near $x = \xi(t_1)$, we see that there exists an interval $t_1 \in I \subset \mathbb{R}$ such that $\xi|_I = \widetilde{\xi}|_I$. This implies S is open in J. Since J is connected, $S = J$, which implies $\xi|_J = \widetilde{\xi}|_J$. Thus any two integral curves that agree at one point agree on their common domain.

For each $x \in D$, let $\mathcal{F}^x$ be the union of all domains of integral curves for F originating at x at time 0. Define $\phi^x : \mathcal{F}^x \to D$ by letting $\phi^x(t) = \xi(t)$, where ξ is any integral curve starting at x and defined on an open interval containing 0 and t. Since all such integral curves agree at t by the argument above, ϕ^x is well–defined, and is obviously the unique maximal integral curve starting at p.

Now let $\mathcal{F} = \{(t, x) \in \mathbb{R} \times D : t \in \mathcal{F}^x\}$ and define $\phi : \mathcal{F} \to D$ by $\phi(t, x) = \phi^x(t)$. We also write $\phi_t(x) = \phi(t, x)$. By definition, ϕ satisfies property (a) in the statement of the fundamental theorem: for each $x \in D$, ϕ^x is the unique maximal integral curve for F starting at x. To verify the group laws, fix any $x \in D$ and $s \in \mathcal{F}^x$, and write $y = \phi(s, x) = \phi^x(s)$. The curve $\xi : (\mathcal{F}^x - s) \to D$ defined by $\xi(t) = \phi^x(t + s)$ starts at y, and Lemma 4.A.1 shows that ξ is an integral curve for F. Since ϕ is a function, ξ agrees with ϕ^y on their common domain, which is equivalent to

$$\forall s \in \mathcal{F}^x, t \in \mathcal{F}^{\phi(s,x)} : (s + t \in \mathcal{F}^x) \implies (\phi(t, \phi(s, x)) = \phi(t + s, x)). \tag{4.A.1}$$

The fact that $\phi(0,x) = x$ for all $x \in D$ is obvious. By maximality of ϕ^x, the domain of ξ cannot be larger than $\mathcal{F}^y$, which means that $\mathcal{F}^x - s \subset \mathcal{F}^y$. Since $0 \in \mathcal{F}^x$, this implies $-s \in \mathcal{F}^y$, and the group law (4.A.1) implies that $\phi^y(-s) = x$. Applying the same argument with $(-s, y)$ in place of (s, x), we find that $\mathcal{F}^y + s \subset \mathcal{F}^x$, which is the same as $\mathcal{F}^y \subset \mathcal{F}^x - s$. This proves (b).

Next we show that $\mathcal{F}$ is open in $\mathbb{R} \times D$ (so it is a flow domain) and that $\phi : \mathcal{F} \to D$ is PC^r. Define a subset $W \subset \mathcal{F}$ as the set of all $(t,x) \in \mathcal{F}$ such that ϕ is defined and PC^r on a product neighborhood of (t,x) of the form $J \times U \subset \mathcal{F}$, where $J \subset \mathbb{R}$ is an open interval containing 0 and t and $U \subset D$ is a neighborhood of x. Then W is open in $\mathbb{R} \times D$, and the restriction $\phi|_W \in PC^r(W, D)$, so it suffices to show that $W = \mathcal{F}$. Suppose this is not the case. Then there exists some point $(\tau, x_0) \in \mathcal{F} \setminus W$. For simplicity, assume $\tau > 0$; the argument for $\tau < 0$ is similar (and can be obtained, for instance, by considering the flow for $-F$).

Let $t_0 = \inf\{t \in \mathbb{R} : (t, x_0) \notin W\}$ [Lee12, Figure 9.6]. By Theorem 4.2.1, ϕ is defined and PC^r in some product neighborhood of $(0, x_0)$, so $t_0 > 0$. Since $t_0 \le \tau$ and $\mathcal{F}^{x_0}$ is an open interval containing 0 and τ, it follows that $t_0 \in \mathcal{F}^{x_0}$. Let $y_0 = \phi^{x_0}(t_0)$. By Theorem 4.2.1 again, there exists $\varepsilon > 0$ and a neighborhood U_0 of y_0 such that $(-\varepsilon, \varepsilon) \times U_0 \subset W$. We will use the group law (4.A.1) to show that ϕ admits a PC^r extension to a neighborhood of (t_0, x_0), which contradicts our choice of t_0.

Choose some $t_1 < t_0$ such that $t_1 + \varepsilon > t_0$ and $\phi^{x_0}(t_1) \in U_0$. Since $t_1 < t_0$, we have $(t_1, x_0) \in W$, so there is a product neighborhood $(t_1 - \delta, t_1 + \delta) \times U_1 \subset W$ for some $\delta > 0$. By definition of W, this implies ϕ is defined and PC^r on $[0, t_1 + \delta) \times U_1$. Because $\phi(t_1, x_0) \in U_0$, we can choose U_1 small enough that ϕ maps $\{t_1\} \times U_1$ into U_0. Define $\widetilde{\phi} : [0, t_1 + \varepsilon) \times U_1 \to D$ by

$$\forall (t,x) \in [0, t_1 + \varepsilon) \times U_1 : \widetilde{\phi}(t,x) = \begin{cases} \phi_t(x), & x \in U_1,\ 0 \le t < t_1, \\ \phi_{t-t_1} \circ \phi_{t_1}(x), & x \in U_1,\ t_1 - \varepsilon < t < t_1 + \varepsilon. \end{cases}$$

The group law for ϕ guarantees that these definitions agree where they overlap, and our choices of U_1, t_1, and ε ensure that this defines a PC^r map. By Lemma 4.A.1, each map $t \mapsto \widetilde{\phi}(t,p)$ is an integral curve of F, so $\widetilde{\phi}$ is a PC^r extension of ϕ to a neighborhood of (t_0, x_0), contradicting our choice of t_0. This completes the proof that $W = \mathcal{F}$.

Finally, we prove (c). The fact that D_t is open is an immediate consequence of the fact that $\mathcal{F}$ is open. From part (b) we deduce that

$$\begin{aligned} x \in D_t &\implies t \in \mathcal{F}^x \implies \mathcal{F}^{\phi_t(x)} = \mathcal{F}^x - t \\ &\implies -t \in \mathcal{F}^{\phi_t(x)} \implies \phi_t(x) \in D_{-t}, \end{aligned}$$

which shows that ϕ_t maps D_t to D_{-t}. Moreover, the group laws then show that $\phi_{-t} \circ \phi_t$ is equal to the identity on D_t. Reversing the roles of t and $-t$ shows that $\phi_t \circ \phi_{-t}$ is the identity on D_{-t}, which completes the proof. □

4.B Perturbation of Differential Inclusions

In the proof of the perturbation results of Section 4.4, we relied on a result due to Filippov. For completeness, we reproduce the statement of the result we required, and clarify some vague points in the statement.

Assumption 4.B.1 ([Fil88, Chapter 2, §8, Theorem 1])**.** *In the domain $\mathcal{F}$ a set–valued function $F(t,x)$ satisfies the* basic conditions *if for all $(t,x) \in \mathcal{F}$ the set $F(t,x)$ is nonempty, bounded, and closed, convex, and the function F is upper semicontinuous in t,x.*

Here, $\mathcal{F}$ is understood to be a subset of $\mathbb{R} \times \mathbb{R}^d$, and F is upper semicontinuous as a *multi-function* $F : \mathcal{F} \to 2^{\mathbb{R}^d}$ [Cla90, §2.1].

Theorem 4.B.1 ([Fil88, Chapter 2, §8, Theorem 1])**.** *Let $F(t,x)$ satisfy Assumption 4.B.1 in the open domain $\mathcal{F}$; $t_0 \in [a,b]$, $(t_0,x_0) \in \mathcal{F}$; let all the solutions of the problem*

$$\dot{x} \in F(t,x),\ x(t_0) = x_0 \tag{4.B.1}$$

exist for all $t \in [a,b]$ and their graphs lie in $\mathcal{F}$.

Then for any $\varepsilon > 0$ there exists a $\delta > 0$ such that for any $t_0^* \in [a,b]$, x_0^* and $F^*(t,x)$ satisfying the conditions

$$|t_0^* - t_0| \le \delta,\ |x_0^* - x_0| \le \delta,\ d_{\mathcal{F}}(F^*, F) \le \delta$$

and Assumption 4.B.1, each solution of the problem

$$\dot{x}^* \in F^*(t,x^*),\ x^*(t_0^*) = x_0^* \tag{4.B.2}$$

exists for all $t \in [a,b]$ and differs from some solution of (4.B.1) by not more than ε.

Here, a "solution of the problem (4.B.1)" on the interval $[a,b] \subset \mathbb{R}$ is an absolutely continuous function $y : [a,b] \to \mathbb{R}^d$ [Fol99, pg. 105]; its "graph lies in $\mathcal{F}$" if $\{(t,y(t)) : t \in [a,b]\} \subset \mathcal{F}$.

Chapter 5

Conclusion and Future Directions

This thesis contributes intrinsic techniques for state space metrization and numerical simulation (Chapter 2), reduction and smoothing (Chapter 3), and first–order approximation (Chapter 4) of the non–smooth flow yielded by hybrid dynamical models for periodic gaits. In each context, we sought generic structures that do not vanish under perturbation. Though tailored to the dynamics of legged locomotion, the tools we derived are not restricted to this setting, and hence may find fruitful application in the study of rhythmic hybrid phenomena arising in electrical circuits [SD81], robotic manipulation [Bue+94], power systems [HR07], biochemistry [GP78], biology [MS90], or neuroscience [Biz+13].

We contend that, taken together, these contributions provide the essential elements of a hybrid dynamical systems theory for legged locomotion. First, they closely parallel results available in the classical (smooth) dynamical systems theory: we generalized simulation and linearization techniques from the classical to the hybrid setting while preserving convergence and approximation properties. Second, they sharply divide hybrid from classical dynamical systems theory: whereas we demonstrated that hybrid models of periodic gaits undergoing isolated footfall transitions generically reduce to a classical system, we showed that no such reduction is possible when two or more limbs can touch down nearly simultaneously. Third, they yield foundational tools upon which we expect to construct a more elaborate edifice. We devote the remainder of this chapter to our plans for contributing to the goal, outlined in the Introduction, of establishing a *systems theory* for *sensorimotor control*.

5.1 Towards Sensorimotor Control Theory

In this thesis, we contributed fundamental elements of a dynamical systems theory for rhythmic locomotion (and hence, by a change–of–coordinates, manipulation [JK13a]). This provides a foundation upon which a systems–level theory for sensorimotor control may be built. However, substantial work remains to establish the unified analytical, computational, and experimental framework described in the Introduction. Here we propose possible extensions in support of this vision.

Analytical elements: *intrinsically self–consistent techniques for dynamical modeling.* Classical notions of observability for linear [Kal59] and nonlinear [Son84] control systems are tacitly built upon the topological and metric properties of Euclidean space; thus the intrinsic state space metric we introduced in Section 2.2 provides the possibility of obtaining observability criteria in general hybrid control systems. Qualitative approximation for piecewise–differentiable maps [KS95] may enable generalization of the route to model reduction explored in Sections 3.3 and 3.4 to the non–smooth flow constructed in Section 4.2. Necessary and sufficient conditions for optimality in the calculus of variations rely on a first–order variation of the flow; thus the Bouligand derivative of our piecewise–differentiable flow could support a tractable specialization of the general maximum principle [Sus99] to our setting.

Computational elements: *tractable algorithms for studying models on a computer.* The approximate deadbeat control architecture in Section 3.6.3 provides a method to stabilize hybrid oscillators at a superexponential rate and only requires inverting a (linearized controllability) matrix [O'R81]; this computationally–tractable technique could be used for instance to stabilize *hybrid zero dynamics* subsystems [Gri+02; Wes+03]. Scalable algorithms for optimal control of constrained nonlinear systems utilize finite–dimensional approximations that rely on uniformly convergent numerical simulations [Pol97, Chapter 4], thus the (uniformly convergent) simulation algorithm we derived in Section 2.3 may support generalization of the *consistent approximations* framework [Pol97] to the hybrid setting.

Experimental elements: *practical procedures for transforming between models and data.* Generalizing classical parameter identification algorithms [Lju99] to hybrid models for locomotion is challenging due to seemingly unavoidable discrete decision variables that assign observations to hybrid modes. To avoid this discrete subproblem, it is possible to formulate an equivalent estimation problem for the smooth subsystem that generically arises near periodic orbits [Bur+12]. Preliminary results indicate this approach can be used to probe perturbation recovery in running cockroaches [Bur+13b]. Generalizations to inverse modeling within subclasses of hybrid models based on recent advances in machine learning [Elh+12] are doomed to succeed in simulation [Bur+14; Elh+14]; the practical relevance of this approach must to be validated experimentally, e.g. for turning control in minimally–actuated robots [Hoo+10].

5.2 Frontiers in Robotics, Neuromechanics, & Rehab

In parallel with the effort to derive elements of a systems theory for sensorimotor control described in the previous section, we also plan to pursue the complementary aim of obtaining advancements within individual disciplines using existing techniques. Conducting these studies in a nascent systems framework lends support for the systems approach while exposing critical foci for subsequent efforts at abstraction and generalization.

5.2.1 Dynamic and Dexterous Robotics

Robots succeed in structured and sterile environments. Hand–tuning can achieve spectacular maneuvers executed in open–loop [Mon+12; JK13b], but these behaviors are sensitive to the experimental preparation. If artifacts are to accomplish useful tasks outside the laboratory, we must develop systematic techniques for synthesizing new behaviors and adapting mechanical designs.

Synthesis of dynamic multi–legged maneuvers

Were the dynamics of legged locomotion smooth as a function of state, then receding–horizon model predictive control provides an effective approach to maneuver synthesis [Gar+89]. This approach generalizes to fixed footfall sequences [Mom+05], but is intractable for multi–legged maneuvers due to the combinatorial explosion of the set of possible footfall sequences. Enumerating footfall sequences may be unavoidable when the flow has discontinuities arising from rigid collision mechanics [Rem+10]. Focusing instead on models that yield a piecewise–differentiable flow as in Chapter 4 provides the opportunity to apply scalable non–smooth optimization algorithms to search directly over the intrinsic hybrid state space of Chapter 2 while avoiding the combinatorial footfall sequence subproblem. Preliminary evidence suggests this approach synthesizes higher jumps for a vertical hopper [Bur+14] than that achievable with a simple sinusoid [Agu+12].

Data–driven improvements to mechanical design

Facilitated by the rise of rapid prototyping techniques [Cha+02; Woo+08; Mut+14] and commercial interest [Rai+08], a menagerie of legged robots have been built in recent years that achieve unprecedented levels of mobility. Proposing modifications to the mechanical design of an existing robot that improves locomotion performance (as measured by speed, specific resistance [GK51], or mean time–to–failure [BT09]) remains an art that relies largely on laborious mechanical prototyping. Analytical and computational models can provide qualitative [Hoo+10] and quantitative [Zha+13] insights for robot design. Tailoring these models to the physical system through parameter identification [Bur+12] and inverse modeling [Elh+14] techniques may improve the fidelity of their predictions, allowing roboticists to implement only the most promising mechanical revisions devised in simulation.

5.2.2 Principles of Neuromechanical Sensorimotor Control

Neural and mechanical feedback in perturbation recovery

Although the nervous system effects exquisite control over the body, experiments with decerebrate cats that walk [She10; Bro11b] and cockroaches that reject large perturbations extremely rapidly [JF02] indicate that neural feedback is not solely responsible for producing stable gaits. Perturbing the sensorimotor loop can reveal mechanisms contributing to the observed closed–loop behavior [Rot+14]. One such study concludes that neural feedback in cockroaches occurs at a significant delay—one to two strides—following a large lateral perturbation [Moo+10; Rev+13]. Associating mechanical models to experimental data enables systematic characterization of the role played by neural and mechanical feedback in perturbation recovery [Bur+13b].

Modeling humans embedded amid automation

Human interaction with the physical world is increasingly mediated by automation. Factory workers facilitate and monitor repetitive or intricate manufacturing tasks to ensure process safety and product quality. Captains of air and watercraft oversee autopilot systems and intervene to compensate for unexpected equipment failures or environmental disturbances. Doctors perform minimally–invasive surgeries via compact but high–precision endoscopic robots. Drivers rely on lanekeeping assistance and automated braking during highway driving, with the prospect of vehicles that drive themselves (at least until the first snowfall) on the immediate horizon. The proliferation of these semiautonomous systems raises critical concerns regarding safety and reliability of the closed–loop behavior, as little is known about the effect of such intermediaries on the behavior of the coupled human/automation system.

5.2.3 Automated Tools for Diagnosis and Rehabilitation

Despite steady progress in closely–related engineering and science disciplines, the quantitative diagnostic and rehabilitative tools available to physiatrists remain primitive. There are many challenges involved in translating engineering methods and scientific insights into clinical practice, not least of which is the daunting task of integrating findings from disparate fields into a unified framework tailored to a class of patients. Considering that the overarching goal of physiatry is to restore functionality while respecting the constraints imposed by a patient's trauma or disease, the systems approach provides a natural framework to achieve this integration. Focusing on the design and control of prostheses, exoskeletons, and other assistive devices, a need arises for dynamical behavior synthesis and data–driven design of assistive devices, as well as an understanding of the mechanisms governing neuromechanical perturbation recovery and the closed–loop dynamics of humans interacting with semi–autonomous artifacts. These advances must ultimately be integrated with real–time and adaptive brain–machine interfaces and low–power sensor networks distributed throughout the body and environment.

5.3 Interdisciplinary Collaboration and Training

The contributions of this thesis were motivated and influenced to a significant degree by experimental biomechanics. Although it is possible to construct artifacts (by means of stiff materials, reinforced joints, and a willful neglect of damage to motor gearboxes) whose behavior exhibits the extreme sensitivity with respect to initial conditions inherent in models of rigid impact, this sensitivity is not typically observed in nature's locomotors. Thus we sought *intrinsically self–consistent modeling techniques* that preclude such pathologies. And although locomotion arises at the bewilderingly complex interface of aero–, hydro–, and terra–dynamics, strikingly simple behaviors consistently emerge across scale, material, and morphology. This lead us to eschew dichotomies that divide the perception → action loop (Figure 1.2) and focus instead on *emergent phenomena in closed–loop systems*.

This collaborative interdisciplinary approach must be deliberately cultivated. Science is a sociological phenomenon [Kuh70], hence crossing the disciplinary divide requires shared conceptual frameworks and cross–disciplinary training. We envision a hierarchical progression [And72] where advancements in robotics, neuromechanics, and rehabilitation merge in a systems–level study of sensorimotor control. This approach addresses the challenge inherent in disciplinary integration [Nis+07; Sch+09] while facilitating synergistic cross–pollination of methods and mechanisms [Mil+12; Cow+14]. The additional effort required will be justified by the benefits conferred to each discipline's individual practitioners.

The closest analogue for our aim is the integration of synthetic [BS05; HC10] and systems [Kit02b; Hoo+04] biology. Although these remain distinct fields, they traffic largely in the same physical media: biological molecules, cells, and tissues. In contrast, the natural and artificial building blocks of sensorimotor control are fundamentally different [Vog98]; exceptions notwithstanding [Cha+02; Woo+08; Mut+14], animals and robots make use of fundamentally different materials, sensors, actuators, and processors. This gap is particularly challenging to bridge pedagogically, where a significant portion of a practitioner's expertise is simply not applicable in other disciplines. Since systems–level insights necessarily abstract away from the detailed physics giving rise to a phenomena of interest, they provide a natural medium through which advancements in one domain may be directly translated to another. Thus we envision the systems approach comprising a core component of training for the next generation of engineers, scientists, and clinicians working at the disciplinary interface.

Bibliography

[AG58] M. A. Aizerman and F. R. Gantmacher. "Determination of Stability by Linear Approximation of a Periodic Solution of a System of Differential Equations with Discontinuous Right–Hand Sides". In: *The Quarterly Journal of Mechanics and Applied Mathematics* 11.4 (1958), pp. 385–398. DOI: 10.1093/qjmam/11.4.385 (cit. on pp. 49, 79).

[AG94] B. Aulbach and B. M. Garay. "Partial linearization for noninvertible mappings". In: *Zeitschrift für Angewandte Mathematik und Physik (ZAMP)* 45 (4 1994), pp. 505–542. DOI: 10.1007/BF00991895 (cit. on pp. 74, 77).

[AS05] A. D. Ames and S. S. Sastry. "A Homology Theory for Hybrid Systems: Hybrid Homology". In: *Hybrid Systems: Computation and Control*. Ed. by M. Morari and L. Thiele. Vol. 3414. Lecture Notes in Computer Science. Springer Berlin / Heidelberg, 2005, pp. 86–102. DOI: 10.1007/978-3-540-31954-2_6 (cit. on pp. 10, 21, 22).

[AS11] M. M. Ankaralı and U. Saranlı. "Control of underactuated planar pronking through an embedded spring–mass Hopper template". In: *Autonomous Robots* 30.2 (2011), pp. 217–231. DOI: 10.1007/s10514-010-9216-x (cit. on pp. 42, 62).

[Abb04] B. Abbaci. "On a theorem of Philip Hartman". In: *Comptes Rendus Mathematique* 339.11 (2004), pp. 781 –786. DOI: 10.1016/j.crma.2004.10.010 (cit. on pp. 7, 74, 77).

[Agu+12] J. Aguilar, A. Lesov, K. Wiesenfeld, and D. I. Goldman. "Lift–off dynamics in a simple jumping robot". In: *Physical Review Letters* 109.174301 (2012). DOI: 10.1103/PhysRevLett.109.174301 (cit. on p. 101).

[Ale84] R. M. Alexander. "The Gaits of Bipedal and Quadrupedal Animals". In: *The International Journal of Robotics Research* 3.2 (1984), pp. 49–59. DOI: 10.1177/027836498400300205 (cit. on pp. 37, 79).

[Alo06] U. Alon. *An introduction to systems biology: design principles of biological circuits*. CRC press, 2006 (cit. on p. 7).

[And+06] E. Andrianantoandro, S. Basu, D. K. Karig, and R. Weiss. "Synthetic biology: new engineering rules for an emerging discipline". In: *Molecular Systems Biology* 2.1 (2006), pp. 1–14. DOI: 10.1038/msb4100073 (cit. on p. 7).

[And+99] E. Anderson, Z. Bai, C. Bischof, S. Blackford, J. Demmel, J. Dongarra, J. Du Croz, A. Greenbaum, S. Hammarling, A. McKenney, and D. Sorensen. *LAPACK Users' Guide*. Society for Industrial and Applied Mathematics, 1999 (cit. on p. 7).

[And72] P. W. Anderson. "More Is Different". In: *Science* 177.4047 (1972), pp. 393–396. URL: http://www.jstor.org/stable/1734697 (cit. on p. 103).

[BF93] R. Blickhan and R. J. Full. "Similarity in multilegged locomotion: Bouncing like a monopode". In: *Journal of Comparative Physiology A* 173.5 (5 1993), pp. 509–517. DOI: 10.1007/BF00197760 (cit. on p. 5).

[BS05] S. A. Benner and A. M. Sismour. "Synthetic biology". In: *Nature Reviews Genetics* 6.7 (2005), pp. 533–543. DOI: 10.1038/nrg1637 (cit. on pp. 7, 103).

[BT09] K. Byl and R. Tedrake. "Metastable walking machines". In: *The International Journal of Robotics Research* 28.8 (2009), pp. 1040–1064. DOI: 10.1177/0278364909340446 (cit. on p. 101).

[BTZ82] A. Ben-Tal and J. Zowe. "Necessary and sufficient optimality conditions for a class of nonsmooth minimization problems". English. In: *Mathematical Programming* 24.1 (1982), pp. 70–91. DOI: 10.1007/BF01585095 (cit. on p. 94).

[BWF] Burroughs Wellcome Fund. *Career Awards at the Scientific Interface*. Accessed July 2014. URL: http://www.bwfund.org (cit. on p. 3).

[Baj88] R. Bajcsy. "Active perception". In: *Proceedings of the IEEE* 76.8 (1988), pp. 966–1005. DOI: 10.1109/5.5968 (cit. on p. 2).

[Bal00] P. Ballard. "The Dynamics of Discrete Mechanical Systems with Perfect Unilateral Constraints". In: *Archive for Rational Mechanics and Analysis* 154.3 (2000), pp. 199–274. DOI: 10.1007/s002050000105 (cit. on p. 32).

[Ban22] S. Banach. "Sur les opérations dans les ensembles abstraits et leur application aux équations intégrales". In: *Fundamenta Mathematicae* 3.1 (1922), pp. 133–181 (cit. on p. 93).

[Bar+95] S. G. Bartels, L. Kuntz, and S. Scholtes. "Continuous selections of linear functions and nonsmooth critical point theory". In: *Nonlinear Analysis: Theory, Methods & Applications* 24.3 (1995), pp. 385–407. DOI: 10.1016/0362-546X(95)91645-6 (cit. on p. 79).

[Ber67] N. A. Bernstein. *The co–ordination and regulation of movements*. Pergamon Press Ltd., 1967 (cit. on pp. 3, 5).

[Ber84] L. v. Bertalanffy. *General system theory: Foundations, development, applications*. Braziller New York, 1984 (cit. on p. 6).

[Bir+09] P. Birkmeyer, K. Peterson, and R. Fearing. "DASH: A dynamic 16g hexapedal robot". In: *Proceedings of the IEEE International Conference on Intelligent Robots and Systems*. 2009, pp. 2683–2689. DOI: 10.1109/IROS.2009.5354561 (cit. on pp. 5, 6).

[Biz+13] F. Bizzarri, A. Brambilla, and G. Storti Gajani. "Lyapunov exponents computation for hybrid neurons". In: *Journal of Computational Neuroscience* 35.2 (2013), pp. 201–212. DOI: 10.1007/s10827-013-0448-6 (cit. on pp. 79, 95, 99).

[Bli+07] R. Blickhan, A. Seyfarth, H. Geyer, S. Grimmer, H. Wagner, and M. Günther. "Intelligence by mechanics". In: *Philosophical Transactions of the Royal Society A: Mathematical, Physical and Engineering Sciences* 365.1850 (2007), pp. 199–220. DOI: 10.1098/rsta.2006.1911 (cit. on p. 4).

[Bli89] R. Blickhan. "The spring-mass model for running and hopping". In: *Journal of Biomechanics* 22.11–12 (1989), pp. 1217 –1227. DOI: 10.1016/0021-9290(89)90224-8 (cit. on p. 5).

[Bod40] H. Bode. "Relations between attenuation and phase in feedback amplifier design". In: *The Bell System Technical Journal* 19.3 (1940), pp. 421–454. DOI: 10.1002/j.1538-7305.1940.tb00839.x (cit. on p. 8).

[Bro11a] L. Brouwer. "Beweis der invarianz desn-dimensionalen gebiets". German. In: *Mathematische Annalen* 71.3 (1911), pp. 305–313. DOI: 10.1007/BF01456846 (cit. on p. 89).

[Bro11b] T. G. Brown. "The Intrinsic Factors in the Act of Progression in the Mammal". In: *Proceedings of the Royal Society of London. Series B, Containing Papers of a Biological Character* 84.572 (1911), pp. 308–319. DOI: 10.1098/rspb.1911.0077 (cit. on p. 102).

[Bro70] R. Brockett. *Finite dimensional linear systems*. Wiley, 1970 (cit. on p. 7).

[Bue+94] M. Buehler, D. E. Koditschek, and P. J. Kindlmann. "Planning and Control of Robotic Juggling and Catching Tasks". In: *The International Journal of Robotics Research* 13.2 (1994), pp. 101–118. DOI: 10.1177/027836499401300201 (cit. on pp. 41, 66, 70, 99).

[Bur+01] D. Burago, Y. Burago, and S. Ivanov. *A course in metric geometry*. American Mathematical Society Providence, RI, 2001 (cit. on pp. 12–14, 18, 20).

[Bur+11a] S. A. Burden, S. Revzen, and S. S. Sastry. "Dimension reduction near periodic orbits of hybrid systems". In: *Proceedings of the IEEE Conference on Decision and Control*. 2011, pp. 6116–6121. DOI: 10.1109/CDC.2011.6160405 (cit. on pp. 55, 73).

[Bur+11b] S. A. Burden, H. Gonzalez, R. Vasudevan, R. Bajcsy, and S. S. Sastry. "Numerical integration of hybrid dynamical systems via domain relaxation". In: *Proceedings of the IEEE Conference on Decision and Control*. 2011, pp. 3958–3965. DOI: 10.1109/CDC.2011.6161050 (cit. on p. 11).

[Bur+12] S. A. Burden, H. Ohlsson, and S. S. Sastry. "Parameter Identification Near Periodic Orbits of Hybrid Dynamical Systems". In: *Proceedings of the IFAC Symposium on System Identification*. 2012, pp. 1197–1202. DOI: 10.3182/20120711-3-BE-2027.00396 (cit. on pp. 100, 101).

[Bur+13a] S. A. Burden, H. Gonzalez, R. Vasudevan, R. Bajcsy, and S. S. Sastry. "Metrization and simulation of controlled hybrid systems". 2013. URL: http://arxiv.org/abs/1302.4402 (cit. on pp. 53, 62).

[Bur+13b] S. A. Burden, S. Revzen, T. Y. Moore, S. S. Sastry, and R. J. Full. "Using reduced-order models to study dynamic legged locomotion: Parameter identification and model validation". In: *Yearly meeting of the Society for Integrative and Comparative Biology*. 2013. URL: http://www.sicb.org/meetings/2013/schedule/abstractdetails.php?id=405 (cit. on pp. 100, 102).

[Bur+14] S. A. Burden, S. S. Sastry, and R. J. Full. "Optimization for models of legged locomotion: Estimation, synthesis, and design". In: *Yearly meeting of the Society for Integrative and Comparative Biology*. 2014. URL: http://www.sicb.org/meetings/2014/schedule/abstractdetails.php?id=187 (cit. on pp. 100, 101).

[Buz06] G. Buzsáki. *Rhythms of the Brain*. Oxford University Press, 2006 (cit. on p. 7).

[CD91] F. Callier and C. Desoer. *Linear system theory*. Springer, 1991 (cit. on pp. 7, 42, 49, 54, 56, 67).

[Cai+08] C. Cai, R. Goebel, and A. Teel. "Relaxation Results for Hybrid Inclusions". In: *Set–Valued Analysis* 16 (5 2008), pp. 733–757. DOI: 10.1007/s11228-007-0067-3 (cit. on p. 10).

[Car+09] S. G. Carver, N. J. Cowan, and J. M. Guckenheimer. "Lateral stability of the spring–mass hopper suggests a two–step control strategy for running". In: *Chaos: An Interdisciplinary Journal of Nonlinear Science* 19.2 (2009), pp. 026106–026106. DOI: 10.1063/1.3127577 (cit. on pp. 41, 66–68).

[Car78] M. Carver. "Efficient integration over discontinuities in ordinary differential equation simulations". In: *Mathematics and Computers in Simulation* 20.3 (1978), pp. 190–196. DOI: 10.1016/0378-4754(78)90068-X (cit. on p. 11).

[Cha+02] J. G. Cham, S. A. Bailey, J. E. Clark, R. J. Full, and M. R. Cutkosky. "Fast and Robust: Hexapedal Robots via Shape Deposition Manufacturing". In: *The International Journal of Robotics Research* 21.10-11 (2002), pp. 869–882. DOI: 10.1177/027836490202101083 7 (cit. on pp. 101, 103).

[Cha89] R. Chaney. "Optimality conditions for piecewise C^2 nonlinear programming". English. In: *Journal of Optimization Theory and Applications* 61.2 (1989), pp. 179–202. DOI: 10.1007/BF00962796 (cit. on p. 94).

[Cla90] F. H. Clarke. *Optimization and nonsmooth analysis*. Vol. 5. Society for Industrial and Applied Mathematics, 1990 (cit. on p. 98).

[Coh+82] A. Cohen, P. J. Holmes, and R. H. Rand. "The nature of coupling between segmental oscillators of the lamprey spinal generator for locomotion: a model". In: *Journal of Mathematical Biology* 13 (1982), pp. 345–369. DOI: 10.1007/BF00276069 (cit. on p. 41).

[Col+05] S. Collins, A. Ruina, R. Tedrake, and M. Wisse. "Efficient bipedal robots based on passive-dynamic walkers". In: *Science* 307.5712 (2005), pp. 1082–1085. DOI: 10.1126/science.1107799 (cit. on pp. 3, 5, 41, 79).

[Col11] F. S. Collins. "Reengineering Translational Science: The Time Is Right". In: *Science Translational Medicine* 3.90 (2011), p. 90cm17. DOI: 10.1126/scitranslmed.3002747 (cit. on p. 3).

[Cow+14] N. J. Cowan, M. M. Ankaralı, J. P. Dyhr, M. S. Madhav, E. Roth, S. Sefati, S. Sponberg, S. A. Stamper, E. S. Fortune, and T. L. Daniel. "Feedback Control as a Framework for Understanding Tradeoffs in Biology". In: *Integrative and Comparative Biology* 54.2 (2014), pp. 223–237. DOI: 10.1093/icb/icu050 (cit. on p. 103).

[DB+08] M. Di Bernardo, C. J. Budd, P. Kowalczyk, and A. R. Champneys. *Piecewise–smooth dynamical systems: theory and applications*. Springer, 2008 (cit. on p. 79).

[DL11] L. Dieci and L. Lopez. "Fundamental matrix solutions of piecewise smooth differential systems". In: *Mathematics and Computers in Simulation* 81.5 (2011), pp. 932–953. DOI: 10.1016/j.matcom.2010.10.012 (cit. on p. 79).

[De10] A. De. "Neuromechanical control of paddle juggling". MA thesis. The Johns Hopkins University, 2010 (cit. on p. 58).

[Del04] F. Delcomyn. "Insect Walking and Robotics". In: *Annual Review of Entomology* 49.1 (2004). PMID: 14651456, pp. 51–70. DOI: 10.1146/annurev.ento.49.061802.123257 (cit. on p. 4).

[Dic+00] M. H. Dickinson, C. T. Farley, R. J. Full, M. A. R. Koehl, R. Kram, and S. Lehman. "How Animals Move: An Integrative View". In: *Science* 288.5463 (2000), pp. 100–106. DOI: 10.1126/science.288.5463.100 (cit. on p. 5).

[Din+11] J. Ding, J. H. Gillula, H. Huang, M. P. Vitus, W. Zhang, and C. J. Tomlin. "Hybrid Systems in Robotics". In: *IEEE Robotics & Automation Magazine* 18.3 (2011), pp. 33–43. DOI: 10.1109/MRA.2011.942113 (cit. on p. 40).

[Don+08] J. M. Donelan, Q. Li, V. Naing, J. A. Hoffer, D. J. Weber, and A. D. Kuo. "Biomechanical Energy Harvesting: Generating Electricity During Walking with Minimal User Effort". In: *Science* 319.5864 (2008), pp. 807–810. DOI: 10.1126/science.1149860 (cit. on p. 4).

[Edw10] D. H. Edwards. "Neuromechanical simulation". In: *Frontiers in Behavioral Neuroscience* 4.40 (2010). DOI: 10.3389/fnbeh.2010.00040 (cit. on p. 5).

[Elh+12] E. Elhamifar, G. Sapiro, and R. Vidal. "Finding Exemplars from Pairwise Dissimilarities via Simultaneous Sparse Recovery". In: *Advances in Neural Information Processing Systems 25*. Ed. by F. Pereira, C. J. C. Burges, L. Bottou, and K. Q. Weinberger. Curran Associates, Inc., 2012, pp. 19–27. URL: http://papers.nips.cc/paper/4705-finding-exemplars-from-pairwise-dissimilarities-via-simultaneous-sparse-recovery.pdf (cit. on p. 100).

[Elh+14] E. Elhamifar, S. A. Burden, and S. S. Sastry. "Adaptive piecewise–affine inverse modeling of hybrid dynamical systems". In: *Proceedings of the IFAC World Congress*. 2014 (cit. on pp. 100, 101).

[Esp+01] J. M. Esposito, V. Kumar, and G. J. Pappas. "Accurate Event Detection for Simulating Hybrid Systems". English. In: *Hybrid Systems: Computation and Control*. Ed. by M. D. Di Benedetto and A. L. Sangiovanni-Vincentelli. Vol. 2034. Lecture Notes in Computer Science. Springer Berlin / Heidelberg, 2001, pp. 204–217. DOI: 10.1007/3-540-45351-2_19 (cit. on p. 11).

[FH85] T. Flash and N. Hogan. "The coordination of arm movements: an experimentally confirmed mathematical model". In: *The Journal of Neuroscience* 5.7 (1985), pp. 1688–1703 (cit. on p. 5).

[FI04] A. Fehnker and F. Ivančić. "Benchmarks for Hybrid Systems Verification". In: *Hybrid Systems: Computation and Control*. Ed. by R. Alur and G. J. Pappas. Vol. 2993. Lecture Notes in Computer Science. Springer Berlin / Heidelberg, 2004, pp. 381–397. DOI: 10.1007/978-3-540-24743-2_22 (cit. on p. 36).

[FK99] R. Full and D. Koditschek. "Templates and anchors: neuromechanical hypotheses of legged locomotion on land". In: *Journal of Experimental Biology* 202.23 (1999), pp. 3325–3332. URL: http://jeb.biologists.org/content/202/23/3325.abstract (cit. on pp. 3, 41, 62).

[Fer+05] D. P. Ferris, G. S. Sawicki, and A. R. Domingo. "Powered Lower Limb Orthoses for Gait Rehabilitation". In: *Topics in Spinal Cord Injury Rehabilitation* 11.2 (2005), pp. 34–49. DOI: 10.1310/6GL4-UM7X-519H-9JYD (cit. on p. 4).

[Fil88] A. F. Filippov. *Differential equations with discontinuous righthand sides*. Springer, 1988 (cit. on pp. 20, 80, 91, 98).

[Fle00] R. Fletcher. *Practical methods of optimization*. John Wiley & Sons, 2000 (cit. on p. 94).

[Flo83] G. Floquet. “Sur les équations différentielles linéaires à coefficients périodiques”. In: *Annales Scientifiques de lÉcole Normale Supérieure, Sér* 2 (1883), p. 12 (cit. on p. 68).

[Fol99] G. B. Folland. *Real analysis*. Wiley, 1999 (cit. on pp. 16, 80, 98).

[Ful+02] R. J. Full, T. Kubow, J. Schmitt, P. Holmes, and D. E. Koditschek. “Quantifying Dynamic Stability and Maneuverability in Legged Locomotion”. In: *Integrative and Comparative Biology* 42.1 (2002), pp. 149–157. DOI: 10.1093/icb/42.1.149 (cit. on p. 5).

[Füc+12] R. M. Füchslin, A. Dzyakanchuk, D. Flumini, H. Hauser, K. J. Hunt, R. H. Luchsinger, B. Reller, S. Scheidegger, and R. Walker. “Morphological computation and morphological control: Steps toward a formal theory and applications”. In: *Artificial Life* 19.1 (2012), pp. 9–34. DOI: 10.1162/ARTL_a_00079 (cit. on p. 4).

[GH83] J. Guckenheimer and P. Holmes. *Nonlinear oscillations, dynamical systems, and bifurcations of vector fields*. Springer, 1983 (cit. on pp. 7, 48, 49, 68, 69, 77).

[GK51] G. Gabrielli and T. von Karmen. “What Price Speed?” In: *Journal of the American Society for Naval Engineers* 63.1 (1951), pp. 188–200. DOI: 10.1111/j.1559-3584.1951.tb02891.x (cit. on p. 101).

[GN92] J. Guckenheimer and A. Nerode. “Simulation for hybrid systems and nonlinear control”. In: *Proceedings of the IEEE Conference on Decision and Control*. 1992, pp. 2980–2981. DOI: 10.1109/CDC.1992.371267 (cit. on p. 11).

[GP07] A. Girard and G. J. Pappas. “Approximation Metrics for Discrete and Continuous Systems”. In: *IEEE Transactions on Automatic Control* 52.5 (2007), pp. 782–798. DOI: 10.1109/TAC.2007.895849 (cit. on p. 40).

[GP78] L. Glass and J. S. Pasternack. “Stable oscillations in mathematical models of biological control systems”. In: *Journal of Mathematical Biology* 6.3 (1978), pp. 207–223. DOI: 10.1007/BF02547797 (cit. on pp. 41, 70, 99).

[Gar+89] C. E. Garcia, D. M. Prett, and M. Morari. “Model predictive control: theory and practice—a survey”. In: *Automatica* 25.3 (1989), pp. 335–348. DOI: 10.1016/0005-1098(89)90002-2 (cit. on p. 101).

[Ghi+03] R. M. Ghigliazza, R. Altendorfer, P. Holmes, and D. E. Koditschek. “A Simply Stabilized Running Model”. In: *SIAM Journal on Applied Dynamical Systems* 2.2 (2003), pp. 187–218. DOI: 10.1137/S1111111102408311 (cit. on pp. 5, 37, 41, 62).

[Gok08] D. Gokhman. “Topologies for hybrid solutions”. In: *Nonlinear Analysis: Hybrid Systems* 2.2 (2008), pp. 468–473. DOI: 10.1016/j.nahs.2006.12.006 (cit. on p. 10).

[Gol+99] M. Golubitsky, I. Stewart, P.-L. Buono, and J. J. Collins. "Symmetry in locomotor central pattern generators and animal gaits". In: *Nature* 401.6754 (1999), pp. 693–695. DOI: 10.1038/44416 (cit. on pp. 37, 41, 79).

[Gol96] A. Goldbeter. *Biochemical oscillations and cellular rhythms*. Vol. 1. Cambridge University Press, 1996 (cit. on p. 7).

[Gri+02] J. W. Grizzle, G. Abba, and F. Plestan. "Asymptotically stable walking for biped robots: Analysis via systems with impulse effects". In: *IEEE Transactions on Automatic Control* 46.1 (2002), pp. 51–64. DOI: 10.1109/9.898695 (cit. on pp. 41, 49, 79, 100).

[Gri85] S. Grillner. "Neurobiological Bases of Rhythmic Motor Acts in Vertebrates". In: *Science* 228.4696 (1985), pp. 143–149. DOI: 10.1126/science.3975635 (cit. on p. 41).

[Guc75] J. Guckenheimer. "Isochrons and phaseless sets". In: *Journal of Mathematical Biology* 1.3 (1975), pp. 259–273. DOI: 10.1007/BF01273747 (cit. on pp. 68, 69).

[Guf99] C. Guffey. "Costs associated with leg autotomy in the harvestmen Leiobunum nigripes and Leiobunum vittatum (Arachnida: Opiliones)". In: *Canadian Journal of Zoology* 77.5 (1999), pp. 824–830. DOI: 10.1139/z99-026 (cit. on p. 3).

[HB71] B Hess and A Boiteux. "Oscillatory Phenomena in Biochemistry". In: *Annual Review of Biochemistry* 40.1 (1971), pp. 237–258. DOI: 10.1146/annurev.bi.40.070171.001321 (cit. on p. 7).

[HC10] M. A. Hamburg and F. S. Collins. "The Path to Personalized Medicine". In: *New England Journal of Medicine* 363.4 (2010), pp. 301–304. DOI: 10.1056/NEJMp1006304 (cit. on pp. 3, 103).

[HP00] I. A. Hiskens and M. A. Pai. "Trajectory sensitivity analysis of hybrid systems". In: *IEEE Transactions on Circuits and Systems I: Fundamental Theory and Applications* 47.2 (2000), pp. 204–220. DOI: 10.1109/81.828574 (cit. on p. 79).

[HR07] I. A. Hiskens and P. B. Reddy. "Switching–induced stable limit cycles". In: *Nonlinear Dynamics* 50.3 (2007), pp. 575–585. DOI: 10.1007/s11071-006-9175-0 (cit. on pp. 41, 70, 99).

[HS74] M. Hirsch and S. Smale. *Differential equations, dynamical systems, and linear algebra*. Academic Press, 1974 (cit. on pp. 48, 71, 89).

[Har60] P. Hartman. "On local homeomorphisms of Euclidean spaces". In: *Boletín de la Sociedad Matemáticas de Mexicana* 5.2 (1960), pp. 220–241 (cit. on pp. 7, 74, 77).

[Hat02] A. Hatcher. *Algebraic topology*. Cambridge University Press, 2002 (cit. on p. 89).

[Hau+11] H. Hauser, A. J. Ijspeert, R. M. Füchslin, R. Pfeifer, and W. Maass. "Towards a theoretical foundation for morphological computation with compliant bodies". In: *Biological Cybernetics* 105.5–6 (2011), pp. 355–370. DOI: 10.1007/s00422-012-0471-0 (cit. on p. 4).

[Hay+12] G. Haynes, A. Rizzi, and D. E. Koditschek. "Multistable phase regulation for robust steady and transitional legged gaits". In: *The International Journal of Robotics Research* 31.14 (2012), pp. 1712–1738. DOI: 10.1177/0278364912458463 (cit. on p. 41).

[Hir76] M. Hirsch. *Differential topology*. Springer–Verlag, 1976 (cit. on pp. 43, 71, 72, 92).

[Hol+06] P. Holmes, R. J. Full, D. E. Koditschek, and J. Guckenheimer. "The Dynamics of Legged Locomotion: Models, Analyses, and Challenges". In: *SIAM Review* 48.2 (2006), pp. 207–304. DOI: 10.1137/S0036144504445133 (cit. on pp. 5, 41, 42, 62, 64, 69, 79, 95).

[Hoo+04] L. Hood, J. R. Heath, M. E. Phelps, and B. Lin. "Systems Biology and New Technologies Enable Predictive and Preventative Medicine". In: *Science* 306.5696 (2004), pp. 640–643. DOI: 10.1126/science.1104635 (cit. on pp. 3, 7, 103).

[Hoo+10] A. Hoover, S. A. Burden, X. Fu, S. S. Sastry, and R. Fearing. "Bio-inspired design and dynamic maneuverability of a minimally actuated six-legged robot". In: *Proceedings of the IEEE International Conference on Biomedical Robotics and Biomechatronics*. 2010, pp. 869–876. DOI: 10.1109/BIOROB.2010.5626034 (cit. on pp. 5, 6, 37, 100, 101).

[Ins+13] T. R. Insel, S. C. Landis, and F. S. Collins. "The NIH BRAIN Initiative". In: *Science* 340.6133 (2013), pp. 687–688. DOI: 10.1126/science.1239276 (cit. on p. 3).

[Iva98] A. Ivanov. "The stability of periodic solutions of discontinuous systems that intersect several surfaces of discontinuity". In: *Journal of Applied Mathematics and Mechanics* 62.5 (1998), pp. 677–685. DOI: 10.1016/S0021-8928(98)00087-2 (cit. on pp. 79, 93).

[JF02] D. L. Jindrich and R. J. Full. "Dynamic stabilization of rapid hexapedal locomotion". In: *Journal of Experimental Biology* 205.18 (2002), pp. 2803–2823. URL: http://jeb.biologists.org/content/205/18/2803.abstract (cit. on pp. 5, 62, 102).

[JF99] D. L. Jindrich and R. J. Full. "Many-legged maneuverability: dynamics of turning in hexapods". In: *Journal of Experimental Biology* 202.12 (1999), pp. 1603–1623. URL: http://jeb.biologists.org/content/202/12/1603.abstract (cit. on p. 5).

[JK13a] A. M. Johnson and D. E. Koditschek. "Legged Self–Manipulation". In: *IEEE Access* 1 (2013), pp. 310–334. DOI: 10.1109/ACCESS.2013.2263192 (cit. on p. 100).

[JK13b] A. M. Johnson and D. E. Koditschek. "Toward a vocabulary of legged leaping". In: *IEEE International Conference on Robotics and Automation*. 2013, pp. 2568–2575. DOI: 10.1109/ICRA.2013.6630928 (cit. on p. 101).

[JL01] O. Janin and C. H. Lamarque. "Comparison of several numerical methods for mechanical systems with impacts". In: *International Journal for Numerical Methods in Engineering* 51.9 (2001), pp. 1101–1132. DOI: 10.1002/nme.206 (cit. on p. 35).

[Joh+12] A. M. Johnson, G. C. Haynes, and D. E. Koditschek. "Standing self-manipulation for a legged robot". In: *Proceedings of the IEEE International Conference on Intelligent Robots and Systems*. 2012, pp. 272–279. DOI: 10.1109/IROS.2012.6386214 (cit. on p. 37).

[Joh+99] K. H. Johansson, M. Egerstedt, J. Lygeros, and S. S. Sastry. "On the regularization of Zeno hybrid automata". In: *Systems & Control Letters* 38.3 (1999), pp. 141–150. DOI: 10.1016/S0167-6911(99)00059-6 (cit. on pp. 10, 26).

[KF99] T. M. Kubow and R. J. Full. "The role of the mechanical system in control: a hypothesis of self–stabilization in hexapedal runners". In: *Philosophical Transactions of the Royal Society of London. Series B: Biological Sciences* 354.1385 (1999), pp. 849–861. DOI: 10.1098/rstb.1999.0437 (cit. on p. 5).

[KH07] R. P. Kukillaya and P. J. Holmes. "A hexapedal jointed–leg model for insect locomotion in the horizontal plane". In: *Biological Cybernetics* 97.5–6 (2007), pp. 379–395. DOI: 10.1007/s00422-007-0180-2 (cit. on p. 5).

[KK02] E. Klavins and D. E. Koditschek. "Phase regulation of decentralized cyclic robotic systems". In: *The International Journal of Robotics Research* 21.3 (2002), pp. 257–275. DOI: 10.1177/027836402320556430 (cit. on pp. 41, 79).

[KS95] L. Kuntz and S. Scholtes. "Qualitative aspects of the local approximation of a piecewise differentiable function". In: *Nonlinear Anal.* 25.2 (1995), pp. 197–215. DOI: 10.1016/0362-546X(94)00202-S (cit. on p. 100).

[Kal59] R. Kalman. "On the general theory of control systems". In: *IRE Transactions on Automatic Control* 4.3 (1959), pp. 110–110. DOI: 10.1109/TAC.1959.1104873 (cit. on pp. 7, 100).

[Kel75] J. Kelley. *General topology*. Springer, 1975 (cit. on pp. 11, 12, 18).

[Kim+06] S. Kim, J. Clark, and M. Cutkosky. "iSprawl: Design and tuning for high-speed autonomous open-loop running". In: *The International Journal of Robotics Research* 25.9 (2006), pp. 903–912. DOI: 10.1177/0278364906069150 (cit. on pp. 5, 6, 37).

[Kit02a] H. Kitano. "Computational systems biology". In: *Nature* 420.6912 (2002), pp. 206–210. DOI: 10.1038/nature01254 (cit. on p. 7).

[Kit02b] H. Kitano. "Systems Biology: A Brief Overview". In: *Science* 295.5560 (2002), pp. 1662–1664. DOI: 10.1126/science.1069492 (cit. on pp. 6, 7, 103).

[Kiw85] K. C. Kiwiel. *Methods of descent for nondifferentiable optimization*. Springer, 1985 (cit. on p. 94).

[Kla+00] E. Klavins, H. Komsuoglu, R. J. Full, and D. E. Koditschek. "The Role of Reflexes Versus Central Pattern Generators in Dynamical Legged Locomotion". In: *Neurotechnology for Biomimetic Robots*. MIT Press, 2000 (cit. on p. 4).

[Kod+04] D. E. Koditschek, R. J. Full, and M. Buehler. "Mechanical aspects of legged locomotion control". In: *Arthropod Structure & Development* 33.3 (2004), pp. 251–272. DOI: 10.1016/j.asd.2004.06.003 (cit. on pp. 4, 5).

[Kod92] D. E. Koditschek. "Task encoding: Toward a scientific paradigm for robot planning and control". In: *Robotics and Autonomous Systems* 9.1–2 (1992), pp. 5–39. DOI: 10.1016/0921-8890(92)90031-S (cit. on p. 2).

[Kuh70] T. S. Kuhn. *The structure of scientific revolutions*. Second. University of Chicago Press, 1970 (cit. on p. 103).

[Kuk+09] R. P. Kukillaya, J. Proctor, and P. J. Holmes. "Neuromechanical models for insect locomotion: Stability, maneuverability, and proprioceptive feedback". In: *Chaos: An Interdisciplinary Journal of Nonlinear Science* 19.2 (2009), p. 026107. DOI: 10.1063/1.3141306 (cit. on pp. 5, 41, 42, 64).

[LB11] D. V. Lee and A. A. Biewener. "BigDog-Inspired Studies in the Locomotion of Goats and Dogs". In: *Integrative and Comparative Biology* (2011). DOI: 10.1093/icb/icr061 (cit. on p. 4).

[Lat12] M. L. Latash. "The bliss (not the problem) of motor abundance (not redundancy)". In: *Experimental Brain Research* 217.1 (2012), pp. 1–5. DOI: 10.1007/s00221-012-3000-4 (cit. on p. 5).

[LeV07] R. LeVeque. *Finite difference methods for ordinary and partial differential equations*. Society for Industrial and Applied Mathematics, 2007 (cit. on p. 29).

[Lee12] J. M. Lee. *Introduction to smooth manifolds*. Springer–Verlag, 2012 (cit. on pp. 17, 40, 43–45, 56, 66, 71, 73, 74, 80, 82, 87, 89, 93, 96, 97).

[Lem+95] C. Lemaréchal, A. Nemirovskii, and Y. Nesterov. "New variants of bundle methods". English. In: *Mathematical Programming* 69.1-3 (1995), pp. 111–147. DOI: 10.1007/BF01585555 (cit. on p. 94).

[Li+13] C. Li, T. Zhang, and D. I. Goldman. "A Terradynamics of Legged Locomotion on Granular Media". In: *Science* 339.6126 (2013), pp. 1408–1412. DOI: 10.1126/science.1229163 (cit. on pp. 5, 41).

[Lju99] L. Ljung. *System identification: theory for the user*. Prentice–Hall, 1999 (cit. on pp. 7, 100).

[Loe+99] G. E. Loeb, I. E. Brown, and E. J. Cheng. "A hierarchical foundation for models of sensorimotor control". English. In: *Experimental Brain Research* 126.1 (1999), pp. 1–18. DOI: 10.1007/s002210050712 (cit. on p. 5).

[Lue69] D. G. Luenberger. *Optimization by vector space methods*. John Wiley & Sons, 1969 (cit. on p. 7).

[Lyg+03] J. Lygeros, K. H. Johansson, S. N. Simic, J. Zhang, and S. S. Sastry. "Dynamical properties of hybrid automata". In: *IEEE Transactions on Automatic Control* 48.1 (2003), pp. 2–17. DOI: 10.1109/TAC.2002.806650 (cit. on pp. 25, 41, 45–47, 79).

[MS90] R. E. Mirollo and S. H. Strogatz. "Synchronization of Pulse–Coupled Biological Oscillators". In: *SIAM Journal on Applied Mathematics* 50.6 (1990), pp. 1645–1662. DOI: 10.1137/0150098 (cit. on pp. 79, 99).

[Ma+04] Y. Ma, S. Soatto, J. Košecká, and S. S. Sastry. *An invitation to 3–D vision*. Springer, 2004 (cit. on p. 2).

[Mar+11] J. Markowitz, P. Krishnaswamy, M. F. Eilenberg, K. Endo, C. Barnhart, and H. Herr. "Speed adaptation in a powered transtibial prosthesis controlled with a neuromuscular model". In: *Philosophical Transactions of the Royal Society B: Biological Sciences* 366.1570 (2011), pp. 1621–1631. DOI: 10.1098/rstb.2010.0347 (cit. on p. 4).

[May10] C. G. Mayhew. "Hybrid Control for Topologically Constrained Systems". PhD thesis. University of California at Santa Barbara, 2010 (cit. on p. 7).

[McG90] T. McGeer. "Passive dynamic walking". In: *The International Journal of Robotics Research* 9.2 (1990), p. 62. DOI: 10.1177/027836499000900206 (cit. on pp. 5, 41).

[McS34] E. J. McShane. "Extension of range of functions". In: *Bulletin of the American Mathematical Society* 40.12 (1934), pp. 837–843. DOI: 10.1090/S0002-9904-1934-05978-0 (cit. on p. 16).

[Mes68] M. D. Mesarović. *Systems theory and biology*. Springer, 1968 (cit. on p. 7).

[Mil+12] L. A. Miller, D. I. Goldman, T. L. Hedrick, E. D. Tytell, Z. J. Wang, J. Yen, and S. Alben. "Using Computational and Mechanical Models to Study Animal Locomotion". In: *Integrative and Comparative Biology* 52.5 (2012), pp. 553–575. DOI: 10.1093/icb/ics115 (cit. on p. 103).

[Mil73] J. G. Miller. "Living Systems: The Organism". English. In: *The Quarterly Review of Biology* 48.1 (1973), pp. 92–276. URL: http://www.jstor.org/stable/2820539 (cit. on p. 7).

[Mom+05] K. D. Mombaur, H. G. Bock, J. P. Schlöder, and R. W. Longman. "Open-loop stable solutions of periodic optimal control problems in robotics". In: *Zeitschrift für Angewandte Mathematik und Mechanik (ZAMM)* 85.7 (2005), pp. 499–515. DOI: 10.1002/zamm.200310190 (cit. on p. 101).

[Mon+12] J.-M. Mongeau, B. McRae, A. Jusufi, P. Birkmeyer, A. M. Hoover, R. Fearing, and R. J. Full. "Rapid Inversion: Running Animals and Robots Swing like a Pendulum under Ledges". In: *PLoS ONE* 7.6 (2012), e38003. DOI: 10.1371/journal.pone.0038003 (cit. on pp. 6, 101).

[Moo+10] T. Y. Moore, S. Revzen, S. A. Burden, and R. J. Full. "Adding inertia and mass to test stability predictions in rapid running insects". In: *Yearly meeting of the Society for Integrative and Comparative Biology*. 2010. URL: http://sicb.org/meetings/2010/schedule/abstractdetails.php3?id=1290 (cit. on p. 102).

[Mun00] J. R. Munkres. *Topology*. Prentice–Hall, 2000 (cit. on p. 12).

[Mur+94] R. M. Murray, Z. Li, and S. S. Sastry. *A mathematical introduction to robotic manipulation*. CRC Press, 1994 (cit. on pp. 2, 63, 64).

[Mut+14] J. T. Muth, D. M. Vogt, R. L. Truby, Y. Mengüç, D. B. Kolesky, R. J. Wood, and J. A. Lewis. "Embedded 3D Printing of Strain Sensors within Highly Stretchable Elastomers". In: *Advanced Materials* (2014). DOI: 10.1002/adma.201400334 (cit. on pp. 101, 103).

[NK93] A. Nerode and W. Kohn. "Models for hybrid systems: Automata, topologies, controllability, observability". In: *Hybrid Systems*. Ed. by R. Grossman, A. Nerode, A. Ravn, and H. Rischel. Vol. 736. Lecture Notes in Computer Science. Springer Berlin / Heidelberg, 1993, pp. 317–356. DOI: 10.1007/3-540-57318-6_35 (cit. on p. 10).

[NRI] National Science Foundation. *National Robotics Initiative*. 2014. URL: http://www.nsf.gov/nri (cit. on p. 2).

[Ner+02] S. Nersesov, V. Chellaboina, and M. Haddad. "A generalization of Poincare's theorem to hybrid and impulsive dynamical systems". In: *Proceedings of the American Control Conference*. Vol. 2. 2002, pp. 1240–1245. DOI: 10.1109/ACC.2002.1023189 (cit. on p. 49).

[Nis+07] K. Nishikawa, A. A. Biewener, P. Aerts, A. N. Ahn, H. J. Chiel, M. A. Daley, T. L. Daniel, R. J. Full, M. E. Hale, T. L. Hedrick, A. K. Lappin, T. R. Nichols, R. D. Quinn, R. A. Satterlie, and B. Szymik. "Neuromechanics: an integrative approach for understanding motor control". In: *Integrative and Comparative Biology* 47.1 (2007), pp. 16–54. DOI: 10.1093/icb/icm024 (cit. on pp. 2, 4, 103).

[Nyq32] H. Nyquist. "Regeneration theory". In: *The Bell System Technical Journal* 11.1 (1932), pp. 126–147. DOI: 10.1002/j.1538-7305.1932.tb02344.x (cit. on p. 8).

[O'R81] J. O'Reilly. "The discrete linear time invariant time–optimal control problem—An overview". In: *Automatica* 17.2 (1981), pp. 363–370. DOI: 10.1016/0005-1098(81)90053-4 (cit. on pp. 67, 100).

[OA11] Y. Or and A. D. Ames. "Stability and Completion of Zeno Equilibria in Lagrangian Hybrid Systems". In: *IEEE Transactions on Automatic Control* 56.6 (2011), pp. 1322–1336. DOI: 10.1109/TAC.2010.2080790 (cit. on p. 48).

[OED] OED Online. *Oxford English Dictionary*. Accessed July 2014. URL: http://www.oed.com (cit. on pp. 1, 4).

[Ort90] J. Ortega. *Numerical analysis: a second course*. Vol. 3. Society for Industrial Mathematics, 1990 (cit. on pp. 75, 76).

[PG09] I. Poulakakis and J. W. Grizzle. "The spring loaded inverted pendulum as the hybrid zero dynamics of an asymmetric hopper". In: *IEEE Transactions on Automatic Control* 54.8 (2009), pp. 1779–1793. DOI: 10.1109/TAC.2009.2024565 (cit. on p. 42).

[PS03] L. Paoli and M. Schatzman. "A numerical scheme for impact problems II: The multidimensional case". In: *SIAM Journal on Numerical Analysis* 40.2 (2003), pp. 734–768. DOI: 10.1137/S003614290037873X (cit. on pp. 11, 34).

[PW09] P. E. M. Purnick and R. Weiss. "The second wave of synthetic biology: from modules to systems". In: *Nature Reviews Molecular Cell Biology* 10.6 (2009), pp. 410–422. DOI: 10.1038/nrm2698 (cit. on p. 7).

[Pfe+07] R. Pfeifer, M. Lungarella, and F. Iida. "Self-Organization, Embodiment, and Biologically Inspired Robotics". In: *Science* 318.5853 (2007), pp. 1088–1093. DOI: 10.1126/science.1145803 (cit. on p. 4).

[Pol84] D. Pollard. *Convergence of Stochastic Processes*. Springer, 1984 (cit. on p. 10).

[Pol97] E. Polak. *Optimization: algorithms and consistent approximations*. Springer–Verlag, 1997 (cit. on pp. 16, 28, 94, 100).

[Pro+10] J. Proctor, R. P. Kukillaya, and P. J. Holmes. "A phase–reduced neuro–mechanical model for insect locomotion: feed–forward stability and proprioceptive feedback". In: *Philosophical Transactions of the Royal Society A: Mathematical, Physical and Engineering Sciences* 368.1930 (2010), pp. 5087–5104. DOI: 10.1098/rsta.2010.0134 (cit. on p. 5).

[QR98] R. Quinn and R. Ritzmann. "Construction of a hexapod robot with cockroach kinematics benefits both robotics and biology". In: *Connection Science* 10.3 (1998), pp. 239–254. DOI: 10.1080/095400998116422 (cit. on p. 4).

[RD12] P. Reist and R. D'Andrea. "Design and Analysis of a Blind Juggling Robot". In: *IEEE Transactions on Robotics* 28.6 (2012), pp. 1228–1243. DOI: 10.1109/TRO.2012.2205493 (cit. on p. 5).

[RG12] S. Revzen and J. M. Guckenheimer. "Finding the dimension of slow dynamics in a rhythmic system". In: *Journal of The Royal Society Interface* 9.70 (2012), pp. 957–971. DOI: 10.1098/rsif.2011.0431 (cit. on p. 68).

[RS97] D. Ralph and S. Scholtes. "Sensitivity analysis of composite piecewise smooth equations". English. In: *Mathematical Programming* 76.3 (1997), pp. 593–612. DOI: 10.1007/BF02614400 (cit. on pp. 88, 95).

[Rai+08] M. H. Raibert, K. Blankespoor, G. Nelson, R. Playter, and the BigDog Team. "BigDog, the Rough–Terrain Quadruped Robot". In: *Proceedings of the IFAC World Congress* (2008). Ed. by C. Myung, pp. 10822–10825. DOI: 10.3182/20080706-5-kr-1001.01833 (cit. on p. 101).

[Rai+86] M. H. Raibert, M. Chepponis, and H. B. Brown, Jr. "Running on four legs as though they were one". In: *IEEE Journal of Robotics and Automation* 2.2 (1986), pp. 70–82. DOI: 10.1109/JRA.1986.1087044 (cit. on p. 37).

[Rai86] M. H. Raibert. "Legged robots". In: *Communications of the ACM* 29.6 (1986), pp. 499–514. DOI: 10.1145/5948.5950 (cit. on pp. 66, 79).

[Ram+04] M. Ramos, D. J. Irschick, and T. E. Christenson. "Overcoming an evolutionary conflict: Removal of a reproductive organ greatly increases locomotor performance". In: *Proceedings of the National Academy of Sciences of the United States of America* 101.14 (2004), pp. 4883–4887. DOI: 10.1073/pnas.0400324101 (cit. on p. 4).

[Rem+10] C. D. Remy, K. Buffinton, and R. Siegwart. "Stability Analysis of Passive Dynamic Walking of Quadrupeds". In: *The International Journal of Robotics Research* 29.9 (2010), pp. 1173–1185. DOI: 10.1177/0278364909344635 (cit. on pp. 66, 79, 101).

[Rev+13] S. Revzen, S. A. Burden, T. Y. Moore, J.-M. Mongeau, and R. J. Full. "Instantaneous kinematic phase reflects neuromechanical response to lateral perturbations of running cockroaches". In: *Biological Cybernetics* 107.2 (2013), pp. 179–200. DOI: 10.1007/s00422-012-0545-z (cit. on p. 102).

[Rev09] S. Revzen. "Neuromechanical Control Architectures of Arthopod Locomotion". PhD thesis. University of California at Berkeley, 2009 (cit. on p. 68).

[Rie+10] J. A. Rieffel, F. J. Valero-Cuevas, and H. Lipson. "Morphological communication: exploiting coupled dynamics in a complex mechanical structure to achieve locomotion". In: *Journal of The Royal Society Interface* 7.45 (2010), pp. 613–621. DOI: 10.1098/rsif.2009.0240 (cit. on p. 4).

[Rie77] R. Riedl. "A Systems–Analytical Approach to Macro–Evolutionary Phenomena". English. In: *The Quarterly Review of Biology* 52.4 (1977), pp. 351–370. URL: http://www.jstor.org/stable/2823251 (cit. on p. 7).

[Rit+00] R. E. Ritzmann, R. D. Quinn, J. T. Watson, and S. N. Zill. "Insect Walking and Biorobotics: A Relationship with Mutual Benefits". In: *BioScience* 50.1 (2000), pp. 23–33. DOI: 10.1641/0006-3568(2000)050[0023:IWABAR]2.3.CO;2 (cit. on p. 4).

[Roc03] R. Rockafellar. "A Property of Piecewise Smooth Functions". In: *Computational Optimization and Applications* 25.1/3 (2003), pp. 247–250. DOI: 10.1023/A:1022921624832 (cit. on p. 79).

[Ros58] R. Rosen. "A relational theory of biological systems". In: *The Bulletin of Mathematical Biophysics* 20.3 (1958), pp. 245–260. DOI: 10.1007/BF02478302 (cit. on p. 7).

[Rot+14] E. Roth, S. Sponberg, and N. J. Cowan. "A comparative approach to closed-loop computation". In: *Current Opinion in Neurobiology* 25 (2014), pp. 54–62. DOI: 10.1016/j.conb.2013.11.005 (cit. on pp. 2, 102).

[Rud76] W. Rudin. *Principles of mathematical analysis*. McGraw–Hill, 1976 (cit. on p. 31).

[SA93] S. Schaal and C. Atkeson. "Open loop stable control strategies for robot juggling". In: *Proceedings of the IEEE International Conference on Robotics and Automation*. 1993, pp. 913–918. DOI: 10.1109/ROBOT.1993.292260 (cit. on p. 5).

[SB89] S. Sastry and M. Bodson. *Adaptive control: stability, convergence, and robustness*. 1989 (cit. on p. 7).

[SD81] S. S. Sastry and C. A. Desoer. "Jump behavior of circuits and systems". In: *IEEE Transactions on Circuits and Systems* 28.12 (1981), pp. 1109–1124. DOI: 10.1109/TCS.1981.1084943 (cit. on p. 99).

[SF] Simons Foundation. *Targeted Grants in the Mathematical Modeling of Living Systems*. Accessed July 2014. URL: http://www.simonsfoundation.org (cit. on p. 3).

[SH00a] J. Schmitt and P. Holmes. "Mechanical models for insect locomotion: dynamics and stability in the horizontal plane - II. Application". In: *Biological Cybernetics* 83.6 (2000), pp. 517–527. DOI: 10.1007/s004220000180 (cit. on p. 5).

[SH00b] J. Schmitt and P. Holmes. "Mechanical models for insect locomotion: dynamics and stability in the horizontal plane I. Theory". In: *Biological Cybernetics* 83.6 (2000), pp. 501–515. DOI: 10.1007/s004220000181 (cit. on pp. 5, 41, 62, 63).

[SH01] J. Schmitt and P. Holmes. "Mechanical models for insect locomotion: stability and parameter studies". In: *Physica D: Nonlinear Phenomena* 156.1–2 (2001), pp. 139–168. DOI: 10.1016/S0167-2789(01)00271-8 (cit. on p. 5).

[SH06] J. Seipel and P. Holmes. "Three-dimensional Translational Dynamics and Stability of Multi-legged Runners". In: *The International Journal of Robotics Research* 25.9 (2006), pp. 889–902. DOI: 10.1177/0278364906069045 (cit. on p. 37).

[SS99] J. Scholz and G. Schöner. "The uncontrolled manifold concept: identifying control variables for a functional task". In: *Experimental Brain Research* 126.3 (1999), pp. 289–306. DOI: 10.1007/s002210050738 (cit. on p. 5).

[ST10] R. G. Sanfelice and A. R. Teel. "Dynamical properties of hybrid systems simulators". In: *Automatica* 46.2 (2010), pp. 239 –248. DOI: 10.1016/j.automatica.2009.09.026 (cit. on pp. 10, 32, 33).

[SZ92] H. Schramm and J. Zowe. "A Version of the Bundle Idea for Minimizing a Nonsmooth Function: Conceptual Idea, Convergence Analysis, Numerical Results". In: *SIAM Journal on Optimization* 2.1 (1992), pp. 121–152. DOI: 10.1137/0802008 (cit. on p. 94).

[Sar+01] U. Saranli, M. Buehler, and D. E. Koditschek. "Rhex: A simple and highly mobile hexapod robot". In: *The International Journal of Robotics Research* 20.7 (2001), pp. 616–631. DOI: 10.1177/02783640122067570 (cit. on pp. 5, 6, 37).

[Sas99] S. S. Sastry. *Nonlinear Systems: Analysis, Stability, and Control*. Springer, 1999 (cit. on p. 77).

[Sch+02] J. Schmitt, M. Garcia, R. Razo, P. Holmes, and R. J. Full. "Dynamics and stability of legged locomotion in the horizontal plane: a test case using insects". In: *Biological Cybernetics* 86.5 (2002), pp. 343–353. DOI: 10.1007/s00422-001-0300-3 (cit. on p. 5).

[Sch+09] K. Schwenk, D. K. Padilla, G. S. Bakken, and R. J. Full. "Grand challenges in organismal biology". In: *Integrative and Comparative Biology* 49.1 (2009), pp. 7–14. DOI: 10.1093/icb/icp034 (cit. on pp. 4, 6, 103).

[Sch12] S. Scholtes. *Introduction to piecewise differentiable equations*. Springer–Verlag, 2012. DOI: 10.1007/978-1-4614-4340-7 (cit. on pp. 79–81, 84, 86, 88, 93, 95, 96).

[Sch98] M. Schatzman. "Uniqueness and continuous dependence on data for one–dimensional impact problems". In: *Mathematical and Computer Modelling* 28.4—8 (1998), pp. 1–18. DOI: 10.1016/S0895-7177(98)00104-6 (cit. on p. 58).

[Sco04] S. H. Scott. "Optimal feedback control and the neural basis of volitional motor control". In: *Nature Reviews Neuroscience* 5.7 (2004), pp. 532–546. DOI: 10.1038/nrn1427 (cit. on p. 5).

[Sey+03] A. Seyfarth, H. Geyer, and H. Herr. "Swing–leg retraction: a simple control model for stable running". In: *Journal of Experimental Biology* 206.15 (2003), pp. 2547–2555. DOI: 10.1242/jeb.00463 (cit. on p. 41).

[Sha+91] L. Shampine, I. Gladwell, and R. Brankin. "Reliable solution of special event location problems for ODEs". In: *ACM Transactions on Mathematical Software* 17.1 (1991), pp. 11–25. DOI: 10.1145/103147.103149 (cit. on p. 11).

[She10] C. S. Sherrington. "Flexion–reflex of the limb, crossed extension–reflex, and reflex stepping and standing". In: *The Journal of Physiology* 40.1–2 (1910), pp. 28–121. URL: http://jp.physoc.org/content/40/1-2/28.short (cit. on p. 102).

[Shi+10] A. S. Shiriaev, L. B. Freidovich, and S. V. Gusev. "Transverse linearization for controlled mechanical systems with several passive degrees of freedom". In: *IEEE Transactions on Automatic Control* 55.4 (2010), pp. 893–906. DOI: 10.1109/TAC.2010.2042000 (cit. on p. 41).

[Sim+05] S. N. Simic, K. H. Johansson, J. Lygeros, and S. S. Sastry. "Towards a geometric theory of hybrid systems". In: *Dynamics of Continuous, Discrete, and Impulsive Systems B: Applications & Algorithms* 12.5–6 (2005), pp. 649–687 (cit. on pp. 10, 14, 17, 18, 22, 58).

[Soa13] S. Soatto. "Actionable Information in Vision". In: *Machine Learning for Computer Vision*. Ed. by R. Cipolla, S. Battiato, and G. M. Farinella. Vol. 411. Studies in Computational Intelligence. Springer Berlin / Heidelberg, 2013, pp. 17–48. DOI: 10.1007/978-3-642-28661-2_2 (cit. on p. 2).

[Son84] E. D. Sontag. "A concept of local observability". In: *Systems & Control Letters* 5.1 (1984), pp. 41–47. DOI: 10.1016/0167-6911(84)90007-0 (cit. on p. 100).

[Sus99] H. J. Sussmann. "A nonsmooth hybrid maximum principle". In: *Stability and Stabilization of Nonlinear Systems*. Ed. by D. Aeyels, F. Lamnabhi-Lagarrigue, and A. van der Schaft. Vol. 246. Lecture Notes in Control and Information Sciences. Springer Berlin / Heidelberg, 1999, pp. 325–354. DOI: 10.1007/1-84628-577-1_17 (cit. on p. 100).

[TJ02] E. Todorov and M. Jordan. "Optimal feedback control as a theory of motor coordination". In: *Nature Neuroscience* 5.11 (2002), pp. 1226–1235. DOI: 10.1038/nn963 (cit. on p. 5).

[TM05] L. H. Ting and J. M. Macpherson. "A limited set of muscle synergies for force control during a postural task". In: *Journal of Neurophysiology* 93.1 (2005), pp. 609–613. DOI: 10.1152/jn.00681.2004 (cit. on pp. 5, 41).

[TM07] L. H. Ting and J. L. McKay. "Neuromechanics of muscle synergies for posture and movement". In: *Current Opinion in Neurobiology* 17.6 (2007), pp. 622–628. DOI: 10.1016/j.conb.2008.01.002 (cit. on p. 5).

[Tab07] P. Tabuada. "Event–Triggered Real–Time Scheduling of Stabilizing Control Tasks". In: *IEEE Transactions on Automatic Control* 52.9 (2007), pp. 1680–1685. DOI: 10.1109/TAC.2007.904277 (cit. on p. 40).

[Tav09] L. Tavernini. "Generic asymptotic error estimates for the numerical simulation of hybrid systems". In: *Nonlinear Analysis: Hybrid Systems* 3.2 (2009), pp. 108–123. DOI: 10.1016/j.nahs.2008.11.002 (cit. on pp. 11, 39).

[Tav87] L. Tavernini. "Differential automata and their discrete simulators". In: *Nonlinear Analysis: Theory, Methods & Applications* 11.6 (1987), pp. 665–683. DOI: 10.1016/0362-546X(87)90034-4 (cit. on pp. 10, 11).

[Td90] R. Thomas and R. d'Ari. *Biological feedback*. CRC press, 1990 (cit. on p. 7).

[Tod04] E. Todorov. "Optimality principles in sensorimotor control". In: *Nature neuroscience* 7.9 (2004), pp. 907–915. DOI: 10.1038/nn1309 (cit. on p. 5).

[Utk77] V. Utkin. "Variable structure systems with sliding modes". In: *IEEE Transactions on Automatic Control* 22.2 (1977), pp. 212–222. DOI: 10.1109/TAC.1977.1101446 (cit. on p. 20).

[Vog07] S. Vogel. "The emergence of comparative biomechanics". In: *Integrative and Comparative Biology* 47.1 (2007), pp. 13–15. DOI: 10.1093/icb/icm004 (cit. on p. 4).

[Vog98] S. Vogel. *Cats' paws and catapults: Mechanical worlds of nature and people*. W. W. Norton & Company, Inc., 1998 (cit. on p. 103).

[WA12] E. D. Wendel and A. D. Ames. "Rank deficiency and superstability of hybrid systems". In: *Nonlinear Analysis: Hybrid Systems* 6.2 (2012), pp. 787–805. DOI: 10.1016/j.nahs.2011.09.002 (cit. on pp. 49, 75, 79).

[WF86] R. Womersley and R. Fletcher. "An algorithm for composite nonsmooth optimization problems". English. In: *Journal of Optimization Theory and Applications* 48.3 (1986), pp. 493–523. DOI: 10.1007/BF00940574 (cit. on p. 94).

[Wes+03] E. R. Westervelt, J. W. Grizzle, and D. E. Koditschek. "Hybrid zero dynamics of planar biped walkers". In: *IEEE Transactions on Automatic Control* 48.1 (2003), pp. 42–56. DOI: 10.1109/TAC.2002.806653 (cit. on pp. 40, 41, 62, 100).

[Wey+09] P. G. Weyand, M. W. Bundle, C. P. McGowan, A. Grabowski, M. B. Brown, R. Kram, and H. Herr. "The fastest runner on artificial legs: different limbs, similar function?" In: *Journal of Applied Physiology* 107.3 (2009), pp. 903–911. DOI: 10.1152/japplphysiol.00174.2009 (cit. on p. 5).

[Wie48] N. Wiener. *Cybernetics: or control and communication in the animal and the machine*. Second. MIT Press, 1948 (cit. on p. 3).

[Win01] A. T. Winfree. *The geometry of biological time*. Vol. 12. Springer, 2001 (cit. on p. 7).

[Woo+08] R. J. Wood, S. Avadhanula, R. Sahai, E. Steltz, and R. S. Fearing. "Microrobot Design Using Fiber Reinforced Composites". In: *Journal of Mechanical Design* 130.5, 052304 (2008), p. 052304. DOI: 10.1115/1.2885509 (cit. on pp. 101, 103).

[Zei95] E Zeidler. *Applied functional analysis and its applications*. Springer–Verlag, 1995 (cit. on p. 92).

[Zha+01] J. Zhang, K. H. Johansson, J. Lygeros, and S. S. Sastry. "Zeno hybrid systems". In: *International Journal of Robust and Nonlinear Control* 11.5 (2001), pp. 435–451. DOI: 10.1002/rnc.592 (cit. on p. 24).

[Zha+13] T. Zhang, F. Qian, C. Li, P. Masarati, A. M. Hoover, P. Birkmeyer, A. Pullin, R. S. Fearing, and D. I. Goldman. "Ground fluidization promotes rapid running of a lightweight robot". In: *The International Journal of Robotics Research* 32.7 (2013), pp. 859–869. DOI: 10.1177/0278364913481690 (cit. on p. 101).

[Zie89] W. P. Ziemer. *Weakly Differentiable Functions*. Graduate Texts in Mathematics. Springer, 1989 (cit. on p. 28).

[dB05] A. d'Avella and E. Bizzi. "Shared and specific muscle synergies in natural motor behaviors". In: *Proceedings of the National Academy of Sciences of the United States of America* 102.8 (2005), pp. 3076–3081. DOI: 10.1073/pnas.0500199102 (cit. on p. 5).

[ÅK14] K. J. Åström and P. Kumar. "Control: A perspective". In: *Automatica* 50.1 (2014), pp. 3–43. DOI: 10.1016/j.automatica.2013.10.012 (cit. on p. 7).